

(NASA-CR-138804) DEVELOPMENT OF HIGH
TEMPERATURE MATERIALS FOR SOLID PROPELLANT
ROCKET NOZZLE APPLICATIONS Quarterly
Progress Report, 1 Jul. (North Carolina
State Univ.) 177 p HC \$11.50 CSCI 21H

N74-28236
THRU
N74-28238
Unclas
43162

G3/28

177

Twelfth Quarterly Progress Report

Covering the Period 1 July 1973 - 30 September 1973

**DEVELOPMENT OF HIGH TEMPERATURE MATERIALS
FOR SOLID PROPELLANT ROCKET NOZZLE APPLICATIONS**

NGR 34-002-108

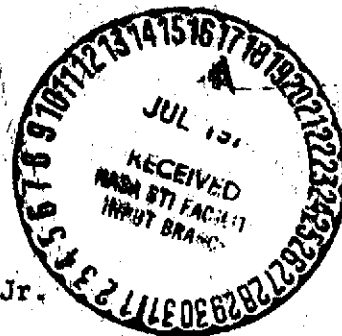
For

National Aeronautics and Space Administration

14 January 1974

By

Charles R. Manning, Jr.
Professor
and
Lynn D. Laneback
Research Assistant



Department of Materials Engineering
North Carolina State University
Raleigh, North Carolina

N 74-28236

Twelfth Quarterly Progress Report
Covering the Period 1 July 1973 - 30 September 1973

DEVELOPMENT OF HIGH TEMPERATURE MATERIALS
FOR SOLID PROPELLANT ROCKET NOZZLE APPLICATIONS

NGR 34-002-108

For
National Aeronautics and Space Administration

14 January 1974

By
Charles R. Manning, Jr.
Professor
and
Lynn D. Lineback
Research Assistant

Department of Materials Engineering
North Carolina State University
Raleigh, North Carolina

INTRODUCTION AND BACKGROUND

During the period from July 1, 1969 to present, work has been performed on the NASA Grant NGR 34-002-108 entitled "Development of High Temperature Materials for Solid Propellant Rocket Nozzle Applications" at North Carolina State University. This work has resulted in the production of a material which has recently been patented by NASA (U.S. Patent 2,706,385 entitled "Thermal Shock Resistant Hafnia Ceramic Material). The material is a hafnia matrix-tungsten fiber composite which has exhibited superior thermal shock resistance. As the result of tests, the material is believed to be capable of meeting the requirements of solid propellant rocket nozzles applications: thermal shock resistance, mechanical erosion resistance, and chemical erosion resistance, as well as high melting temperatures.

While the melting point of hafnia is not as high as that of the material currently used for the application (graphite), it is believed to be sufficiently high to avoid melting. The mechanical and chemical erosion resistance is clearly superior, however. The problem of thermal shock resistance has been overcome by the incorporation of tungsten metal fibers in the composite material. It is believed that better control of solid propellant rocket engines can be realized by incorporating this material in the region of the nozzle throat section such that the throat cross sectional area increases during flight may be reduced.

As a result of extensive testing a composite material containing 90 wt. pct. of yttria stabilized hafnia and 10 wt. pct. of tungsten fibers was selected as a candidate material for incorporation into

throat inserts for small scale test nozzles.. These inserts of composite material have been hot pressed to final shape as illustrated by half section in Figure 1. The ceramic composite core is encased in a graphite case which completes the throat section of the small scale motor.

Three composite nozzles were submitted to the Scout Project Office, NASA Langley, and two nozzles have been test fired. The results of these firings are described below.

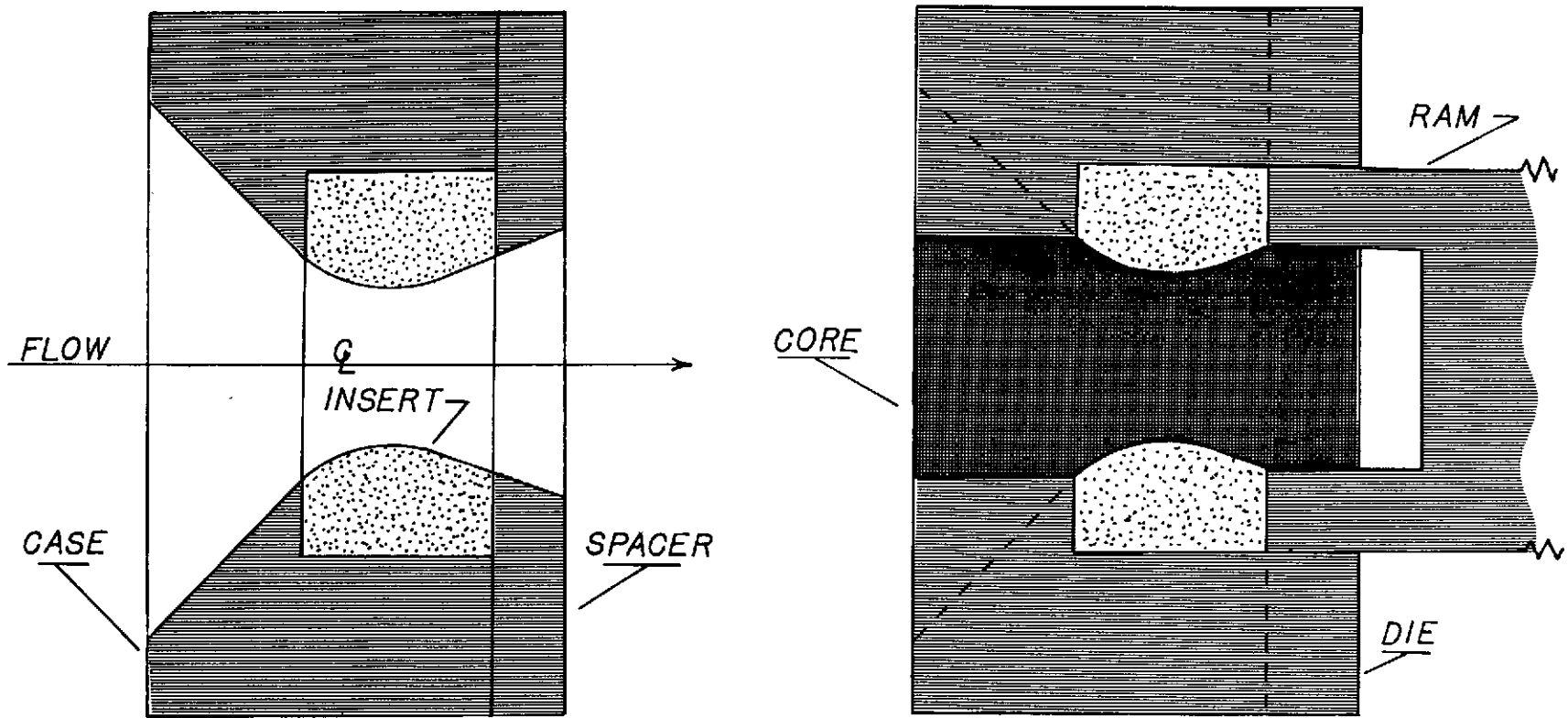


Figure 1. Schematic of nozzle throat section die and insert.

TEST FIRING OF NOZZLES CONTAINING INSERTS

Two nozzles of the design previously described were test fired by Allegheny Ballistics Laboratory in small motor cases with solid fuel charges. One of the nozzles was fabricated from graphite, a second contained a hafnia-tungsten composite insert. From Figures 2 and 3 it may be observed that no catastrophic thermal shock occurred but severe erosion of the throat sections of the hafnia based inserts did occur. In general, the erosion was more severe in the hafnia-based insert. Closer observation indicates that although some melting did occur in the hafnia based nozzle, the primary mode of failure was by thermal erosion.

In general, the hot pressing temperatures and pressures were not high enough to produce a strong body. In the development of the material, temperatures in excess of 2100°C were found to produce bodies with good thermal shock resistance and with no spalling. When fabricating the test nozzles, this temperature was seldom if ever, reached because of the limitations of the induction heating equipment. Thus, it is believed that if a higher temperature can be reached a stronger material less susceptible to thermal spalling yet resistant to thermal shock can be obtained.

Several nozzles should be fabricated at temperatures of 2100°C or above and these nozzles should be test fired as before.

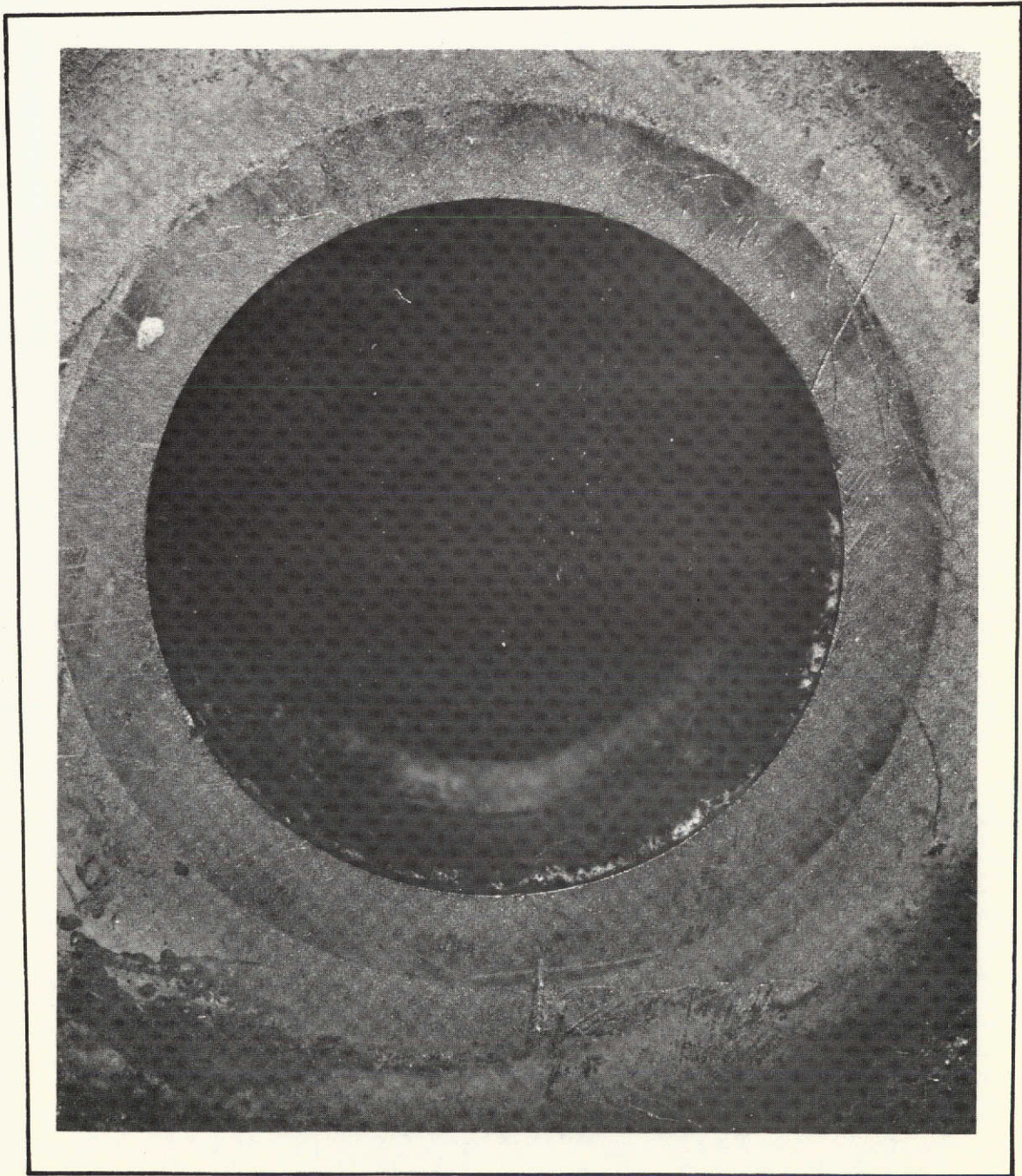


Figure 2 Graphite Rocket Nozzle after Static Test Firing.

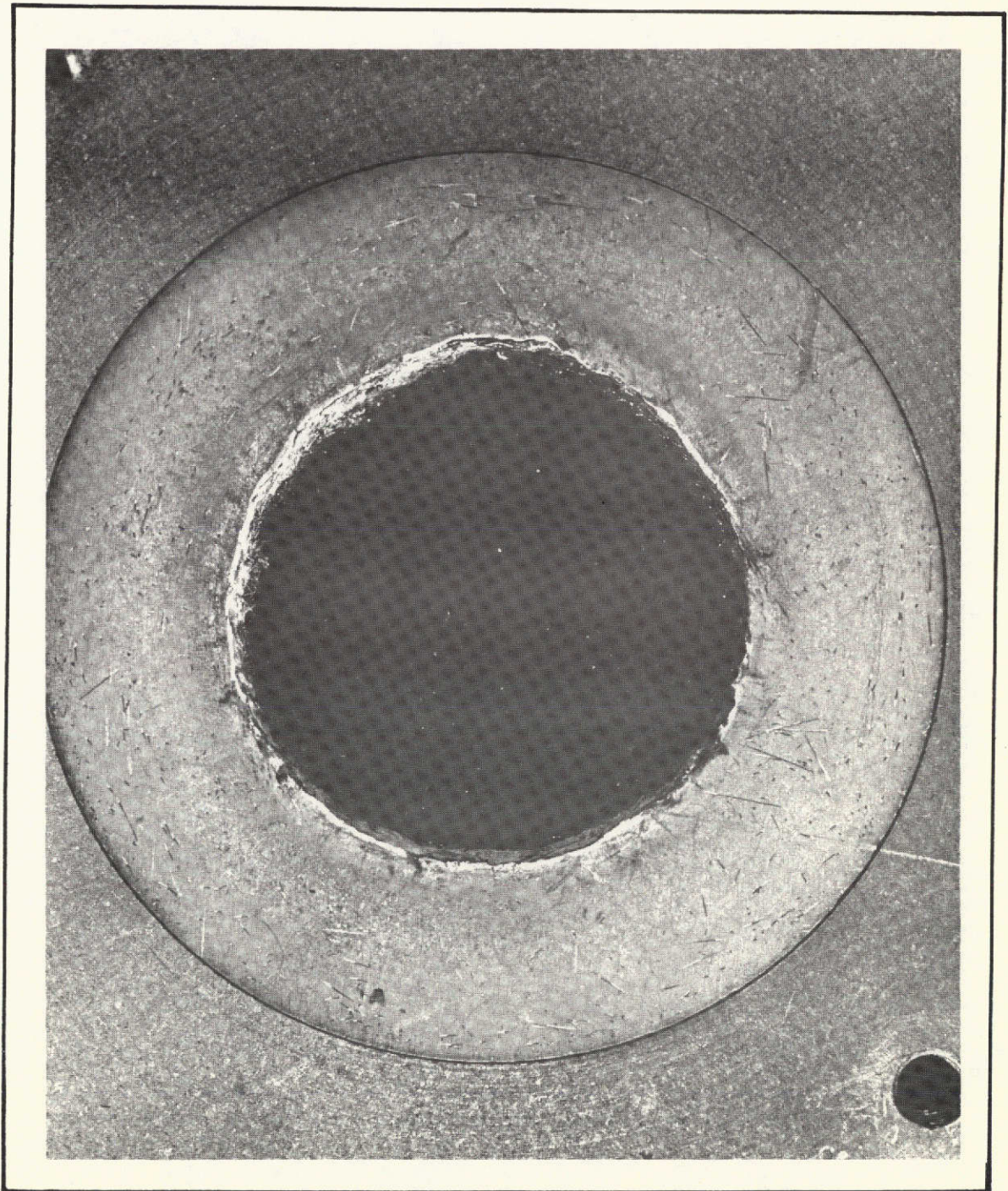


Figure 3 Hafnia-tungsten Rocket Insert after Static Test Firing.

CONTINUATION OF RESEARCH

During the first two years of the grant, a number of materials were investigated for possible application as solid propellant nozzle materials. As has been reported in a number of progress reports, hafnium carbide and zirconium carbide based materials were found to be unsatisfactory due to their lack of oxidation resistance at elevated temperatures. As a result, hafnium dioxide, which is very stable in an oxidizing atmosphere, was investigated as a possible candidate material.

Good thermal shock resistance of hafnia which had been partially stabilized with yttrium, had been observed by J. D. Buckley ("Stabilization of the Phase Transformations in Hafnium Oxide", Ph.D. Dissertation, Iowa State University, 1967) as the result of an earlier investigation. On this basis, hafnia was considered as a candidate material for the matrix of a ceramic-based composite material. Initially, graphite was considered as the dispersed phase material. Lineback and Manning ("Factors Affecting the Thermal Shock Behavior of Yttria Stabilized Hafnia Based Graphite and Tungsten Composites", pp. 137-147, in Materials Science Research, Vol. 5, "Ceramics in Severe Environments", H. Palmour and W. W. Kriegel, editors, Plenum Press, New York, 1971) reported that any additions of graphite were harmful to the thermal shock resistance. It was further reported in this paper that small additions of about 10 wt. pct. tungsten fibers significantly improved the thermal shock resistance of partially stabilized hafnia. In his Master of Science thesis derived from this work, Lineback ("Factors Affecting the Thermal Shock Resistance of Several Hafnia Based Composites

Containing Graphite or Tungsten", Masters thesis, North Carolina State University, 1971) (appendix) observed that the addition of fibers decreased both the fracture strength and modulus of elasticity. The ratio of the fracture strength to modulus of elasticity was increased, however; that is to say that the strain to failure was increased. The classical concepts of thermal shock resistance indicated that the maximum temperature differential to which a material may be exposed without thermal shock failure is directly proportional to this ratio:

$$\Delta T = \frac{\sigma_f s}{\sigma E} A + \frac{ck}{Lh}$$

where $\sigma_f s$ is the fracture strength; α , the coefficient of linear thermal expansion; E , the modulus of elasticity; A , c , and L , geometric factors; k , the thermal conductivity; and h , the coefficient of surface heat transfer. On the basis of this observation, Lineback ("Model for Thermal Stress Resistance of Truly Elastic Materials Containing More Than One Crack", Ph.D. Dissertation, North Carolina State University, 1973, work under this grant) (appendix) developed a model for the thermal shock resistance of ceramic materials. The model has been applied successfully to data other than that for the hafnia material.

The model, which was developed along lines similar to Hasselman's microcrack theory ("Unified Theory of Thermal Shock Fracture Initiation and Crack Propagation in Brittle Ceramics", J. Amer. Cer. Soc. 52, (11), 600-604, 1969), related the thermal stress resistance of ceramic materials to the measured materials properties of fracture strength, effective modulus of elasticity, and coefficient linear thermal expansion through the intrinsic materials properties of surface energy

and intrinsic modulus of elasticity by virtue of the microstructure (i.e. crack sizes and numbers). It is felt that the knowledge gained during this investigation in the past, as expressed by Lineback's model, would allow the refinement of present materials as well as the development of new high temperature materials having excellent thermal shock resistances..

PROPOSALS FOR CONTINUED WORK

On the foundation of the knowledge gained thus far in this investigation, a number of specific proposals are made below for continued work. They include analysis of the materials currently developed during this investigation after test firing of the engine, fabrication of full size nozzles upon satisfactory testing of small scale engines, improvement of present material, and development of new materials.

It is proposed that an intensive investigation be made of the microstructure and mechanical properties of the composite material to establish its thermal shock resistance, as well as, the chemical and mechanical erosion resistance. These fired materials would be compared with unfired materials to establish change in microstructure and physical properties. This investigation would be beneficial in establishing the possibility of this material for use in restartable engines which are subject to more than one thermal cycle.

It is proposed that work continue in the improvement of this material such that its applications may be broadened. A detailed investigation of the microstructure may lead to significant improvements in the strain to failure and consequently in the temperature differential to cause thermal failure. These improvements would allow the use of higher burning temperature materials and consequently improvements in the efficiency of solid propellant engines.

It is further proposed that new ceramic based composite materials for application on high temperature nozzle inserts be investigated. Due to the knowledge gained during this investigation, it is believed

that other ceramic matrix composite materials can be developed which may be used for similar applications. Perhaps, for example, zirconia-hafnia alloys may be developed as matrix material. Hafnium or zirconium metal fibers may prove a more stable dispersed phase. Other materials such as reaction bonded silicon nitride may be adaptable to the application as well.

APPENDIX

ABSTRACT

LINEBACK, LYNN DAVID. Factors Affecting the Thermal Shock Resistance of Several Hafnia Based Composites Containing Graphite or Tungsten. (Under the direction of CHARLES RICHARD MANNING, Jr.).

The thermal shock resistance of hafnia based composites containing graphite powder or tungsten fibers was investigated in terms of material properties which include thermal expansion, thermal conductivity, compressive fracture stress, modulus of elasticity, and phase stability in terms of the processing parameters of hot pressing pressure and/or density, degree of stabilization of the hafnia, and composition. All other parameters were held constant or assumed constant. For these materials the thermal shock resistance was directly proportional to the compressive fracture stress to modulus of elasticity ratio and was not affected appreciably by the small thermal expansion or thermal conductivity changes. This ratio was found to vary strongly with the composition and density such that the composites containing graphite had relatively poor thermal shock resistance, while the composites containing tungsten had superior thermal shock resistance.

N74-28237

i

FACTORS AFFECTING THE THERMAL SHOCK RESISTANCE
OF SEVERAL HAFNIA BASED COMPOSITES CONTAINING
GRAPHITE OR TUNGSTEN

by

LYNN DAVID LINEBACK

A thesis submitted to the Graduate Faculty of
North Carolina State University at Raleigh
in partial fulfillment of the
requirements for the Degree of
Master of Science

DEPARTMENT OF MATERIALS ENGINEERING

RALEIGH

1 9 7 1

APPROVED BY:

Chairman of Advisory Committee

ACKNOWLEDGEMENTS

This investigation was performed primarily under the guidance of the author's committee chairman, C. R. Manning, Jr. and his initiation of the investigation; aid in performing the investigation, rapidly procuring equipment and supplies, and "acquiring a fundamental understanding;" and moral support are gratefully acknowledged. A. A. Fahmy, of the advisory committee, is also due a note of thanks for pertinent discussions and editing of the thesis manuscript. J. Bailey, also of the advisory committee, is acknowledged for his many corrections to the manuscript.

A group of people, too numerous to mention, has also contributed to the investigation. Especially deserving, however, are M. W. Haller for his aid in modulus of elasticity measurements and the author's wife, T. M. Lineback, for aid in construction of equipment, testing, and editing of the manuscript.

Finally, the National Aeronautics and Space Administration is acknowledged for financial support in the form of the NGR 34-002-108 grant supervised by J. P. Howell for the Scout office at Langley Research Center, Hampton, Virginia.

TABLE OF CONTENTS

	Page
LIST OF FIGURES	iv
INTRODUCTION	1
LITERATURE SURVEY	2
THEORETICAL CONSIDERATIONS	6
APPROACH TO PROBLEM	14
PROCEDURE	17
Materials	17
Fabrication	17
Stabilization	18
Density	19
Coefficient of Linear Thermal Expansion	19
Coefficient of Thermal Conductivity	20
Modulus of Elasticity and Compressive Fracture Strength	21
Thermal Shock	22
RESULTS AND DISCUSSION OF RESULTS	24
Coefficient of Thermal Expansion	24
Coefficient of Thermal Conductivity	27
Modulus of Elasticity and Compressive Fracture Stress	32
Thermal Shock	38
CONCLUSION	41
PROPOSALS FOR FUTURE WORK	43
REFERENCES	45

LIST OF FIGURES

	Page
1. Nondimensional time vs. nondimensional stress for various values of Biot's modulus	12
2. Coefficient of linear thermal expansion vs. percent stabilization in yttria stabilized hafnia hot pressed at one thousand pounds per square inch	25
3. Coefficient of linear thermal expansion vs. atomic percent graphite in eighty five percent yttria stabilized hafnia hot pressed at ten thousand pounds per square inch	26
4. Coefficient of linear thermal expansion vs. weight percent tungsten in seventy percent yttria stabilized hafnia hot pressed at eight thousand pounds per square inch	28
5. Coefficient of thermal conductivity vs. percent stabilization in yttria stabilized hafnia hot pressed at ten thousand pounds per square inch	29
6. Coefficient of thermal conductivity vs. atomic percent graphite in eighty five percent yttria stabilized hafnia hot pressed at ten thousand pounds per square inch	30
7. Coefficient of thermal conductivity vs. weight percent tungsten in seventy percent yttria stabilized hafnia hot pressed at eight thousand pounds per square inch	31
8. Modulus of elasticity vs. atomic percent graphite in eighty five percent yttria stabilized hafnia hot pressed at ten thousand pounds per square inch	34
9. Compressive fracture stress vs. atomic percent graphite in eighty five percent yttria stabilized hafnia hot pressed at ten thousand pounds per square inch	35
10. Modulus of elasticity vs. weight percent tungsten in seventy percent yttria stabilized hafnia hot pressed at eight thousand pounds per square inch	36
11. Compressive fracture stress vs. weight percent tungsten in seventy percent yttria stabilized hafnia hot pressed at eight thousand pounds per square inch	37
12. Ratio of compressive fracture stress to modulus of elasticity vs. weight percent tungsten in seventy percent yttria stabilized hafnia hot pressed at eight thousand pounds per square inch	39

INTRODUCTION

Throat areas of solid propellant rocket nozzles are subjected to severe thermal shock, mechanical erosion, and chemical erosion (6, 22, 33). In the past this area of the nozzle has been made from such materials as graphite, tungsten and alumina. All these materials are lacking resistance to one or more of the above areas of degradation (19, 20, 23, 24, 32). Graphite while having excellent thermal shock resistance has poor chemical and mechanical erosion resistance. Tungsten is heavy, hard to fabricate, and has poor chemical erosion resistance. Alumina, on the other hand, has poor thermal shock resistance.

Hafnia based composites containing either graphite or tungsten were investigated in an attempt to optimize thermal shock resistance, mechanical erosion and chemical erosion. This paper discusses the thermal shock behavior of the base material and composites containing the base material with either graphite or tungsten in terms of the thermal shock resistance parameters of thermal expansion, thermal conductivity, modulus of elasticity and compressive fracture stress. These parameters were investigated in terms of the material and processing parameters of degree of stabilization of hafnia, hot pressing pressure and density, and graphite or tungsten content. All other parameters were held constant.

No attempt has been made to describe the behavior in terms of composite theory; the microscopic modulus of elasticity, fracture stress, thermal expansion, or thermal conductivity; ceramic-metal interfacial bonding; or currently popular theories of thermal shock resistance attributed to microcrack distribution, propagation, and interaction.

In the past a large volume of work has been devoted to the problem of thermal shock. In general, however, the majority of that work is concerned with the selection of materials for given thermal shock environments. The majority of those materials are metal or metal based materials.

Within the field of ceramic materials some work has been done in the area of increasing thermal shock resistance by adjusting porosity and density. The results are not in general agreement. Only recently has work been done in the area of composite materials with ceramic bases which may be more thermal shock resistant than the base material. The work as a whole was not done to improve thermal shock resistance but to improve the high temperature mechanical properties such as fracture stresses. Some workers fortunately did do some secondary work on the thermal shock resistance of these materials. These materials are the ones of interest to this investigation.

Baskin et al. (5) in 1959 fabricated a series of thoria based composites containing mild steel, type 430 stainless steel, molybdenum, niobium, Zircalloy-2 and zirconium wire by vacuum hot pressing with a pressure of twenty five hundred pounds per square inch at a temperature of fifteen hundred degrees centigrade for twenty minutes. These specimens were thermal shock tested by quenching from one thousand degrees centigrade into mercury. These investigators report that specimens having densities of ninety-five percent of theoretical and containing five, ten, and twenty weight percent molybdenum fiber withstood increasing numbers of thermal shock cycles. In general, they report that

any addition of molybdenum fibers was beneficial to thermal shock resistance. Composites containing up to twenty weight percent molybdenum powder, however, fractured during the first thermal shock exposure as did all base material without molybdenum additions.

Baskin et al. (5) reported the compressive fracture stress and modulus of elasticity for a series of ninety one percent of theoretical density specimens. The fracture stress to modulus ratios for these materials are as follows: zero weight percent molybdenum has a ratio of 5.5×10^{-3} ; five weight percent, 2.0×10^{-3} ; ten weight percent, 2.3×10^{-3} ; twenty weight percent, 4.0×10^{-3} .

The addition of niobium fibers was also reported to increase the thermal shock resistance similar to that of the molybdenum additions. Some loss of thermal shock resistance was noted if the niobium wire carburized and the molybdenum additions were considered more satisfactory.

Additions of Zircalloy-2 and zirconium did not improve the thermal shock resistance due to embrittlement of both additions. The steel additions did not substantially improve thermal shock resistance because of softening and subsequent extrusion of the steel from the composites during hot pressing.

Blakeley and White (7) in 1960 described a nickel-magnesia composite refractory material cold pressed at ten thousand pounds per square inch and sintered. They proposed that a high fracture stress to modulus of elasticity ratio was desirable for optimum thermal shock resistance. They reported that small additions of nickel to magnesia improved the

thermal shock resistance while having little effect upon strength. Larger additions of nickel increased strength moderately and significantly increased thermal shock resistance. At eighty percent nickel the strength fell abruptly and an addition of seventy five percent nickel gave the best thermal shock resistance. The investigators report that their results (which were not given) agreed with their proposed criteria for improving thermal shock resistance.

Walton and Poulos (31) in 1962 placed four to five volume percent Nichrome and type 430 stainless steel wires in fired silica and alumina by slip casting. They, however, did not report values for any parameters of thermal shock resistance.

Tinklepaugh et al. (28, 29, 30) in the late 1950's and 1960's did extensive work on alumina-metal composites. He and his group made composites containing five, ten, and twenty weight percent molybdenum hot pressed at fourteen, fifteen, and sixteen hundred degrees centigrade. These materials, having unidirectionally oriented continuous fibers, were studied primarily for their mechanical properties at elevated temperatures. Some work was done in the area of thermal shock resistance. They found that the composites containing ten and twenty weight percent molybdenum were superior to the base material in thermal shock resistance. The compressive fracture stress to modulus of elasticity ratios of these materials was difficult to obtain from their work but, in general, the ten and twenty weight percent materials had significantly higher ratios than did the five weight percent material.

Hafnia of unspecified density and degree of stabilization was hot pressed with twenty weight percent molybdenum wires by Tinklepaugh et al.

The four specimens fabricated did not fracture due to thermal shock and were in general considered to be superior to the base material.

Arias (3, 4) added fifteen mole percent titanium powder to 5.33 weight percent stabilized zirconia and fabricated composites by hot pressing and by cold pressing and sintering. In all cases he reported that the thermal shock resistance of these materials was better than that of the base material.

The addition of the titanium increased the modulus of rupture from approximately sixteen thousand pounds per square inch to approximately thirty thousand pounds per square inch. The modulus of elasticity also increased from twenty million pounds per square inch to thirty million pounds per square inch. This gives a ratio of 0.8×10^{-3} for the zirconia and a ratio of 1.0×10^{-3} for the composite.

THEORETICAL CONSIDERATIONS

Thermal Stressing and Shock

If a perfectly elastic homogeneous body has been deformed, six strains may be induced by three displacements along the three major axis, x, y, and z (25):

$$\epsilon_{ij} = \frac{1}{2} \left(\frac{\delta u_i}{\delta x_j} + \frac{\delta u_j}{\delta x_i} \right) \quad (1)$$

where u, v, and w are displacements. These equations through differentiation and elimination of displacements yield the following set of compatibility equations:

$$\frac{\delta^2 \epsilon_{ij}}{\delta x_k \delta x_l} + \frac{\delta^2 \epsilon_{kl}}{\delta x_i \delta x_j} = \frac{\delta^2 \epsilon_{ik}}{\delta x_j \delta x_l} + \frac{\delta^2 \epsilon_{jl}}{\delta x_i \delta x_k} \quad (2)$$

By Hooke's law:

$$\epsilon_i = \frac{\sigma_i}{E} \quad (3)$$

where σ_i is a stress along the i axis and E is Young's modulus. Likewise

$$\epsilon_j = \frac{-\mu \sigma_i}{E} \quad \text{and} \quad \epsilon_k = \frac{-\mu \sigma_i}{E}$$

where μ is Poisson's ratio.

Now if a temperature gradient ΔT is applied:

$$\epsilon_i = \frac{1}{E} [\sigma_i - \mu(\sigma_j + \sigma_k)] + \alpha \Delta T \quad (4)$$

where α is the coefficient of linear thermal expansion. Because free

thermal expansion does not produce angular distortion, the relationships between the shearing stresses and strains are unaffected:

$$\gamma_{ij} = \frac{\tau_{ij}}{G} \quad (5)$$

where $G = \frac{E}{2(1+\mu)}$.

Now if the body is restrained by a hydrostatic pressure p , (4) reduces to:

$$0 = \frac{1}{E} [p - \mu(p+p)] + \alpha \Delta T \quad (6)$$

or $p = \frac{-\alpha E \Delta T}{1-2\mu}$.

If the forces about any cube in the material are summed, the body forces on the cube may be obtained:

$$\frac{\delta \sigma_i}{\delta x_i} + \frac{\delta \tau_{ij}}{\delta x_j} + \frac{\delta \tau_{ik}}{\delta x_k} = X_i \quad (7)$$

where X_i are the body forces. If $x_i = p$ for the case of (6), then (7) becomes:

$$X_i = \frac{-\alpha E}{1-2\mu} \frac{\delta T}{\delta x_i} \quad (8)$$

If the body is unrestrained, the thermal stresses may be obtained by superimposing (8) onto (7) and changing signs to obtain the general case:

$$\frac{\delta \sigma_i}{\delta x_i} + \frac{\delta \tau_{ij}}{\delta x_j} + \frac{\delta \tau_{ik}}{\delta x_k} = \left(\frac{\alpha E}{1-2\mu} \right) \frac{\delta T}{\delta x_i} \quad (9)$$

Now if the surface of the material is heated or cooled by a fluid which is considered to remain at a constant temperature at all times, the temperature at any point within the body at any time may be found as a function of displacement from the heat surface x_j and time t .

Carslaw and Jaeger and others (8, 10, 14, 18) suggest the following function for three dimensions:

$$\frac{\delta^2 T_j}{\delta x_j^2} + \frac{\delta^2 T_j}{\delta x_j^2} + \frac{\delta^2 T_j}{\delta x_k^2} - \frac{1}{K} \frac{\delta T}{\delta t} = 0 \quad (10)$$

where K is the thermal diffusivity and is equal to $\frac{k}{\rho c}$ where k is the thermal conductivity, ρ is the density and c is the specific heat.

If a semi-infinite solid is bounded by the surface $x=0$ then (10) may be reduced to

$$\frac{\delta^2 T}{\delta x^2} - \frac{1}{K} \frac{\delta T}{\delta t} = 0 \quad (10a)$$

If the initial temperature of this solid at any point is a function of x and the surface is kept at $T=0$ the solution of (10a) will be of the form:

$$T = \frac{1}{\sqrt{4\pi Kt}} \int_0^{\infty} f(x') \left\{ e^{-(x-x')^2/4Kt} - e^{-(x+x')^2/4Kt} \right\} dx' \quad (11)$$

If the initial temperature T_0 at time $t=0$ is uniform within the body, the temperature as a function of x and t is given by a specific solution of (11):

$$T = T_0 \operatorname{erf} \left\{ \frac{x}{\sqrt{4Kt}} \right\} \quad (12)$$

where $\operatorname{erf}(u) = \frac{2}{\sqrt{\pi}} \int_0^u e^{-u^2} du$

If the boundary conditions are reversed such that the boundary is kept at some constant temperature T_s and the body is at some initial temperature $T_0 < T_s$ then the temperature or a function of x and t is given by:

$$T = T_0 \operatorname{erfc} \frac{x}{\sqrt{4Kt}} \quad \text{where } \operatorname{erfc}(x) = 1 - \operatorname{erf}(x) \quad (13)$$

For a semi-infinite solid at some uniform temperature T_0 heated by a fluid following Newton's Law of cooling,

$$\frac{\delta T}{\delta x} + h(T - T_0) = 0 \quad (14)$$

where h is the coefficient of surface heat transfer. Temperature as a function of x and t may be found for linear heat flow (10a):

$$T = T_f \left[\operatorname{erfc} \frac{x}{\sqrt{4Kt}} - e^{hx+h^2Kt} \operatorname{erfc} \left\{ \frac{x}{\sqrt{4Kt}} + h\sqrt{Kt} \right\} \right] \quad (15)$$

where T_f is the temperature of the fluid.

Now for the case of a semi-infinite solid, the strain in the y and z directions are equal to zero and the strains in the x direction are not zero. Further, σ_x is taken to be zero and σ_y and σ_z are taken to be equal. Therefore, from (4)

$$\sigma_z = \sigma_y = \left(\frac{\alpha E}{1 - \mu} \right) \Delta T \quad (16)$$

If the initial temperature is taken as zero, the thermal stress distribution for a semi-infinite solid heated on the plane $x=0$ is given by the following equations for the two aforementioned general heating condition:

$$\sigma_z = \sigma_y = \left(\frac{\alpha E}{1-\mu} \right) T_f \operatorname{erfc} \frac{x}{4Kt} \quad (17)$$

$$\sigma_z = \sigma_y = \left(\frac{\alpha E}{1-\mu} \right) T_f \left[\operatorname{erfc} \frac{x}{4Kt} - e^{hx+h^2Kt} \operatorname{erfc} \left\{ \frac{x}{4Kt} + h\sqrt{Kt} \right\} \right] \quad (18)$$

For both conditions the maximum stress occurs at the surface ($x=0$):

$$\sigma_{z_s} = \sigma_{y_s} = \left(\frac{\alpha E}{1-\mu} \right) T_f \quad (19)$$

$$\sigma_{z_s} = \sigma_{y_s} = \left(\frac{\alpha E}{1-\mu} \right) T_f \left[1 - e^{h^2Kt} \operatorname{erfc} (h\sqrt{Kt}) \right] \quad (20)$$

[For large values of h , (20) approaches that of (19). Therefore, for this case (19) may be considered a special case of (20).]

Now if the semi-infinite solid is reduced to a semi-infinite plate of finite half thickness L and if t is limited such that T at L never exceeds the initial temperature T_0 , the stresses on the surface are the sum:

$$\sigma_y = \sigma_z = \left(\frac{\alpha E}{1-\mu} \right) T(x) + C_1 + C_2 \quad (21)$$

where C_1 and C_2 are constants determined by end conditions of the plate.

If the ends are free:

$$C_1 = \frac{1}{2h} \int_0^L T(x) dx \quad (22)$$

and

$$C_2 = \frac{3}{2L^3} \int_0^L T(x)xdx \quad (23)$$

The stresses are now given by

$$\sigma_y = \sigma_z = \left(\frac{\alpha E}{1-\mu} \right) \left[-T(x) + \frac{1}{2L} \int_{-L}^L T(x)dx + \frac{3x}{2L^3} \int_{-L}^L T(x)xdx \right] \quad (24)$$

where

$$T(x) = T_f \left[\operatorname{erfc} \frac{x}{4Kt} - e^{hx+h^2Kt} \operatorname{erfc} \left\{ \frac{x+h\sqrt{Kt}}{4Kt} \right\} \right].$$

Heisler (16) has solved this equation for $x=0$ where the maximum stress occurs and Hlinka et al. (17) have plotted these stresses in terms of the following non-dimensional parameter:

$$\sigma_s^* = \frac{\sigma_x(1-\mu)}{E\alpha T_F} \quad (\text{nondimensional stress}) \quad (25)$$

$$\tau = \frac{Kt}{L^2} \quad (\text{nondimensional time}) \quad (26)$$

$$\beta = \frac{hL}{k} \quad (\text{Biot's Modulus}) \quad (27)$$

Manson (21) plotted the maximum σ^* vs each β (Figure 1) and fitted the curve with an expression of the following form:

$$\sigma_{s \max}^* = A + \frac{C}{\beta} - Fe^{-D/\beta} \quad (28)$$

where A, C, D, and F are constants. (For small values of β the third term may be omitted.)

Thermal stress becomes thermal shock when the maximum stress produced exceeds the fracture stress of the material σ_{fs} . By combining

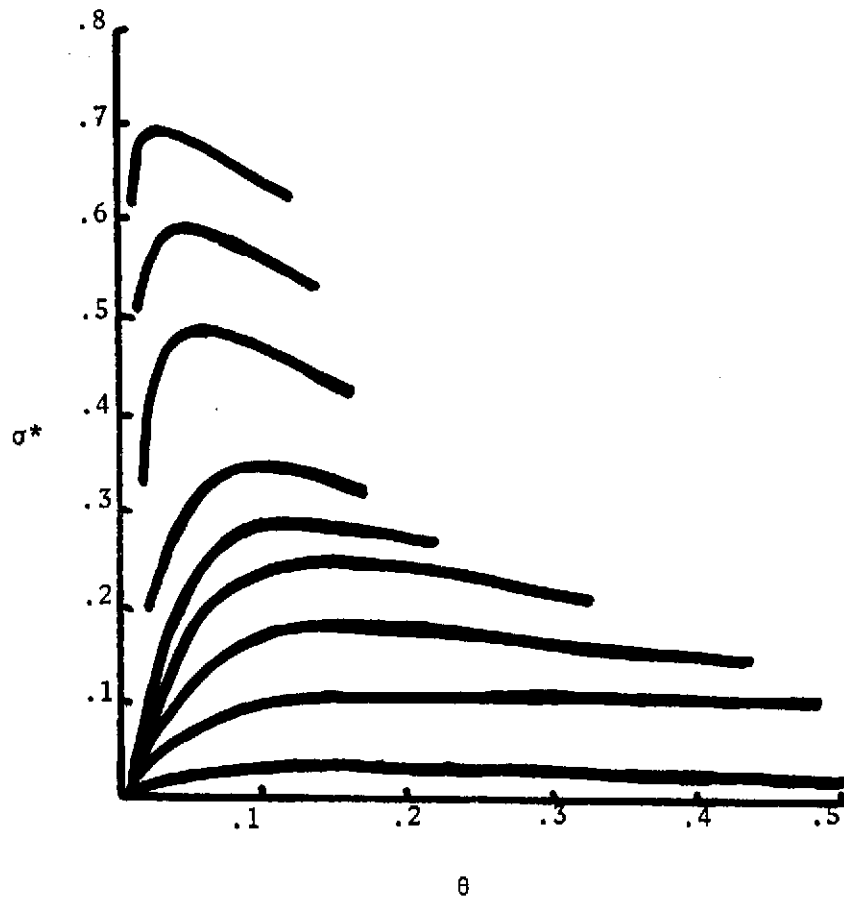


Figure 1. Nondimensional time vs. nondimensional stress for various values of Biot's modulus

(25), (27) and (28) the minimum fluid temperature required to produce thermal shock may be written:

$$T_{f_{\min}} = \frac{\sigma_{fs}(1-\mu)}{\alpha E} \left(A + \frac{ck}{Lh} \right) \quad (29)$$

(This equation applies to cylinders and spheres as well. The constants are changed, however.)

Now for the general case of a semi-infinite thick plate heated by a fluid obeying Newton's Law of Cooling, it may be concluded that thermal shock characteristics of materials in general are not inherent material characteristics but are instead a combination of material physical properties, environmental properties and geometry. From the materials viewpoint the environmental properties (T_f and h) and the geometry (L) are not variables. The physical properties of the material (σ_{fs} , α , E , μ , k) are however the variables of concern. The susceptibility to failure by thermal shock then may be diminished by varying these material physical and mechanical properties as follows:

1. decreasing α
2. decreasing E
3. increasing σ_{fs}
4. increasing k
5. decreasing μ

APPROACH TO PROBLEM

The review of the literature indicated that ceramic based composite materials might be developed for application as rocket motor nozzle throat inserts if the problem of the severe thermal shock environment could be overcome. The work indicated in the Literature Survey suggested that ceramic-metal fiber composite materials could possibly be developed for this application. No previous work was found to have been done in the area of ceramic oxide-graphite composites.

The selection of this group of materials was guided by the environment to which they were to be exposed. The high temperatures generated by the engine dictated materials having the highest melting or sublimation points possible. The environment also dictated materials resistant to oxidizing atmospheres and to wear by solid or semisolid particles impinging upon them in the exhaust gas flow.

Graphite and tungsten had been used previously as materials for this application. Both were unsatisfactory as base materials for reasons previously mentioned. They do have several physical, chemical, and mechanical properties which are suitable for dispersed phases in composite materials for use in thermal shock environments. The graphite has a high sublimation point, high thermal conductivity, low modulus of elasticity, good phase stability, and low density. On the other hand, graphite has low fracture strength, relatively high coefficient of thermal expansion and little oxidation resistance which are detrimental to thermal shock resistance. Tungsten has a high melting point, high thermal conductivity, low thermal expansion, good phase stability, fair erosion resistance, and

high fracture strength. These advantages are contrasted against high modulus of elasticity, high density, poor oxidation resistance, and tendency to become embrittled by interstitial atoms such as hydrogen, carbon, oxygen and nitrogen.

The ceramic base material was not expected to have good thermal shock resistance. It was expected to have good oxidation and mechanical erosion resistance and to be compatible with the dispersed phase. Hafnia was selected because of its high melting point and ability to be stabilized in a manner which allowed phase transformation control. The material is similar to zirconia in all aspects and the knowledge of zirconia behavior was applicable to hafnia.

Hafnia has a higher melting point and was subsequently selected rather than zirconia.

The carbides of hafnium and zirconium have significantly higher melting points than do the oxides. Preliminary work with these carbide materials was discontinued due to their tendency to revert to oxide materials in the presence of oxygen at high temperatures. The borides and nitrides of these materials are not readily available.

Initially it was expected that the thermal shock resistance of the hafnia base would be improved by the addition of either graphite or tungsten. The major contribution was expected to be to the thermal conductivity of the composite materials with secondary contributions to the coefficient of thermal expansion and to the strength with tungsten and to the modulus of elasticity with the graphite. The lower strength of the graphite in small additions was not expected to ap-

preciably lower the strength of the composite base material. The tungsten fibers were expected to improve the strength of the composite without appreciably changing the modulus of elasticity.

PROCEDURE

Materials

Materials used in this investigation were obtained from appropriate vendors. All materials were of a readily available form and little or no subsequent processing was performed on them.

The hafnium oxide and yttrium oxide were supplied by Wah Chag Corporation. Both materials were of a -325 mesh particle size and were of a reactor grade quality. The hafnium oxide was in the low temperature monoclinic crystallographic form and was of sufficient purity that no high temperature body centered tetragonal form was retained upon heating above the transformation temperature and subsequent quenching.

The graphite was supplied by Poco Graphite Inc. and was their TRA graphite. The graphite has a -400 mesh particle size and contained less than five parts per million impurities. The tungsten wire was supplied by General Electric Company and was alloyed with three percent rhenium. Microprobe analysis showed the material to contain a small undetermined amount of iron. The wire was supplied with a five thousandths of an inch diameter and was chopped into lengths of approximately one eighth of an inch corresponding to a 25:1 aspect ratio.

Fabrication

Specimens were fabricated by the vacuum hot pressing technique. Cylindrical specimens varying in diameter from one inch to one-half inch and height from one inch to one-fourth of an inch were formed by induction heating in graphite dies. The temperature was maintained at twenty-one hundred degrees centigrade in a vacuum of less than ten microns

of mercury. Pressures up to ten thousand pounds per square inch were applied during hot pressing.

The tapered graphite dies were machined from Basic Carbon's Graphite A for pressures to four thousand pounds per square inch and Poco Graphite HP-1 for pressure above those. All rams were fabricated from Poco Graphite HP-1 graphite. Tantalum end shields were placed between the ram and specimens to facilitate removal of specimens and to retard carbon diffusion into the specimens.

Pressure was applied by a hydraulic press through a bellows assembly into a vacuum body which was evacuated by a six inch diffusion pump backed by a one hundred and fifty standard cubic foot per minute mechanical pump. The die was located inside a graphite and silica cloth lined induction coil within the vacuum body. The temperature of the outside surface of the die was read by optical pyrometer through a series of sight ports through the vacuum body, coil, and insulation. Die displacement readings for determination of densification termination was measured by a variable differential transducer and the output was read on a strip chart recorder.

Stabilization

Solid solutions of hafnia and yttria were obtained during vacuum hot pressing. At a temperature of twenty-one hundred degrees centigrade it was found that the solid solution was obtained before densification was completed such that both operations could be performed simultaneously.

The degree of stabilization was established by an x-ray technique following Buckley (9), and Dewez and Odell (11). This method involves

measuring the relative intensities of the (111) and $(1\bar{1}\bar{1})$ monoclinic lines and the (111) body centered tetragonal line. The ratios of the three possible combinations give directly from tabulated data the degree of stabilization in terms of the percentage of tetragonal phase present. In general, the degree of stabilization was determined on the end surfaces of specimens which subsequently were exposed to the various tests.

Density

Density determinations were by ASTM Designation B 311-58 entitled Standard Method of Test for Density of Cemented Carbides (2) with no modifications. This technique is the immersion technique and distilled water was the immersion fluid used.

Coefficient of Linear Thermal Expansion

A dilatation interferometer was employed in establishing the coefficient of linear thermal expansion. ASTM Designation C 327-53 entitled Standard Method of Test for Linear Thermal Expansion of Whiteware was followed (1). The tetrahedral specimens were approximately two-tenths of an inch in height. Filtered monochromatic light from the mercury spectrum having a wavelength of 0.5461 microns was employed. The heating rate of the electric furnace was controlled manually to approximately three degrees centigrade per minute. The temperature was measured by use of a chromel-alumel thermocouple and recorded by an automatic electronic recorder. Expansion was measured in the range of one hundred to three hundred degrees centigrade. Linear thermal expansion was plotted against temperature to check for linearity of expansion

in the temperature range investigated. Air correction factors given in the specifications were used to correct for the wave length of the light in air at various temperatures.

Coefficient of Thermal Conductivity

Thermal conductivity of the composite materials was determined by the steady state method described by Haacke and Spitzer (15) in an apparatus designed and constructed by the author. The conductivity is given by

$$K = \epsilon \frac{C \lambda F}{q} \frac{T_x^4 - T_0^4}{T_1 - T_x}$$

where K is the conductivity; ϵ is the emissivity of a heat sink having a surface area F and a uniform temperature T_x . The cross sectional area of the cylindrical specimen is given by q and its length is λ . The uniform temperature of the heat source is T_1 and the temperature of the black body universe enclosing heat source, specimen and heat sink is T_0 . C is the Stephen-Boltzman constant.

The black body universe is a graphite ink coated copper vacuum body evacuated to less than one micron of mercury by a two stage mechanical pump to minimize heat loss from the specimen and heat sink by conduction or convection. This body is immersed in a constant temperature water bath. Temperatures were measured with chromel-alumel thermocouples and potentiometer accurate to one-hundredth of a millivolt. Thermocouples were located in the heat source and heat sink and on the black body universe. Specimens were heated by a chromel heater mounted in the copper heat source. The heat sink was constructed of pure silver and had a graphite

ink coating to raise the emissivity to approximately ninety-nine one-hundredths. Thermal contact between specimens and heat sources and sink was enhanced by a thin layer of silicone vacuum grease and radiation heat loss from the specimen was minimized by use of a polished gold radiation heat shield.

The unit was calibrated with specimens of Corning 7740 glass and International Nickel Company Monel 400 at a source temperature of 350 degrees Kelvin. Measurements of temperature were made at the end of six hours exposure to assure thermal equilibrium and the heat source was maintained at a constant temperature of three-hundred and fifty degrees Kelvin for all specimens. The thermal gradient between the heat source and heat sink at equilibrium ranged from five to ten degrees Kelvin depending upon specimen length.

Modulus of Elasticity and Compressive Fracture Strength

Specimens having a diameter of one-half inch and a height of one-fourth inch were used to determine the modulus of elasticity and compressive fracture strength. The small height to diameter ratio was employed to reduce the effect of barreling on strain measurements obtained from SR-4 strain gauges cemented to each specimen.

Specimens were loaded in compression with a conventional tensile-compressive testing machine. Strain was measured at intervals of two hundred and fifty pounds static load between one thousand and three thousand pounds load. Strain in micro inches per inch were read from the one hundred and twenty ohm gauges having a gauge factor of 2.05 by use of a balanced bridge potentiometer. Polyester films were placed between the

specimens ends and the compression rams to reduce sliding friction on the self aligning heads.

Loading was cycled a minimum of three times to achieve reproducibility of strain readings. The values of stress were plotted against strain to assure linearity.

Compressive fracture stress is given as that stress at which the first crack was observed to cause a discontinuity in the load.

Thermal Shock

Specimens were tested for thermal shock resistance by exposing them to nitrogen plasma generated by non-transferred arc at a temperature of approximately nine thousand degrees centigrade for a period of five seconds and subsequently allowing them to cool slowly in static air. The specimens, nominally one-half inch in diameter and three-eighths inch in height, were heated from one end by the plasma stream emerging with a diameter of one-fourth of an inch and a flow rate of ninety to one hundred and ten standard cubic foot per hour. The criteria for failure was either total disintegration of the specimen or the presence of one or more macroscopic cracks traversing a portion or all of the specimen. The specimens were not thermally cycled.

Stress distributions for this method of heating are given by Sharma (26) as:

$$\sigma_r = \sigma_\theta = -\alpha ET \left[1 - \frac{Z}{\sqrt{a^2 + Z^2}} \right]$$

where T is the uniform temperature of the disc, Z is length from surface on cylindrical axis and a is the radius of the heated zone. The expres-

sion is limited because it is assumed that the body remains at a constant uniform temperature of zero and that the coefficient of surface heat transfer is infinite. Fridman (13) expanded the Sharma expression to include the maximum shearing stresses in the unheated zone. These stresses are at an angle of 45° to the cylindrical axis and are given by

$$\tau = \frac{\alpha ET}{2} \frac{a^2}{r^2} .$$

In three dimensions this expression represents the stresses laying on a surface produced by rotating a line inclined at 45° to the cylindrical axis about the cylindrical axis such that that surface cuts the end surface of the cylinder at a uniform distance, a , from the cylindrical axis.

Although the coefficient of surface heat transfer of nitrogen plasma has not been determined,¹ it is believed to be high enough to use the above expressions for determination of maximum stresses produced by plasma heating.

¹Bennett, W. H. 1970. Personal communication. Department of Physics, North Carolina State University at Raleigh.

RESULTS AND DISCUSSION OF RESULTS

Coefficient of Thermal Expansion

The degree of stabilization of yttria stabilized hafnia did not strongly affect the coefficient of linear thermal expansion as shown in Figure 1. Increases in the density of hafnia at a given degree of stabilization increased the coefficient of linear thermal expansion by a relatively small amount. The broken lines in Figure 2 and subsequent figures represent the limits of the scattering of the observed data due to inaccuracies in determining degree of stabilization and variations in densities when hot pressed at a given pressure.

For hafnia an important expansion criteria is the phase inversion from monoclinic to body centered tetragonal near two thousand degrees centigrade. If the material is to be exposed to temperatures sufficiently high to induce the phase inversion, the lower thermal expansion of the monoclinic phase can be negated by this inversion such that an intermediate degree of stabilization may be more advantageous. Thermal shock testing of the base material indicated that fifty per cent stabilization was an optimum degree. Deviations of ten per cent higher or lower resulted in central cracking upon exposure to the thermal shock environment. Larger deviations resulted in both central cracking and ring cracking due to the shear stresses. These values were generally true for all densities investigated which ranged from 88 to 96 per cent of theoretical density.

Addition of graphite to the base material increased the coefficient of linear thermal expansion slightly. Figure 3 shows that the coefficient approaches that of the pure graphite (8.1×10^{-6} per °K). Likewise, additions of tungsten fiber lowers the coefficient of linear thermal expansion

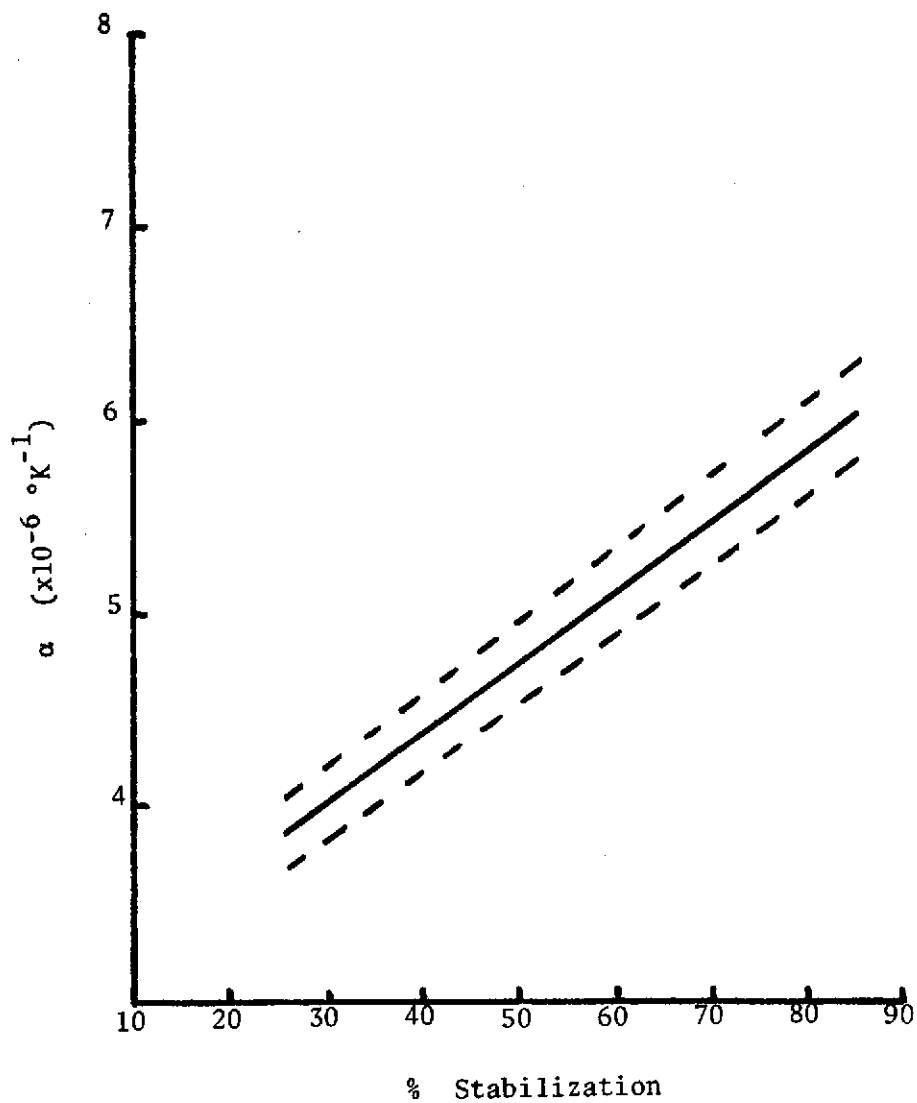


Figure 2. Coefficient of linear thermal expansion vs. percent stabilization in yttria stabilized hafnia hot pressed at one thousand pounds per square inch

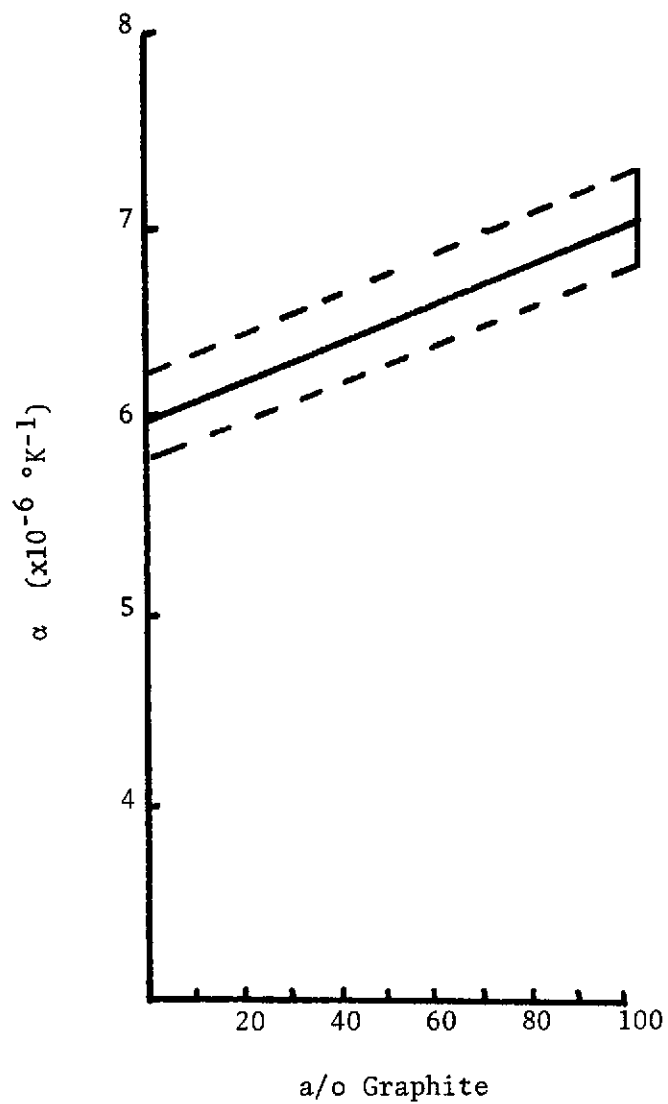


Figure 3. Coefficient of linear thermal expansion vs. atomic percent graphite in eighty five percent yttria stabilized hafnia hot pressed at ten thousand pounds per square inch

as shown in Figure 4. Again, the coefficient approaches that of tungsten (2.5×10^{-6} per $^{\circ}\text{K}$). On this basis, addition of graphite would appear to be detrimental to thermal shock resistance. The influence of both additions will be shown to be secondary to other considerations discussed below.

Coefficient of Thermal Conductivity

The degree of stabilization of yttria stabilized hafnia did not strongly affect the coefficient of thermal conductivity as shown in Figure 5. The data does however support the only data available in the literature (12).

Additions of graphite having a coefficient of thermal conductivity of 1.4 watts per centimeter degree Kelvin did not significantly increase the coefficient of the resulting composite as shown in Figure 6. These data indicate that even at large atomic percentages of graphite, the graphite is a dispersed phase with the hafnia being the controlling matrix. At lower percentages of graphite this conjecture is supported by the small particle size of the graphite. In general, however, no satisfactory hypothesis for this behavior has been drawn.

Additions of tungsten having a coefficient of thermal conductivity of 1.7 watts per centimeter degree Kelvin lowers the conductivity initially and subsequently increases conductivity as shown in Figure 7. The decrease in thermal conductivity with additions to approximately fifteen weight per cent can be attributed to a decrease in percentage of theoretical density. Measurements of conductivity of porous materials made in vacuum may be lower than those made in a fluid environment and deviation

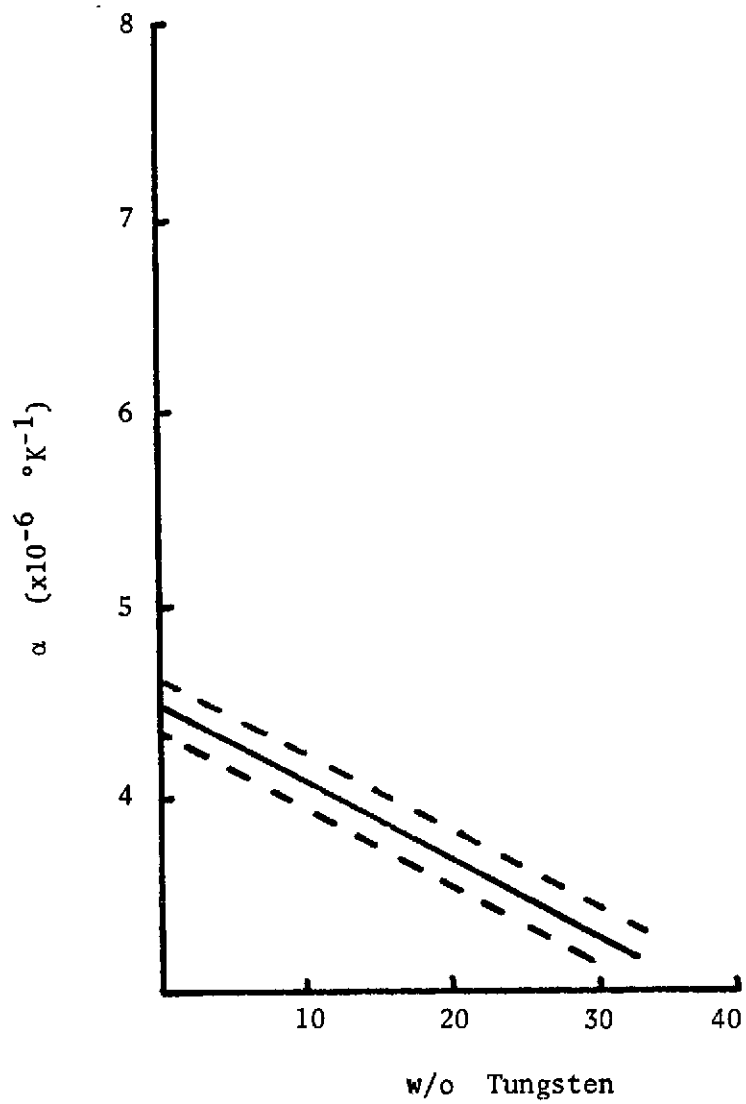


Figure 4. Coefficient of linear thermal expansion vs. weight percent tungsten in seventy percent yttria stabilized hafnia hot pressed at eight thousand pounds per square inch

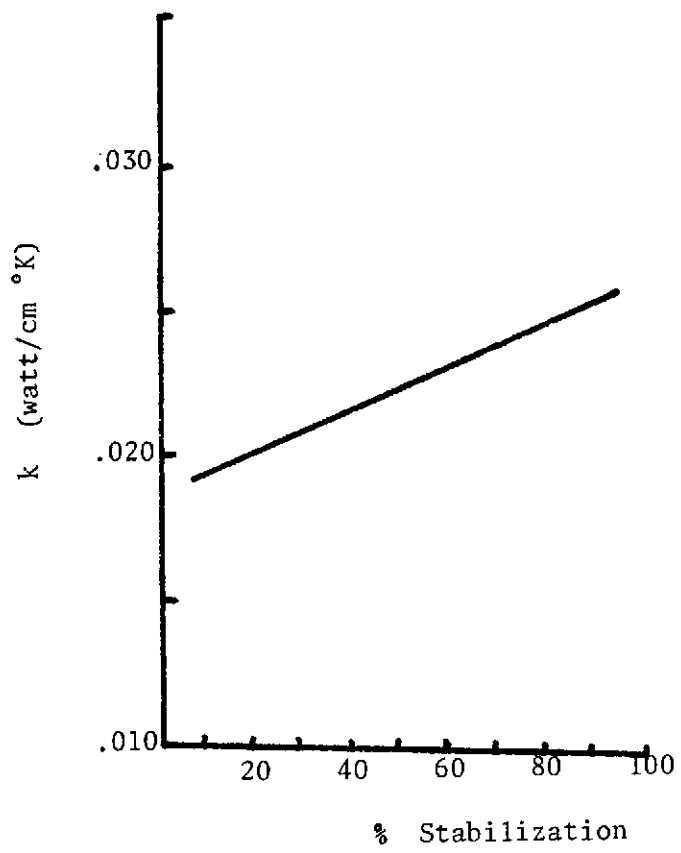


Figure 5. Coefficient of thermal conductivity vs. percent stabilization in yttria stabilized hafnia hot pressed at ten thousand pounds per square inch

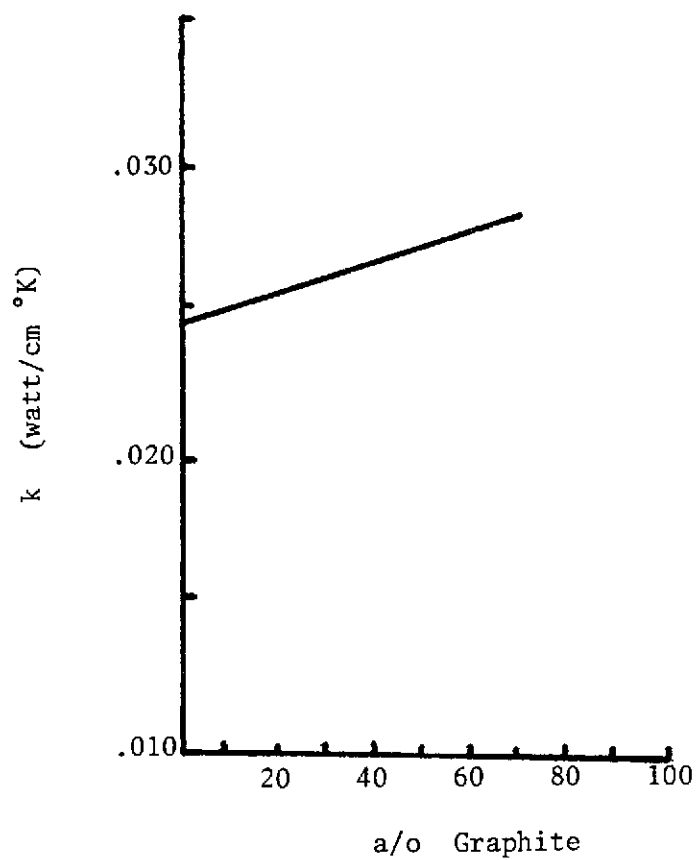


Figure 6. Coefficient of thermal conductivity vs. atomic percent graphite in eighty five percent yttria stabilized hafnia hot pressed at ten thousand pounds per square inch

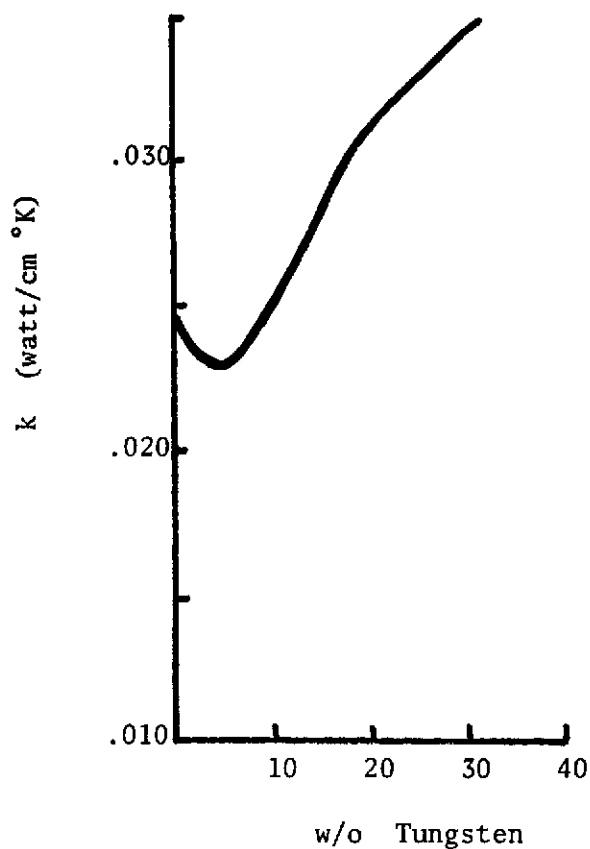


Figure 7. Coefficient of thermal conductivity vs. weight percent tungsten in seventy percent yttria stabilized hafnia hot pressed at eight thousand pounds per square inch

of conductivity due to porosity may be accentuated (12). The effect of this decrease in density on modulus of elasticity and fracture stress is, however, more pronounced.

Modulus of Elasticity and Compressive Fracture Stress

Density was found to have a drastic effect on modulus of elasticity and compressive fracture stress. The base material hot pressed at pressures up to four thousand pounds per square inch had moduli of elasticity of approximately six million pounds per square inch and compressive fracture stresses of approximately forty thousand pounds per square inch. These specimens had a density of approximately eighty eight percent of theoretical.

Specimens hot pressed at eight thousand and ten thousand pounds per square inch were found to have a modulus of approximately sixty seven million pounds per square inch and a compressive fracture stress of approximately one hundred and twenty thousand pounds per square inch. These specimens had density of approximately ninety six percent of theoretical.

Specimens were not hot pressed at pressures between four thousand and eight thousand pounds per square inch and no consistent data is presented for the base material in this range. From the above data, however, the effect of density on thermal shock resistance of the base material may be related primarily to the ratio of the compressive fracture stress to the modulus of elasticity. The low density material had a ratio of 6.6×10^{-3} , while the high density material had a ratio of 1.7×10^{-3} . On the basis of the theory the lower density hafnia would have the greater thermal shock resistance due to the higher ratio.

Additions of any amount of graphite to the base material lowered both the modulus of elasticity and the compressive fracture stress as shown in Figures 8 and 9. The modulus was lowered to approximately ten million pounds per square inch and the compressive fracture stresses, to approximately fifteen thousand pounds per square inch. These data correspond to a ratio of 1.5×10^{-3} which indicates lower thermal shock resistance than that of the base material.

Tungsten additions yielded behavior of the moduli of elasticity and and fraction stresses similar to that of the coefficient of thermal conductivity. Additions of ten to twenty weight percent significantly lowered both the modulus of elasticity and to a lesser degree the compressive fraction stress as shown in Figures 10 and 11. Larger additions increased both parameters again.

The modulus of elasticity of the tungsten is approximately sixty million pounds per square inch. In Figure 10 the composites moduli are shown to approach that of the tungsten. This value is, of course, lower than that of the hafnia base material. Also of importance is the strength of the composites containing additions of tungsten.

The tensile fracture stress of the tungsten material is approximately two hundred and twenty thousand pounds per square inch which is considerably higher than that of the base materials. From Figure 11 it may be observed that addition of tungsten above twenty weight percent not only increased the modulus but also significantly contributed to the strength of the composite such that the compressive fracture stress of the base material and the tensile fracture stress of the tungsten is approached.

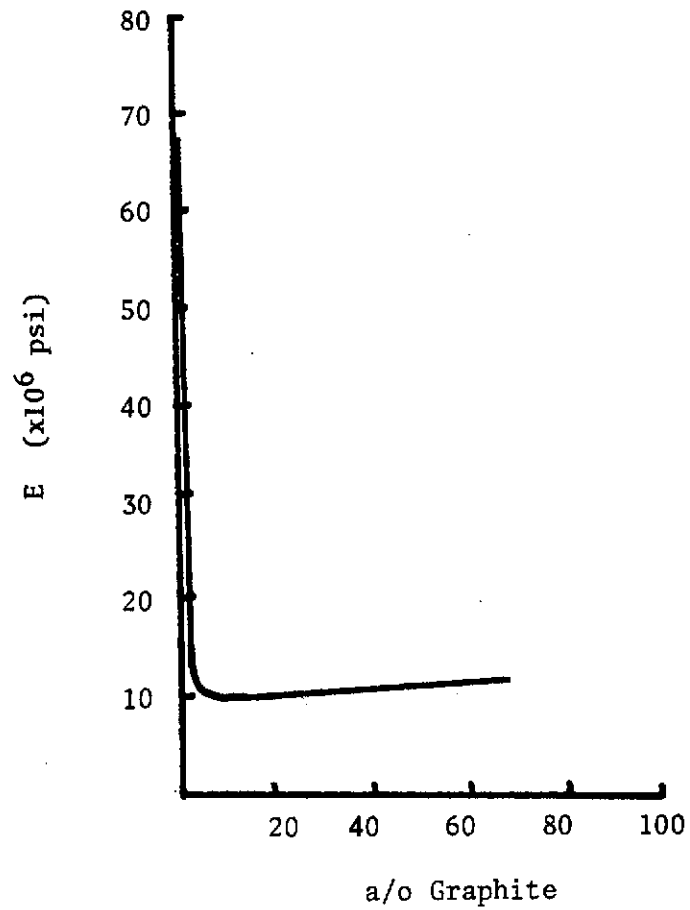


Figure 8. Modulus of elasticity vs. atomic percent graphite in eighty five percent yttria stabilized hafnia hot pressed at ten thousand pounds per square inch

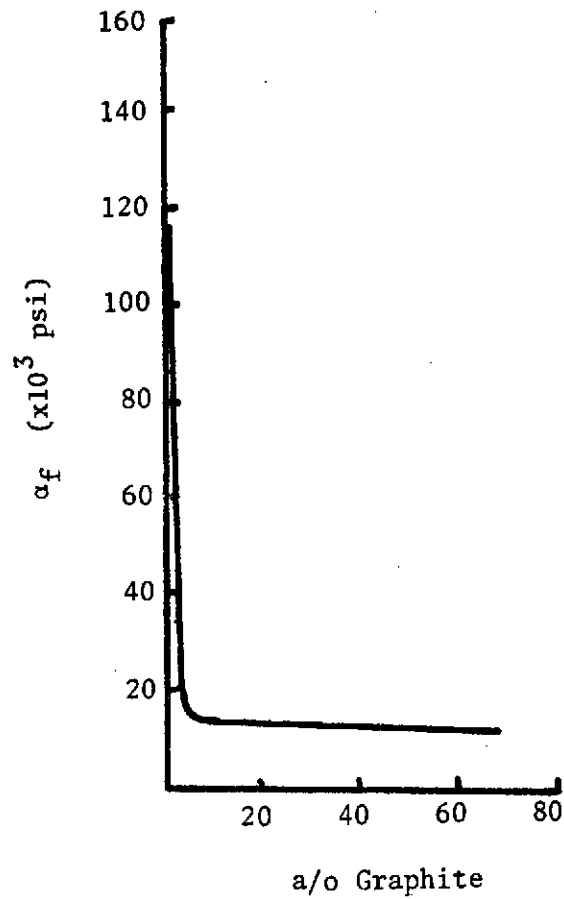


Figure 9. Compressive fracture stress vs. atomic percent graphite in eighty five percent yttria stabilized hafnia hot pressed at ten thousand pounds per square inch

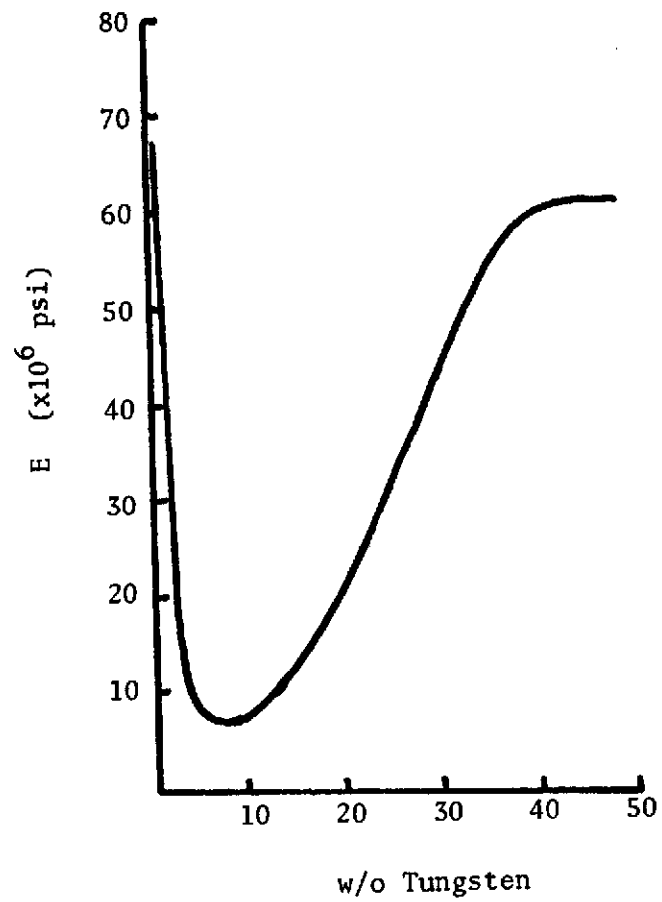


Figure 10. Modulus of elasticity vs. weight percent tungsten in seventy percent yttria stabilized hafnia hot pressed at eight thousand pounds per square inch

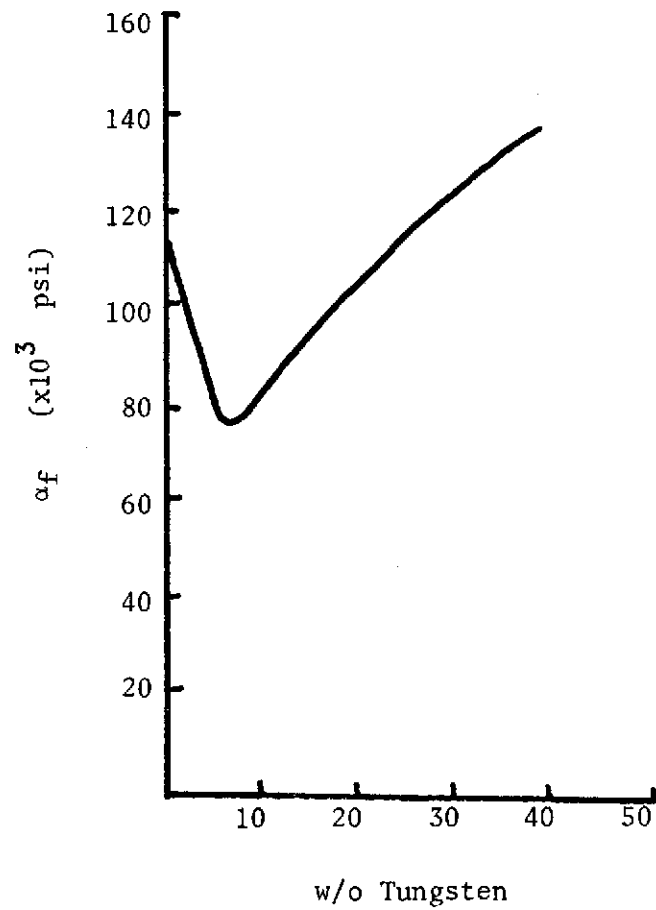


Figure 11. Compressive fracture stress vs. weight percent tungsten in seventy percent yttria stabilized hafnia hot pressed at eight thousand pounds per square inch

Of more significance is the ratios of the moduli and fracture stress shown in Figure 12. These range from the ratio of 1.7×10^{-3} for the high density base material to 12.0×10^{-3} for approximately fifteen weight percent tungsten to approximately 2.0×10^{-3} for large addition of tungsten. Assuming that the thermal shock model presented is correct, then addition of approximately fifteen weight percent tungsten to the base material hot pressed at eight thousand pounds per square inch should increase the thermal shock resistance an order of magnitude. This also represents a two fold increase over that of the low density base material. These assertions are based upon the assumption that for these materials, the changes in coefficients of thermal expansion and thermal conductivity are negligible.

Thermal Shock

Initially, base materials of the high and low densities were exposed to the described thermal stress environment. Of these materials, those stabilized to fifty percent exhibited the best thermal shock resistance. As discussed previously, deviations in stabilization of ten percent higher or lower yield central compressive stress cracking which originated from the heated surface. Larger deviations also resulted in the ring shear stress cracking. In accordance with the compressive fracture stress to modulus of elasticity ratio, the cracking was more pronounced in the higher density specimens.

Additions of any amount of graphite to the base material resulted in explosive thermal shock failure for all specimens. Fragments which could be found of exposed material indicated cracking by both compressive and shear stresses. In general the thermal shock resistance of these materials

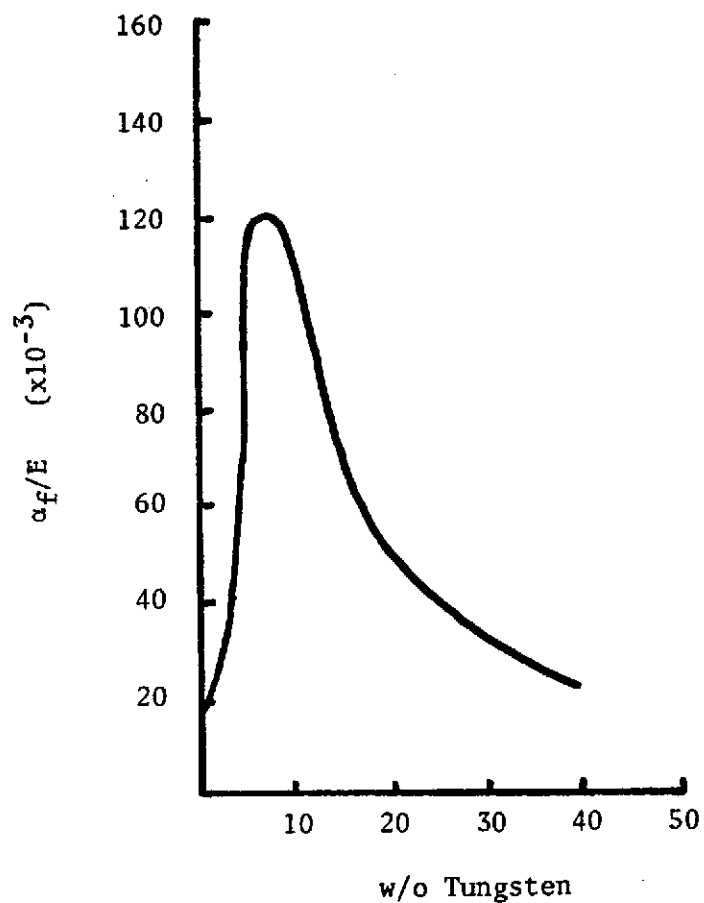


Figure 12. Ratio of compressive fracture stress to modulus of elasticity vs. weight percent tungsten in seventy percent yttria stabilized hafnia hot pressed at eight thousand pounds per square inch

was inferior to that of the base material. This again is indicated by the low compressive fracture stress to modulus of elasticity ratio.

Additions of tungsten, in general, increased thermal shock resistance. No specimen containing tungsten tested exhibited the ring shear stress cracks and only specimens containing amounts of tungsten greater than twenty five weight percent tungsten had any compressive stress cracks. No specimen containing ten to twenty weight percent tungsten was cracked by thermal exposure.

As a supplementary test, specimen discs having a diameter of one inch and a thickness of one-half inch were initially exposed to plasma without cracking. These specimens were subsequently quenched from one thousand degree centigrade into ice water ten times without any cracking. These materials had the highest compressive fracture stress to modulus ratio of any material tested, which may explain the superior thermal shock resistance.

CONCLUSION

1. The thermal shock resistance of the yttria stabilized hafnia can be maximized by stabilizing to fifty percent of the high temperature phase. Lowering the density also increased the thermal shock resistance.
2. The macroscopic modulus of elasticity and compressive fracture stress of yttria stabilized hafnia has been shown to be very sensitive to changes in density.
3. Addition of any amount of graphite to the base material is detrimental to thermal shock resistance. The slight increase in thermal conductivity and significant decrease in modulus of elasticity is more than offset by the drastic decrease in fracture stress and slight increase in thermal expansion.
4. Addition of tungsten wire to the base material can significantly increase thermal shock resistance. The most significant effect in the lowering of the modulus of elasticity by decreasing the density while acting as a strengthening component. The tungsten wire in large quantities can significantly increase thermal conductivity and compressive fracture stress and decrease thermal expansion. These increases are, however, offset by the increase in modulus of elasticity which approaches that of the tungsten metal itself.
5. Knowledge of the macroscopic material parameters thermal conductivity, thermal expansion, modulus of elasticity, and fracture stress have been shown to be helpful in predicting the thermal shock resistance of ceramic based composite materials. In general for ceramic based material such as those investigated, the ratio of the compressive

fracture stress to the modulus of elasticity can be used to predict the thermal shock behavior of the material if the coefficient of thermal expansion and thermal conductivity are not significantly changed.

PROPOSALS FOR FUTURE WORK

This investigation of the effect of macroscopic parameters on thermal shock resistance opens several avenues for further investigation into these and similar ceramic-metal composites materials. In general, an investigation into the microscopic aspects of these materials is warranted. From the macroscopic point of view, the conclusion concerning the correlation of the compressive fracture stress to modulus of elasticity ratio upon the thermal shock resistance can be further investigated.

The following macroscopic investigations are suggested:

1. Introduction of ten to twenty weight percent tungsten powder and tungsten machine turnings into composites of low density to determine the effect of dispersed phase size and shape upon both modulus of elasticity and compressive fracture stress.
2. Substitution of both tantalum and iridium wire in additions of ten to twenty weight percent to establish the effect of moduli different from the tungsten modulus on materials having approximately the same fracture strength, thermal conductivity and thermal expansion. Tantalum has a low modulus (approximately twenty five million pounds per square inch) such that large amounts of tantalum may be added to increase strength without large increase in the macroscopic moduli of elasticity. Iridium with the high modulus (approximately eighty million pounds per square inch) should have the opposite effect at higher concentrations.

The following microscopic investigations are suggested:

1. Investigation of fiber to ceramic bonding.
2. Investigation of composite effects due to dispersed phase

orientation, topology, concentration, and concentration distribution, and particle size and shape.

3. Investigation into micro-elasticity and crack initiation, propagation, and interaction effects upon compressive fracture stress and modulus of elasticity.

REFERENCES

1. American Society for Testing Materials. 1956. Standard method of test for linear expansion of whiteware. ASTM Designation C 327-56.
2. American Society for Testing Materials. 1958. Standard method of test for density of demented carbides. ASTM Designation B 311-58.
3. Arias, A. 1964. Investigation of thermal shock resistance of zirconia with metal additions. NASA TN D-2464.
4. Arias, A. 1966. Thermal shock resistance of zirconia with 15 moles percent titanium. J. Am. Cer. Soc., 49(6):334-338.
5. Baskin, Y., Arenberg, C. A., and Handwerk, J. H. 1959. Thoria reinforced by metal fibers. Am. Cer. Soc. Bull., 38(7):345-348.
6. Bert, C. W. and Hyler, W. S. 1962. Design consideration in selecting materials for large solid-propellant rocket-motor cases. DMIC Report 180.
7. Blakeley, T. H. and White, A. E. S. 1960. Improvement of refractories by the incorporation of metals. Chem. and Ind. (London), 12:305-306.
8. Boley, B. and Weiner, J. 1960. Theory of Thermal Stresses. John Wiley and Sons, Inc., New York.
9. Buckley, J. D. 1967. Stabilization of the phase transformations in hafnium oxide. Unpublished PhD thesis, Department of Ceramic Engineering, Iowa State University, Ames, Iowa.
10. Carslaw, H. and Jaeger, J. 1959. Conductivity of Heat in Solids. Clarendon Press, Oxford, England.
11. Duwez, P. and Odell, F. 1959. Quantitative analysis of cubic and monoclinic zirconia by x-ray diffraction. J. Am. Cer. Soc., 32(5):130.
12. Flynn, D. R. 1969. Thermal conductivity of ceramics, pp.63-123. In J. B. Wachtman (ed.), Mechanical and Thermal Properties of Ceramics. National Bureau of Standards, Special Publication No.303.
13. Fridman, Ya. 1964. Strength and Deformation in Nonuniform Thermal Fields. Consultants Bureau Enterprises, Inc., New York.
14. Gatewood, B. 1957. Thermal Stress. McGraw Hill Book Company, New York.

15. Haacke, G. and Spitzer, D. P. 1965. Method for thermal conductivity measurements on solids. *J. Sci. Instrum.*, 42:702.
16. Heisler, M. P. 1953. Transient thermal stresses in slabs and circular pressures vessels. *J. Appl. Mech.*, 20(6):261-269.
17. Hlinka, J. H., Landau, H. G., and Paschkis, V. 1957. Charts on elastic thermal stresses in heating and cooling of slabs and cylinders. ASME paper No. 57-A-238. Entire.
18. Johns, D. 1965. *Thermal Stress Analysis*. Pergamon Press, Inc., Oxford, England.
19. Johnson, J. R., Signorelli, R. A., and Freche, J. C. 1966. Performance of rocket nozzle materials with several solid propellants. NASA TN D-3428.
20. Kammer, E. W., Smith, N., and Olcott, E. 1963. Thermal shock evaluation of refractory materials on rocker nozzle inserts. NRL Report No. 6005.
21. Manson, S. S. 1961. Thermal stresses and thermal shock, pp.393-418. *In* J. E. Dorn, (ed.), *Mechanical Behavior at Elevated Temperatures*. McGraw Hill Book Company, Inc., New York.
22. Northam, G. B. 1968. Effects of steady-state acceleration on combustion characteristics of an aluminized composite solid propellant. NASA TN D-4914.
23. Peterson, D. A. 1967. Experimental evaluation of high-purity-silica reinforced ablative composites on nozzle sections of 7.8 inch - (19.3 cm) diameter throat storable-propellant rocket engine. NASA TM X-1391.
24. Peterson, D. A. and Meyer, C. L. 1966. Experimental evaluation of several ablative materials as nozzle sections of a storable-propellant rocket engine. NASA TM X-1223.
25. Shames, I. H. 1964. *Mechanics of Deformable Solids*. Prentice-Hall, Inc., Englewood Cliffs, New Jersey.
26. Sharma, R. 1956. Thermal stresses in infinite elastic disks. *J. Appl. Mech.*, 23(4):527.
27. Southern Research Institute. 1962. The thermal properties of 26 solid materials to 5000° F or their destruction temperature. ASD-TDR-62-765, Contract AF-33(616)-7319.

28. Swica, J. J., Hoskyns, W. R., Goss, B. R., Connor, J. H., and Tinklepaugh, J. R. 1960. Metal fiber reinforced ceramics. WACD Technical Report No. 58-452, Part II.
29. Tinklepaugh, J. R., Goss, B. R., Hoskyns, W. R., Connor, J. H., and Button, D. D. 1960. Metal fiber reinforced ceramics. WACD Technical Report No.58-452, Part III.
30. Truesdale, R. S., Swica, J. J., and Tinklepaugh, J. R. 1958. Metal fiber reinforced ceramics. WACD Technical Report No. 58-452, Part I.
31. Walton, J. D. and Poulos, N. E. 1962. Slip cast metal fiber reinforced ceramics. Am. Cer. Soc. Bull., 41(11):778-780.
32. Winter, J. M., Plewes, L. D., and Johnston, J. R. 1966. Experimental evaluation of throat inserts in a storable-propellant rocket engine. NASA TM X-1266.
33. Wong, E. Y. 1968. Solid rocket nozzle design summary. AIAA Paper No.68-655. American Institute of Aeronautics and Astronautics, New York.

1474-28238

MODEL FOR THERMAL STRESS RESISTANCE OF TRULY ELASTIC
MATERIALS CONTAINING MORE THAN ONE CRACK

by

LYNN DAVID LINEBACK

A thesis submitted to the Graduate Faculty of
North Carolina State University at Raleigh
in partial fulfillment of the
requirements for the Degree of
Doctor of Philosophy

DEPARTMENT OF MATERIALS ENGINEERING

RALEIGH

1 9 7 3

APPROVED BY:

Chairman of Advisory Committee

BIOGRAPHY

Lynn D. Lineback was born 26 June 1946 in Forsyth County, North Carolina. He lived in the Pfafftown, North Carolina community of that county and graduated from the Winston-Salem/Forsyth County School System before entering North Carolina State University in Raleigh, North Carolina in the fall of 1964. He received a Bachelor of Science degree in Metallurgical Engineering in 1969 and a Master of Science degree in Materials Engineering in 1971 from that University. He continued his education there and was admitted to candidacy for the Doctor of Philosophy degree in 1972.

ACKNOWLEDGEMENTS

The conviction for, confidence in, and patience with the author during his graduate career as well as in the preparation of this dissertation, by his major professor, Charles R. Manning, Jr., is gratefully acknowledged. The contributions of both an educational and advisory nature to the author by Professor A. A. Fahmy of the advisory committee is especially appreciated. Appreciation is also extended to the other members of the committee, Professors E. M. Schoenborn and R. F. Stoops.

Thanks are extended to a number of people too numerous to name who performed laboratory work over the past four years. The tolerance and patience of the author's wife, Tess, is also gratefully acknowledged.

The financial assistance of the National Aeronautics and Space Administration in the form of two grants is acknowledged. The confidence and aid of R. D. English and V. D. Crowder of the Scout Project Office, NASA Langley, which was essential in obtaining and twice extending one grant, NGR 34-002-108, subsequently supervised by J. D. Buckley and J. P. Howell, is especially appreciated. The aid of W. D. Boatwright of the Hypersonic Vehicles Division, NASA Langley, in obtaining the second grant, NGR 30-002-167, (also monitored by J. P. Howell and J. D. Buckley) is also appreciated.

TABLE OF CONTENTS

	Page
LIST OF TABLES	v
LIST OF FIGURES	vi
TABLE OF NOMENCLATURE	ix
INTRODUCTION	1
MODEL FOR THERMAL STRESS RESISTANCE OF A TRULY ELASTIC MATERIAL CONTAINING MORE THAN ONE CRACK	3
COMPATIBILITY OF THE MODEL WITH EXISTING THERMAL SHOCK RESISTANCE MODELS	30
APPLICATION OF THE MODEL TO THE DATA	36
SUMMARY AND CONCLUSIONS	90
LIST OF REFERENCES	94

LIST OF TABLES

	Page
1. Physical property data for firebricks.	59
2. Physical property data for alumina, zirconia, and magnesia	68
3. Properties of various ceramic materials	71
4. Properties of alumina ceramics	72

LIST OF FIGURES

	Page
1. Lines of constant Griffith energy on a grid of number of cracks <u>vs.</u> crack size	8
2. Lines of constant numbers of cracks on a grid of Griffith energy <u>vs.</u> crack size	9
3. Lines of constant crack size on a grid of Griffith energy <u>vs.</u> number of cracks	10
4. The effect of number of cracks on the locus of the Griffith criteria	13
5. The effect of surface energy on the locus of the Griffith criteria	16
6. The effect of the intrinsic modulus of elasticity on the locus of the Griffith criteria	17
7. Analysis of the Griffith criteria for a strong material at constant strain	19
8. Analysis of the Griffith criteria for a weak material at constant strain	21
9. Analysis of the Griffith criteria at constant stress	22
10. Griffith strain <u>vs.</u> crack size for various numbers of cracks	27
11. Griffith strain <u>vs.</u> crack size for various surface energies	28
12. Minimum thermal strain required to initiate crack propagation as a function of crack length and crack density	33
13. Strength <u>vs.</u> quenching temperature differential	38
14. Applied temperature differential <u>vs.</u> percentage decrease in modulus of elasticity for zircon	41
15. Applied temperature differential <u>vs.</u> percent loss in strength of zircon after thermal shock exposure	42

LIST OF FIGURES (continued)

	Page
16. Relationship between mechanical strength and spalling loss	44
17. Relationship between modulus of elasticity and spalling loss	45
18. Relationship between coefficient of linear thermal expansion and spalling loss	46
19. Relationship between σ/E and spalling loss	49
20. Relationship between $\sigma/E\alpha$ and spalling loss	50
21. Effect of thermal shock on fracture strength	52
22. Experimental data showing relation between final strength and percent reduction in strength	54
23. Experimental data showing relation between initial strength and percent reduction in strength	55
24. Experimental data showing relation between initial and final strength	56
25. Initial transverse strength <u>vs.</u> final transverse strength after thermal shock exposure for various triaxial bodies	57
26. Modulus of rupture <u>vs.</u> modulus of elasticity for selected fireclay plastic refractories	61
27. Modulus of rupture <u>vs.</u> percent spalling loss for selected fireclay plastic refractories	62
28. Modulus of elasticity <u>vs.</u> percent spalling loss for selected plastic refractories	64
29. Strain to failure <u>vs.</u> percent spalling loss for selected fireclay plastic refractories	65
30. Number of cycles to failure <u>vs.</u> critical temperature differential for selected firebricks	67
31. Correlation between thermal-stress-resistance parameter and critical temperature for various substances	73

LIST OF FIGURES (continued)

	Page
32. Correlation between thermal-stress-resistance parameter and critical temperature for aluminas	75
33. Modulus of rupture <u>vs.</u> critical temperature differential for sagger clays	77
34. Modulus of elasticity <u>vs.</u> critical temperature differential for sagger clays	78
35. The relationship between modulus of elasticity and transverse strength determined at room temperature	79
36. Resistance of saggors to spalling	80
37. Thermal conductivity of zirconium oxide with 15 percent titanium as a function of temperature compared with that of stabilized zirconia	83
38. Ratio of compressive fracture stress to modulus of elasticity <u>vs.</u> weight percent tungsten in seventy percent yttria stabilized hafnia	86
39. Modulus of elasticity <u>vs.</u> weight percent tungsten in seventy percent yttria stabilized hafnia	87
40. Compressive fracture stress <u>vs.</u> weight percent tungsten in seventy percent yttria stabilized hafnia	88

TABLE OF NOMENCLATURE

α	(alpha), coefficient of linear thermal expansion
c	crack half width
ΔT	(delta T), temperature differential
ΔT_c	(delta T sub c), critical temperature differential
ΔT_{max}	(delta T sub max), maximum temperature differential
E	modulus of elasticity
E_{eff}	effective modulus of elasticity
E_{int}	intrinsic modulus of elasticity
ϵ	(epsilon), strain
ϵ_g	(epsilon sub g), Griffith strain
ϵ_{ts}	(epsilon sub ts), strain produced by a thermal stress
γ	(gamma), surface energy as defined by Griffith
GE	Griffith energy
GE_{min}	(GE sub min), minimum Griffith energy
l_f	(l sub f), final length of a stressed body
l_i	(l sub i), initial length of an unstressed body
M	number of cracks per cubic cm.
N	number of cracks per square cm.
ν	(nu), Poisson's ratio
π	(pi), constant of 3.141
SE	strain energy
σ	(sigma), stress
σ_{fs}	(sigma sub fs), tensile fracture stress
σ_g	(sigma sub g), Griffith stress
w_t	(w sub t), total amount of work
X	defined energy factor

INTRODUCTION

Designers are often confounded when faced with the chore of selecting materials for use in oxidizing thermal shock environments. Materials such as metals which have excellent thermal shock resistance as a result of their excellent thermal conductivities are, in general, unsatisfactory due to their lack of oxidation resistance. Materials such as polymers are often unsatisfactory due to their low melting or decomposition temperatures. Other materials such as oxide ceramics can tolerate both the high temperatures and the oxidizing atmospheres. They lack thermal shock resistance generally because of their lower thermal conductivities and lack of plasticity.

It is the purpose of this paper to present a model, a priori, for the thermal shock resistance of elastic materials such as oxide ceramics; to apply data, posteriori, to the model to establish its validity; and to make generalized suggestions for the improvement of the thermal shock resistance of elastic materials such as oxide ceramics. Limiting the discussion to brittle elastic materials, the classical concepts of thermal shock resistance (Kingery, 1955) often appear to be invalid because the microstructures of the materials are not taken into account. That is to say that the intrinsic material properties (the properties of the perfect material containing no microstructural defects) when used in the predictive formula often give inaccurate indications of real, existent material thermal shock performance. Recently a major contribution (Haselman, 1969b) has been made which indicated that these intrinsic material properties in conjunction with knowledge of the microstructure can accurately describe the thermal shock performance of existent materials.

The present model is also to be developed on the basis of intrinsic material properties and microstructure. The effect of the microstructure on the measured or extrinsic material properties is to be considered such that the final form of the model may be used to predict the thermal shock resistance of existent materials based upon these "effective" properties without an extensive knowledge of the microstructure.

Existent data published in the literature by the present author as well as many others will be applied to the model when the materials properties have been measured and reported. Microstructural information will be correlated with the thermal shock behavior when available.

MODEL FOR THERMAL STRESS RESISTANCE OF A TRULY ELASTIC
MATERIAL CONTAINING MORE THAN ONE CRACK

If the measure of the total amount of work which can be performed on a material by a thermal stress without causing an unacceptable amount of damage to the material can be taken as a measure of the thermal shock resistance of that material, then, by the appropriate application of heat transfer theory, the value of the maximum temperature differential to which that material can be exposed may be calculated. That is to say that the measure of the thermal shock resistance of a material is a measure of three energies associated with the material:

1. the elastic strain energy,
2. the energy associated with the formation of new surfaces (surface energy), and
3. the kinetic energy associated with the formation and growth of new surfaces (cracks).

When a truly elastic material is stressed in either compression or tension, a finite strain results. These stresses and strains are related by the well known Hook's Law:

$$\sigma = E\varepsilon \quad (1)$$

where σ is the uniaxially applied stress, ε is the resultant strain in the direction of the uniaxially applied stress and E is Young's modulus of elasticity which is the ratio of the applied stress to the resultant strain. The strain is the change in length of the material per unit length or

$$\varepsilon = \ln (l_f/l_i) \quad (2)$$

where l_f is the final length of a specimen of initial length l_i as the result of the applied stress σ . That is to say a force per unit area moves through a distance and a certain amount of work is done per unit volume of material.

Within limits, the work done per unit volume in stressing a material is converted to strain energy which may be defined as:

$$SE = \int \sigma \, d\epsilon \quad (3)$$

or if Hook's Law applies:

$$SE = 1/2 \, \sigma \epsilon \quad (4)$$

or

$$SE = 1/2 \, E \epsilon^2 \quad (5)$$

or

$$SE = \sigma^2 / (2E) \quad (6)$$

The limits, for a truly elastic material, are established when the material, in tension, is stressed to the level necessary to overcome the energy barrier for the creation of a new surface by the breaking of bonds of atoms lying in a plane of fracture. This energy barrier is the surface energy, γ , of the material. Griffith (1920) established a mathematical relationship between the surface free energy and the amount of stress (now known as the Griffith stress) necessary to start a crack of half width c growing:

$$\sigma_g^2 = \frac{2\gamma E}{\pi \nu c} \quad (7)$$

where ν is Poisson's ratio. The equation was later corrected by Griffith (1924) by removing the Poisson's ratio term:

$$\sigma_g^2 = \frac{2\gamma E}{\pi C} \quad (8)$$

If the strain energy put into a material which has been stressed to the Griffith stress is defined as the Griffith energy, GE, then this energy term can be expressed in terms of surface energy and crack size by combining equations (4) and (8):

$$GE = SE = \frac{\sigma_g^2}{2E} = \frac{\gamma}{\pi C} \quad (9)$$

This expression clearly indicates that the Griffith energy, for any material having a given surface energy, is inversely proportional to the crack half width if the modulus of elasticity used in the Griffith expression [equation (8)] is the same as that in the strain energy terms (4) and (5). They are not as may be seen shortly. The modulus of elasticity used in the Griffith expression is that of the material locally, i.e., uncracked, and this modulus shall be described as the intrinsic modulus of elasticity, E_{int} . The modulus of elasticity used in the strain energy equations is that of the body as a whole and this modulus shall be described as the effective modulus of elasticity, E_{eff} . Equation (9) may now be written correctly as:

$$GE = \frac{\gamma}{\pi C} \frac{E_{int}}{E_{eff}} \quad (10)$$

Walsh (1965) noted that uniaxial elastic compression of rocks yielded nonlinear stress-strain behavior and hysteresis with the slope of the stress-strain curve increasing as the stress increased. That is to say that the effective modulus of elasticity increased with increased com-

pressive loads. By analysis he developed a mathematical model which yielded the result that the measured modulus of elasticity of a body containing open cracks is less than that of an uncracked body, i.e., $E_{\text{eff}} < E_{\text{int}}$. This expression, as later developed by Berry (1960a and 1960b) may be written as:

$$E_{\text{eff}} = \frac{E_{\text{int}}}{(1+2\pi Nc^2)} \quad (11)$$

where N is the number of cracks passing through a unit of cross sectional area.

If the unqualified assumptions are made that all the cracks in a material are of the same size and that they are separated from one another by a sufficient distance such that their stress fields do not interact, then the equally unqualified assumption can be made that the number of cracks in this material does not affect the Griffith stress, rather it is the size of these cracks, the surface energy, and the intrinsic modulus of elasticity that affect it. Keeping these assumptions in mind, an extensive amount of information may now be gathered from the two material parameters of γ and E_{int} and the two physical parameters of N and c .

The Griffith energy for a material containing cracks may now be correctly written as:

$$GE = \gamma \left(\frac{1}{\pi c} + 2Nc \right) \quad (12)$$

Again, the amount of work which must be performed upon a material to start a crack growing is independent of the modulus of elasticity of

that material and depends only upon the surface energy, crack size, and crack number. The Griffith energy may be expressed in a different form as:

$$\gamma x = GE \quad (13)$$

where, of course,

$$x = \frac{1}{\pi c} + 2Nc \quad (14)$$

The term x is defined as the energy factor because for a given material, i.e., a given surface energy, this term determines the Griffith energy.

Constant Griffith energy contours are given on a crack size vs. crack number grid in Figure 1. Similarly, lines of constant crack number on grids of Griffith energy vs. crack size and lines of constant crack size on grids of Griffith energy vs. crack number are given in Figures 2 and 3. Figure 2 indicates that for a given number of cracks, as the crack size increases from zero the Griffith energy decreases to a minimum and then increases again with increasing crack size. This minimum value of energy was determined to occur when:

$$N = \frac{1}{2\pi c^2} \quad (15)$$

The minimum Griffith energy then becomes

$$GE_{\min} = \frac{2\gamma}{\pi c_{\min}} = 4\gamma N c_{\min} \quad (16)$$

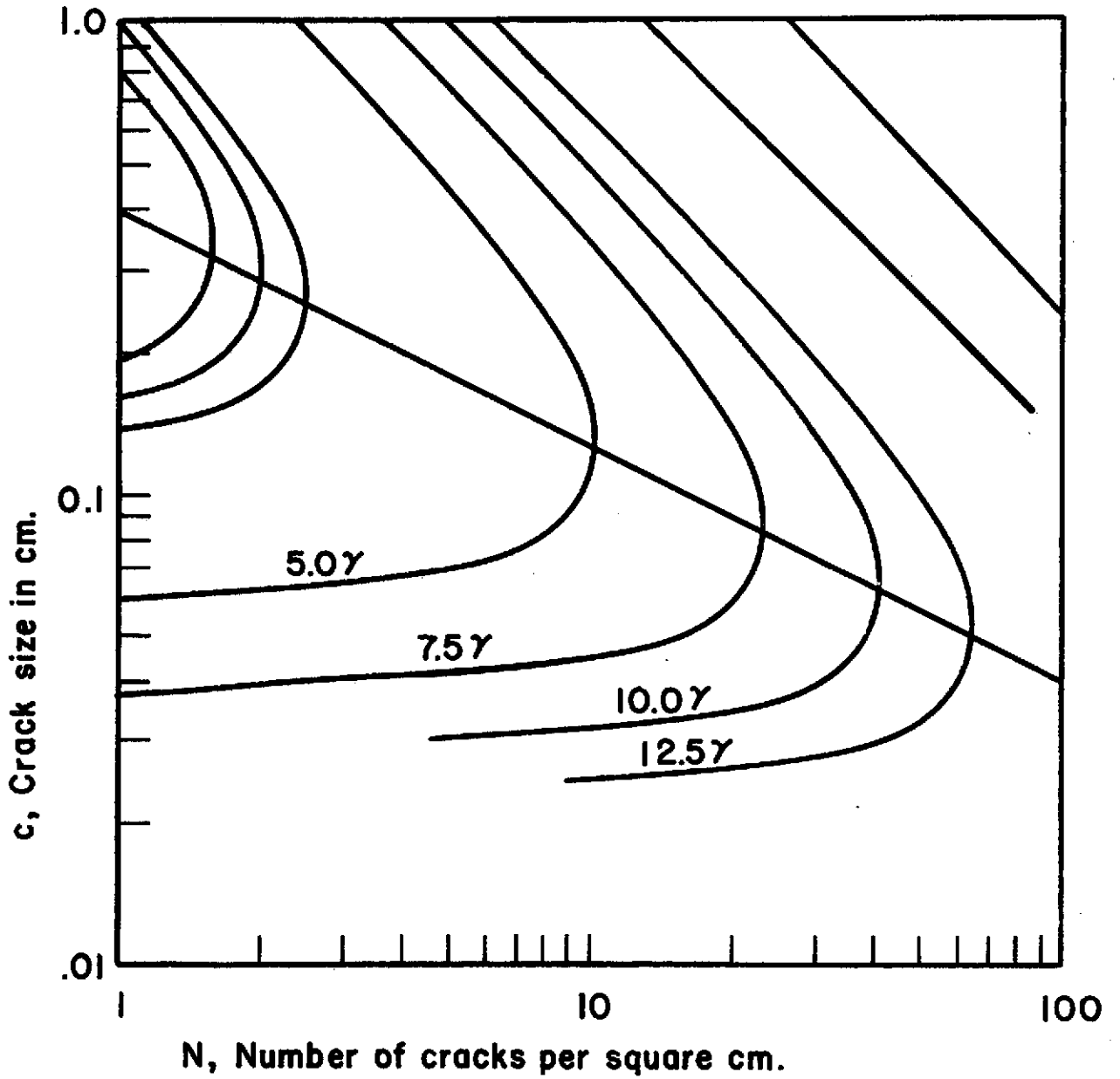


Figure 1. Lines of constant Griffith energy on a grid of number of cracks vs. crack size

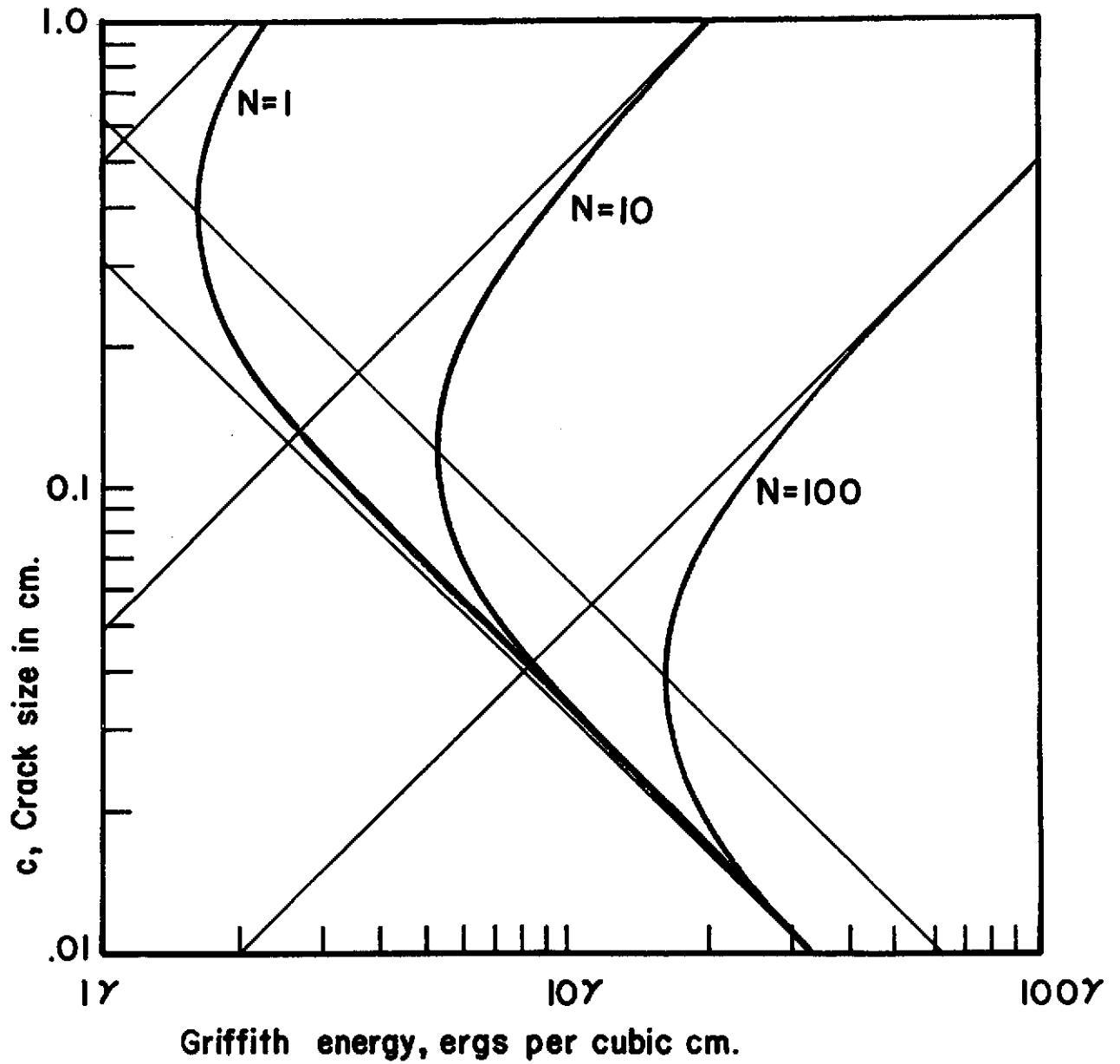


Figure 2. Lines of constant numbers of cracks on a grid of Griffith energy vs. crack size

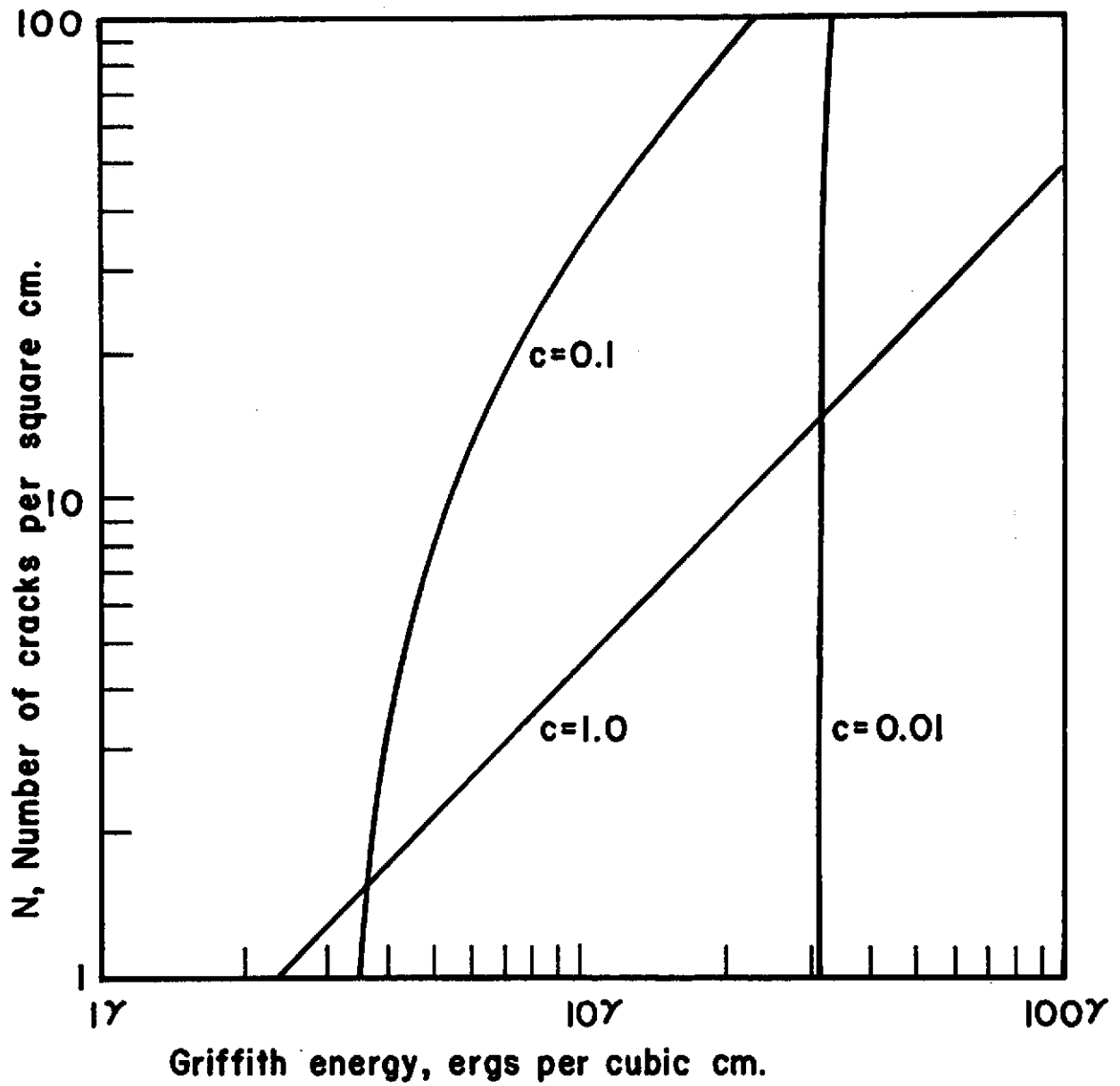


Figure 3. Lines of constant crack size on a grid of Griffith energy vs. number of cracks

or at the minimum Griffith energy the $1/(\pi c)$ term is equal to the $2Nc$ term.

It may be further noted from Figure 2 that as the crack size gets smaller, the Griffith energy approaches the line defined by

$$GE = \gamma/(\pi c) \quad (17)$$

Equation (17) is identical to Equation (9) which was the original expression for Griffith energy without the correction for the effect of open cracks on the modulus of elasticity. Similarly, as the crack size gets large, the Griffith energy approaches a value defined by the following expression:

$$GE = 2\gamma Nc \quad (18)$$

The point of intersection of the lines described by Equations (17) and (18) in Figure 2 gives the crack size for the minimum Griffith energy and indicates half the minimum Griffith energy. The number of cracks may also play an important role as shown in Figure 3. For a given crack size in a given material the Griffith energy always increases with increased numbers of cracks. It is further observed that the rate of increase of Griffith energy is higher for the material having the larger sized cracks.

The results of increases in both crack size and number is shown in Figure 1. Values of Griffith energy for a given material may be increased in two ways:

1. by making the crack size very small, and
2. by making a large number of larger cracks.

In the first instance the effect of number of cracks is small as evidenced by the gentle slope of the contours of Griffith energy. In the second instance, for a given Griffith energy initially as the crack size increases, the number must also increase. However, after passing the point of minimum Griffith energy, the number gets smaller as the crack length increases. Finally, it should be noted that for a given set of crack sizes and numbers, the Griffith energy can always be increased by selecting a material with a higher surface energy.

These changes in Griffith energy are of course reflected in the mechanical behavior of these materials. The effect of changes in crack size and crack number, intrinsic modulus of elasticity, and surface energy can be observed as changes in the Griffith stress, effective modulus of elasticity, and the Griffith strain which is defined as:

$$\epsilon_g = \sigma_g / E_{\text{eff}} \quad (19)$$

A plot can be made of Griffith stress vs. Griffith strain which represents the locus of the Griffith criteria for a truly elastic material containing more than one crack with cracks being independent of one another. The slope of the straight line from any point on the locus drawn to the origin would then represent the effective modulus of elasticity of the material containing cracks.

The effect of increasing the number of cracks in a given material is shown in Figure 4. For initially small crack sizes increases in either or both crack sizes or numbers does not significantly alter the effective modulus of elasticity. In the region above the knee of the

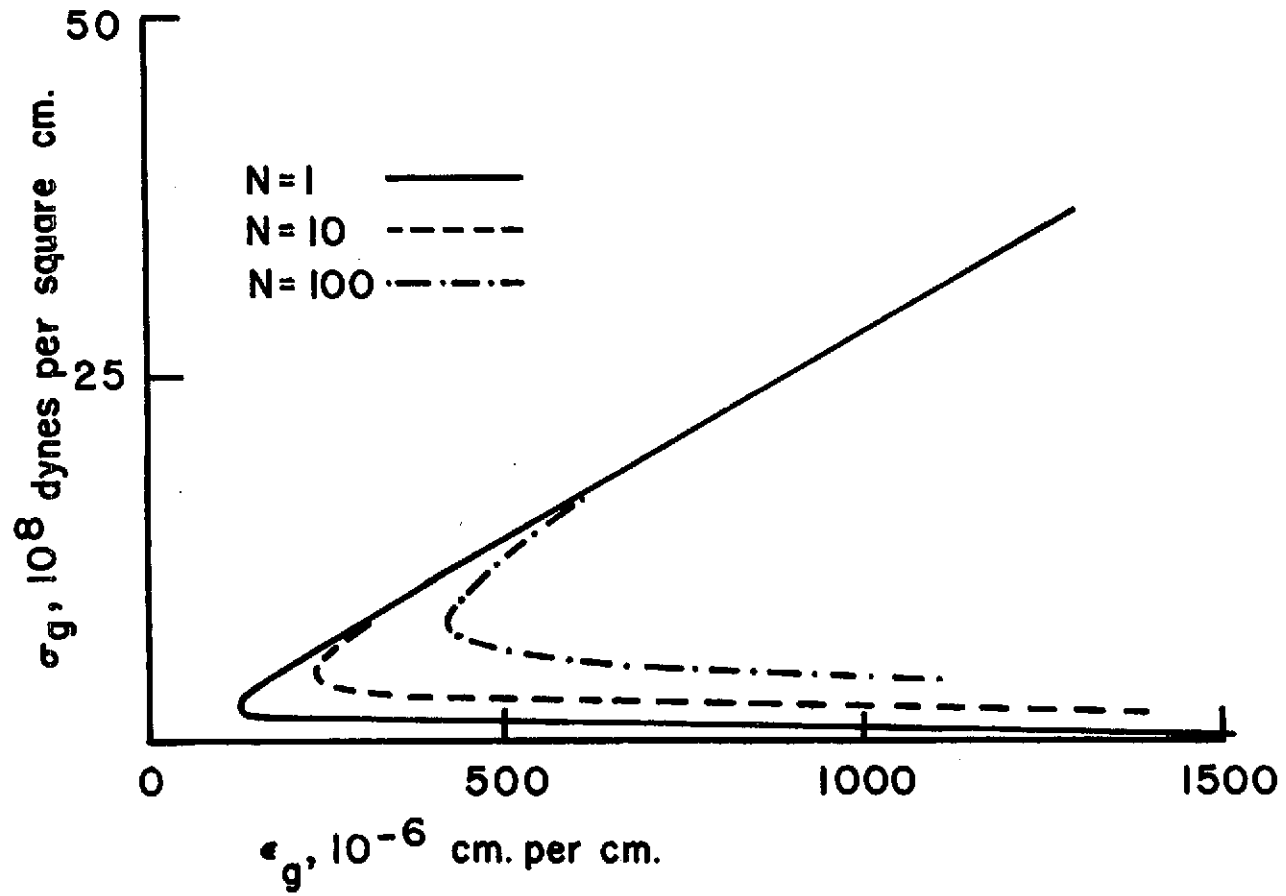


Figure 4. The effect of number of cracks on the locus of the Griffith criteria

of the locus, however, the Griffith stress drops rapidly with increasing crack size. At a point a minimum Griffith strain is reached when the crack size reaches:

$$c^2 = 1/(8\pi N) \quad (20)$$

(This value of c is half that which produces the minimum Griffith energy). Figure 4 indicates that the minimum Griffith strain is larger for larger number of cracks. When the crack reaches a length twice that to produce the minimum Griffith strain, the minimum Griffith energy is reached. It can be shown through the use of Equations (11) and (15) that at this point the effective modulus of elasticity is exactly half that of the intrinsic modulus of elasticity. That is not to say that an increase in intrinsic modulus of elasticity will increase the minimum Griffith energy because Equation (12) clearly indicates that the Griffith energy is a function of only one material parameter, the surface energy. As the crack size increases from this point, the Griffith stress decreases more slowly. It may also be observed that for a given Griffith stress, the Griffith strain is larger for a larger number of cracks. Likewise, the effective modulus of elasticity is lower and the Griffith energy is higher. It is also obvious from Figure 4 that below the knee of the locus for a given number of cracks, an increase in crack size from this point increases the Griffith energy. Therefore, if the effective modulus of elasticity is either larger or smaller than half the intrinsic modulus of elasticity of that material, the Griffith energy of that material, when stressed to the Griffith stress, will not be at a minimum.

The effect of increasing the surface energy is shown in Figure 5. For a given intrinsic modulus of elasticity and number of cracks, increases in crack sizes cause changes in the Griffith stress and Griffith strain similar to those in Figure 4. Increases in surface energy increase the minimum Griffith strain and the minimum Griffith energy. Similarly, for a given Griffith stress little change in Griffith strain occurs for a small value of crack size as a result of increases in surface energy while larger changes occur in the Griffith strain for larger values of crack size.

Figure 6 indicates the effect of intrinsic modulus of elasticity on the locus of the Griffith criteria for a given number of cracks and surface energy. The intrinsic modulus of elasticity has no effect on the Griffith energy but a decrease in intrinsic modulus of elasticity does indicate an increase in the Griffith stress for a given Griffith strain as is expected by the application of Hook's Law.

If the Griffith stress is exceeded, the cracks will begin to increase in size. It is assumed that the cracks which are initially of equal size will grow in concert. Two easily analyzed conditions may exist after the Griffith stress is reached: constant stress or constant strain. The condition of constant strain will be analyzed first because of its simplicity and similarity to materials in a thermally stressed state.

A given material containing a number of cracks is stressed to a point $\sigma > \sigma_g$. In the first analysis the crack number and size are such that ϵ_g is greater than the minimum and σ_g subsequently is

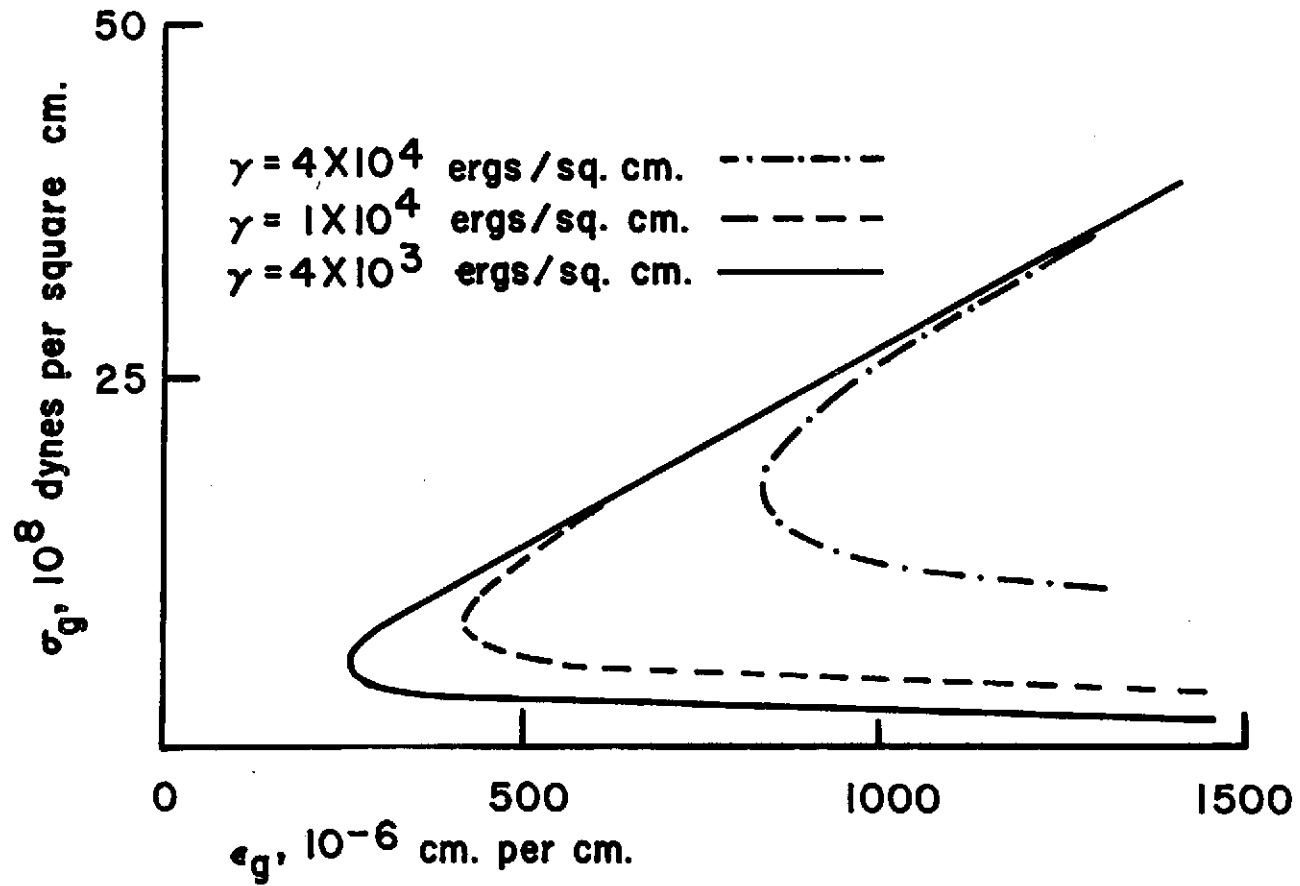


Figure 5. The effect of surface energy on the locus of the Griffith criteria

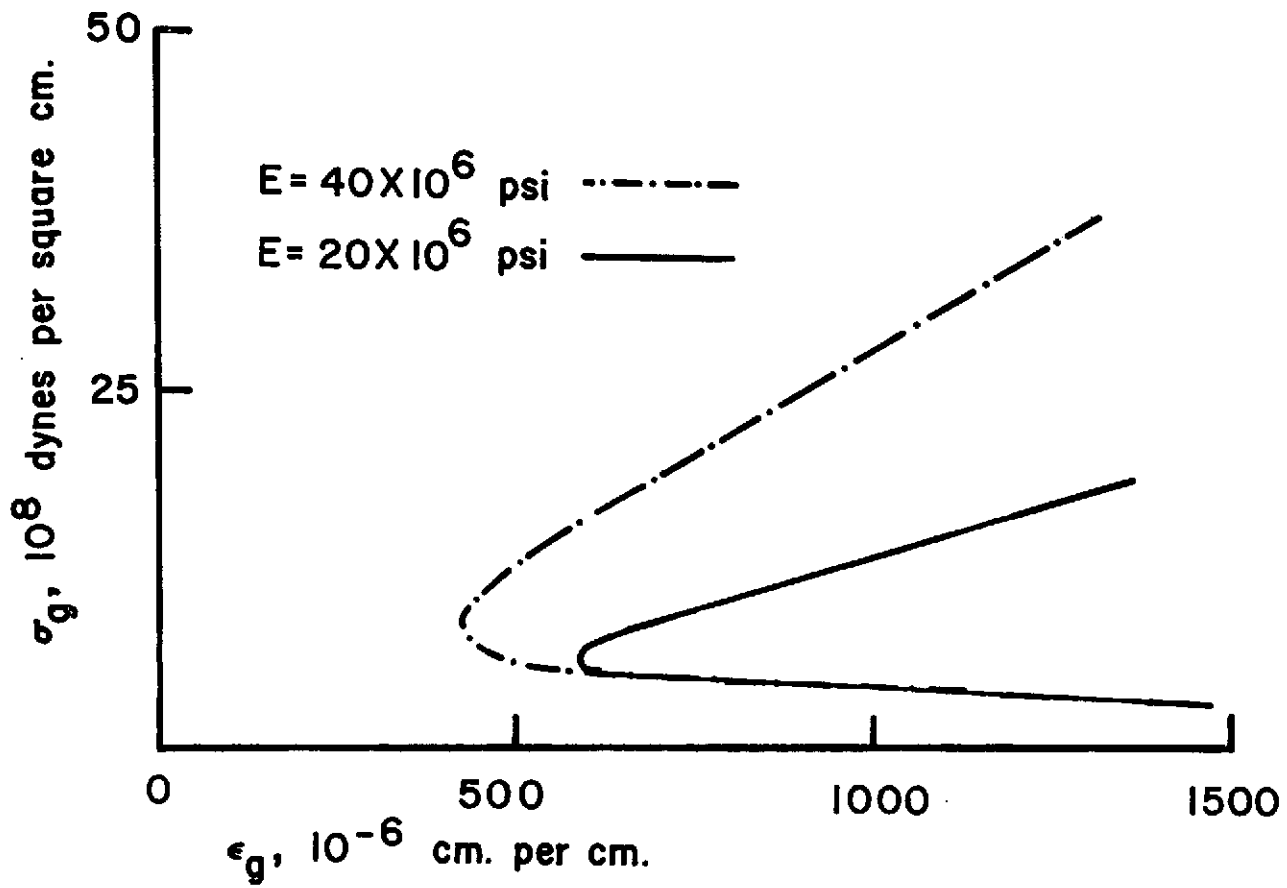


Figure 6. The effect of the intrinsic modulus of elasticity on the locus of the Griffith criteria

above that necessary to produce a minimum as shown in Figure 7 and as indicated by line oa.

If the applied stress is only infinitesimally higher than σ_g then the area oab is only infinitesimally more than the Griffith energy and the cracks will grow, σ_g will decrease and the effective modulus of elasticity will decrease. Point c may represent the condition shortly after σ_g is applied. It is immediately obvious that point c is in the region of instability and that the cracks must continue to grow. Berry (1960b) has shown that the area acd is the kinetic energy of the cracks and that the area oad is the surface energy contribution of the cracks. The area ocb then represents the remainder of the strain energy.

The cracks must continue to grow until the locus of the point is outside the region of instability. This condition would appear to be met at point e but the kinetic energy (ade) is now at a maximum and the cracks must continue to grow until this energy is absorbed by the surface energy term. This condition is met at point f with the final crack size being determined by the Griffith stress at point g. Berry (1960b) indicated that at this point the area efg will be the same as ade.

The cracks are now subcritical. The material contains a residual strain energy (ofb) but this energy is clearly less than the Griffith energy (ogh) and the residual stress σ_f is clearly less than the Griffith stress σ_{g_g} . From the values of σ_{g_a} and σ_{g_g} it can be determined that, for a constant strain condition, initially short cracks grow to very long cracks because of the high kinetic energy associated

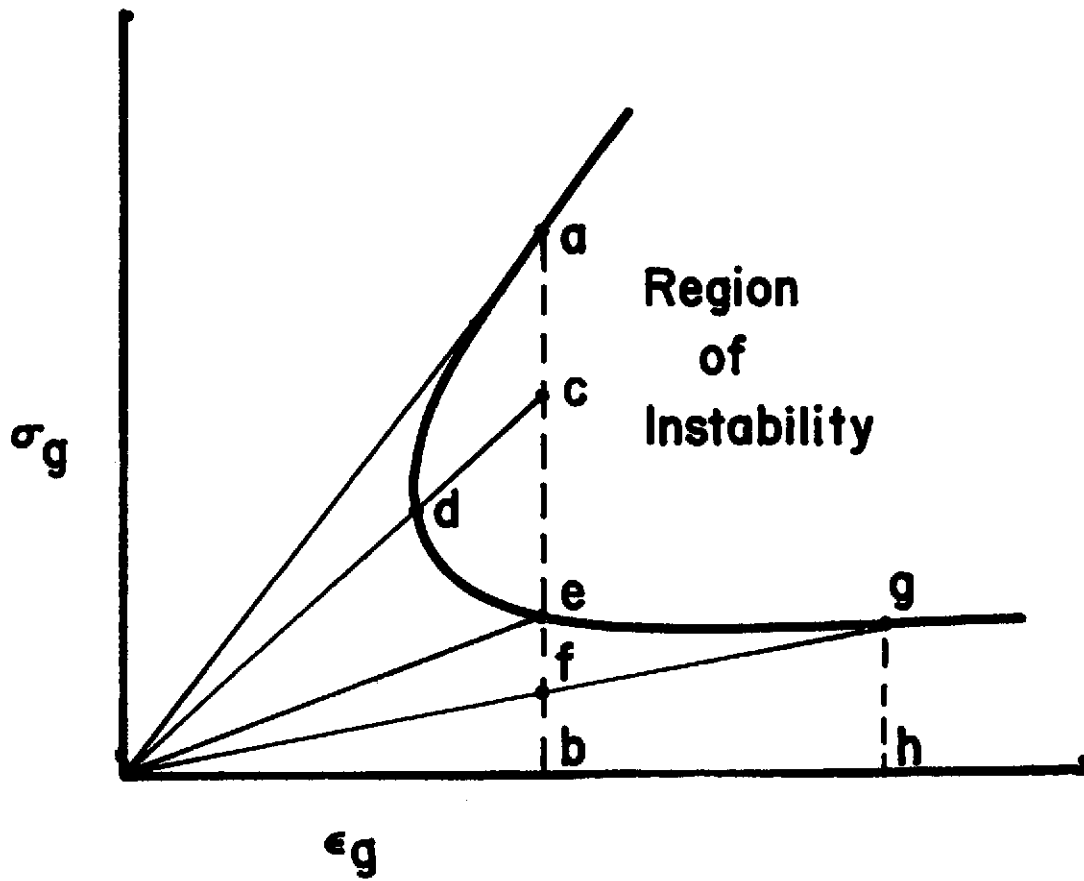


Figure 7. Analysis of the Griffith criteria for a strong material at constant strain

with them. The Griffith stress and thus the fracture stress also drops significantly as does the effective modulus of elasticity.

For values of crack sizes and numbers above those which produce the minimum Griffith strain, the kinetic energy term is less significant. Such a material may be stressed to point a in Figure 8 lying within the region of instability. The strain energy term oab again is larger than the Griffith energy and the cracks must grow in size. When the point c is reached a small amount of kinetic energy remains and must be converted to surface energy and residual strain energy. Thus the cracks grow to point d such that the kinetic energy (afc) equals cde as before. For this case the loss in Griffith stress and consequently fracture stress is slight as may be noted by the positions of σ_{g_f} and σ_{g_e} . The crack length has increased moderately and the effective modulus of elasticity has decreased moderately.

Analysis of a material containing more than one crack at a constant stress may be performed similarly. Figure 9 again gives the locus of the Griffith criteria. The material is stressed to a point a such that the Griffith energy is only slightly exceeded. The cracks begin to grow but the stress level σ_a is maintained to point b. The area (oabc) represents the total amount of work done on the material. The area oae is the surface energy contribution, aeb is the kinetic energy developed and obc is the resultant residual strain energy at fracture. If the material fractures at point b then this strain energy will be converted to kinetic energy but the surface energy term will remain the same. If, on the other hand, the strain is held constant at this point the very

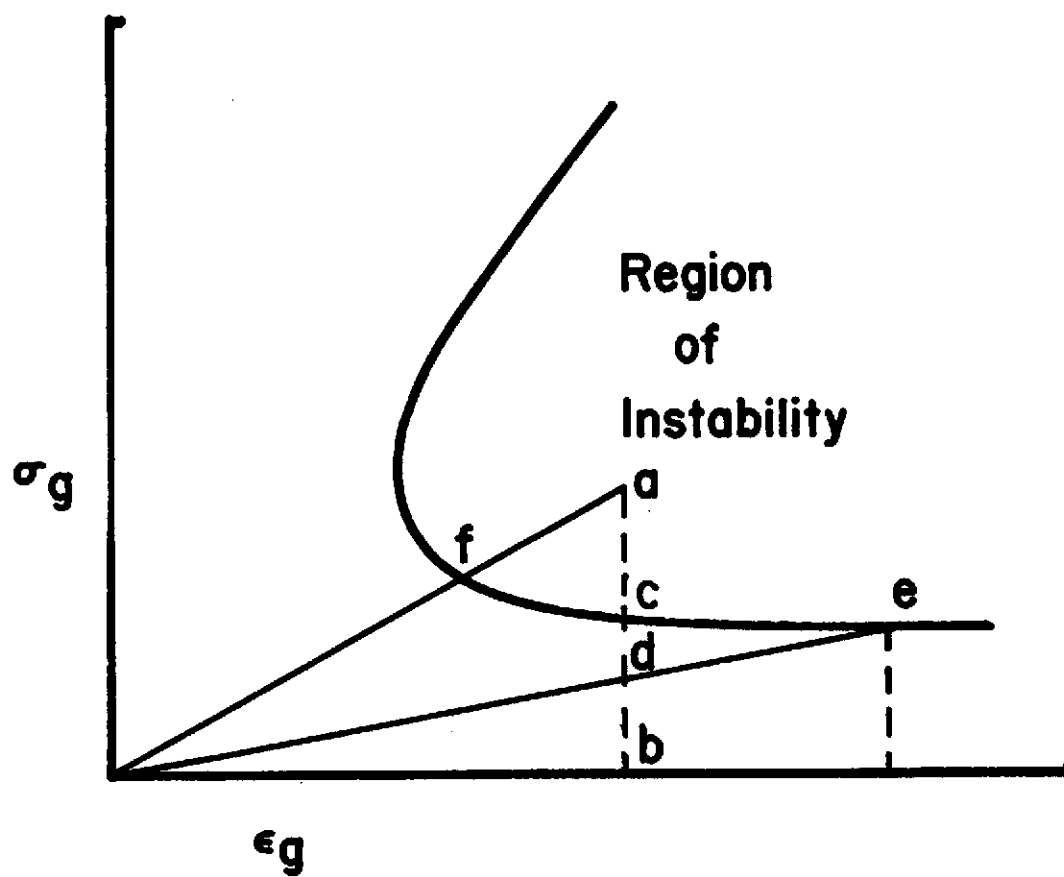


Figure 8. Analysis of the Griffith criteria for a weak material at constant strain

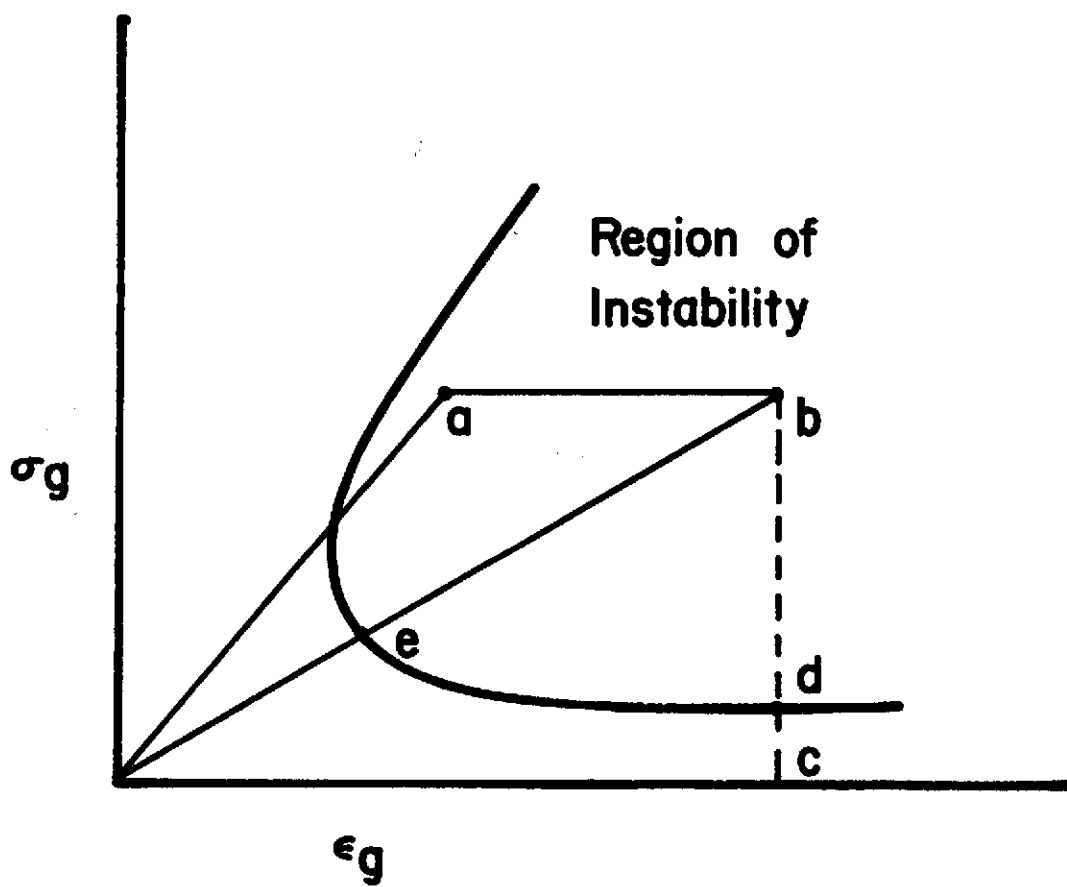


Figure 9. Analysis of the Griffith criteria at constant stress

large amount of kinetic energy $\frac{1}{2} \rho v^2$ must be converted to surface energy. The Griffith stress and effective modulus of elasticity would become very low and the Griffith strain would become very large as a result of the very large cracks. Likewise the Griffith energy would become very large.

In reality the constant strain nor the constant stress case exists except under experimental conditions. Bodies exposed to stresses large enough to be located in the region of instability probably are neither constant stress nor constant strain. The constant strain is probably more nearly correct and it will be used in the model for thermal shock resistance to follow. As such the thermal stress resistances derived from this model will represent minimum values. That is to say the thermal stress resistances are conservative values of use for design purposes when the chance of obtaining unacceptable thermal shock damage must be minimized.

In a real situation a material may be exposed to mechanical stresses as well as thermal stresses. When the sum of these two stresses reach the Griffith stress, cracks of equal size in the material begin to grow in size resulting in a decrease in the Griffith stress and effective modulus of elasticity and an increase or decrease in the Griffith strain depending upon the Griffith criteria of the material. The Griffith energy, that is the energy necessary to start the crack moving again, may be increased or decreased, depending solely upon the size of the cracks since the number of cracks is assumed to remain constant. The new value of the crack size may be determined from the locus of the Griffith criteria as has been shown.

C-2

If it is assumed that the effect of crack size and crack number on the coefficient of thermal expansion is negligible then the thermal strain for a free body may be described as:

$$\epsilon_{ts} = \alpha \Delta T \quad (21)$$

where, for a free body having a coefficient of thermal expansion α , ϵ_{ts} is the thermal strain produced by the temperature differential ΔT . Using Hook's Law one may also write for a body constrained in one dimension with no prestress that:

$$\sigma_{ts} = E_{eff} \epsilon_{ts} = \alpha E_{eff} \Delta T \quad (22)$$

where σ_{ts} is the thermal stress generated. In terms of the temperature differential we may write:

$$\Delta T = \sigma_{ts} / (\alpha E_{eff}) \quad (23)$$

Now recalling Equation (4) the temperature differential may be written in terms of the strain energy and the stress level:

$$\Delta T = 2(SE) / (\alpha \sigma_{fs}) \quad (24)$$

The maximum temperature differential to avoid production of crack growth is then:

$$\Delta T = \frac{2(GE)}{\alpha \sigma_g} = \frac{\sigma_g}{\alpha E_{eff}} = \frac{\epsilon_g}{\alpha} \quad (25)$$

This may also be expressed in terms of crack size and number by appropriate substitution:

$$\Delta T = \left(\frac{2\gamma}{\pi c E_{int}} \right)^{1/2} \frac{(1 + 2 N c^2)}{\alpha} \quad (26)$$

If the criteria for thermal shock damage is that no loss in strength be incurred then Equation (25) may be used as a measure of thermal stress resistance while Equation (26) may be used as a guide for material selection. The latter equation indicates that a high value of surface energy and low values of intrinsic modulus of elasticity and coefficients of thermal expansion are desirable. Obviously the optimum crack size is dependent upon the number of cracks as has been previously discussed in detail. If the crack size is small then Equation (26) reduces to

$$\Delta T = \frac{(2\gamma E_{int}/\pi c)^{1/2}}{\alpha E_{int}} = \sigma/\alpha E_{int} \quad (27)$$

This is the classical concept of increasing thermal shock resistance by selecting a very strong material and it is, in principle, a valid one. In practice many materials, particularly ceramic materials, contain many flaws or microcracks which lower the maximum stress to which they may be exposed.

Previously it has been shown that the energy necessary to start cracks moving or the Griffith energy as it was defined is a function of the surface energy, the crack size, and the crack number only. This is the basis of Equation (26). However, surface energies, crack size, and crack number are very difficult to measure. Fracture stresses, fracture strains, and effective moduli of elasticity and consequently Griffith energies are relatively easy to measure. Therefore while Equation (25) takes into account crack numbers and size it is an easier and perhaps

more accurate measure of the thermal shock resistance of materials. This equation then indicates that the thermal stress resistance can be measured in terms of bulk material or effective material parameters. Quite simply put, the temperature differential necessary for crack propagation in the free body under discussion is directly proportional to the ratio of the Griffith stress (that is a slowly applied stress necessary to start cracks moving) and the effective modulus of elasticity or, more to the point, is directly proportional to the Griffith strain. As indicated by Equation (20) for a given number of cracks in any material the Griffith strain may be increased by increasing or decreasing the crack size above or below the value given by:

$$c^2 = 1/(8\pi N) \quad (20)$$

Thus the thermal shock resistance of any material containing more than one crack decreases to a minimum and then increases again as the crack size increases from zero. The crack size to produce the minimum thermal stress resistance is for all materials a function of the number of cracks. Finally it can be shown mathematically as is shown graphically in Figures 10 and 11 that the minimum Griffith strain and subsequently the minimum thermal shock resistance may be increased by increasing the surface energy and/or number of cracks and by decreasing the intrinsic modulus of elasticity.

If the criteria for thermal stress damage is for no loss of strength when large thermal gradients are to be encountered then a material containing cracks larger than those which produce the minimum thermal stress

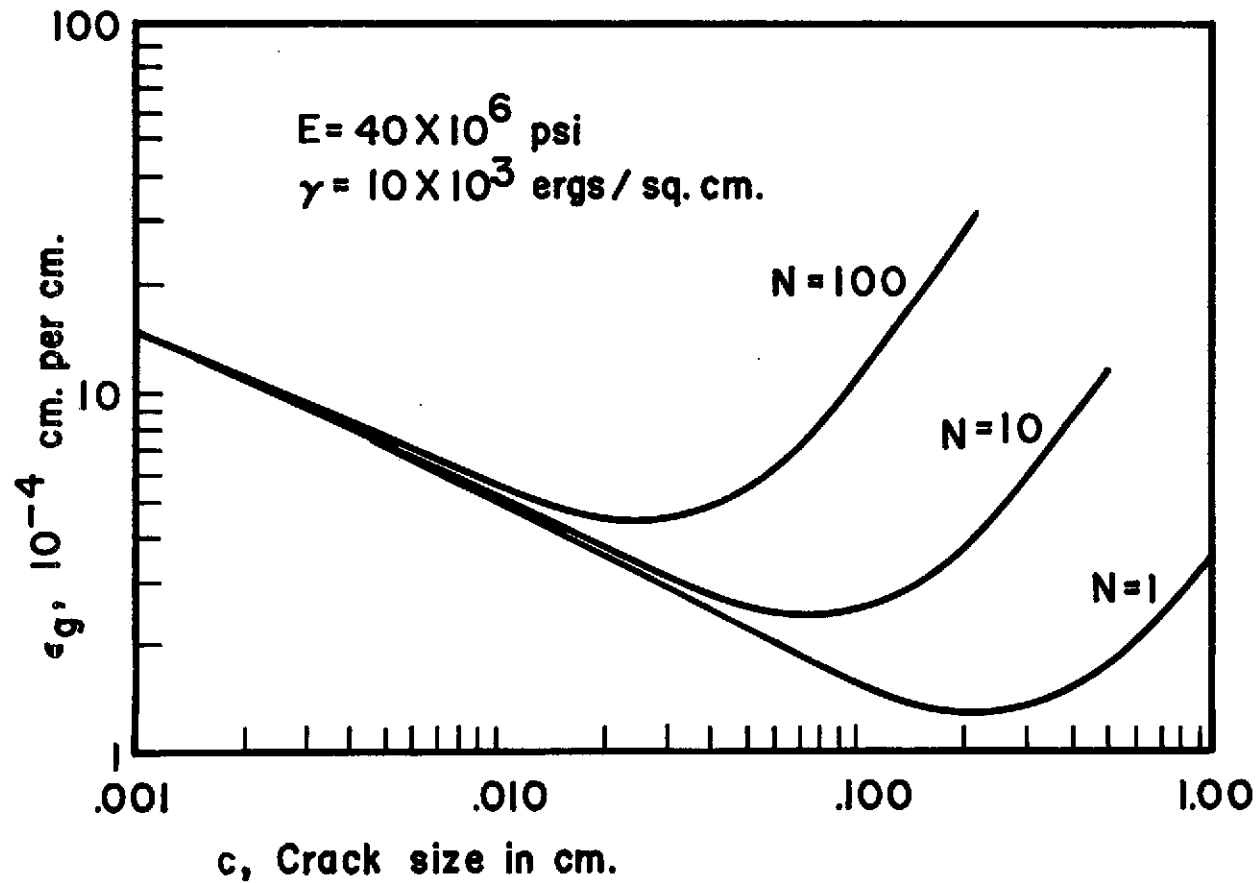


Figure 10. Griffith strain vs. crack size for various numbers of cracks

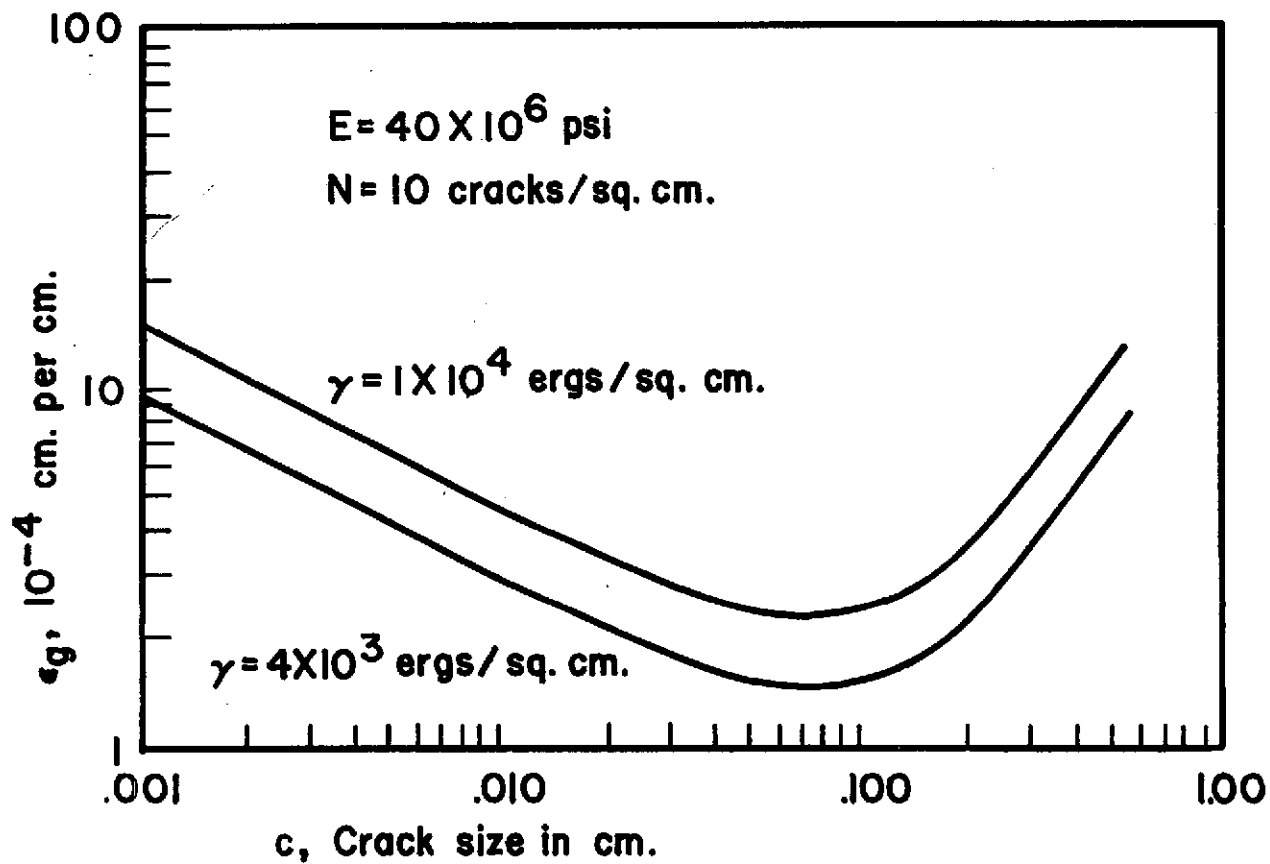


Figure 11. Griffith strain vs. crack size for various surface energies

resistance or minimum Griffith strain must be selected. Here if the Griffith criteria is exceeded the increase in crack size and consequently the decrease in strength is quite small as was previously discussed. A different material having the same strength but containing cracks smaller than those producing the minimum Griffith strain would fail "catastrophically" rather than "quasi-statically" because of the absorption of the kinetic energy associated with the production of very large cracks.

Determination of whether a material will suffer thermal shock damage of "catastrophic" proportions then depends upon whether the crack size is larger or smaller than that needed to produce the minimum Griffith strain. Using Equation (20) and the equation for effective modulus of elasticity (11) it can be shown that the condition of minimum Griffith strain is met in all cases when the effective modulus of elasticity equals eighty percent of the intrinsic modulus of elasticity. Thus materials having effective moduli of elasticity above that value are subject to "catastrophic" thermal shock failure if the Griffith energy condition for crack growth is reached as a result of large thermal differentials.

COMPATIBILITY OF THE MODEL WITH EXISTING THERMAL
SHOCK RESISTANCE MODELS

The present model of thermal shock resistance does not disagree with the classical concepts of thermal shock resistance in any manner except semantically. These classical concepts are based upon the idea of continuum mechanics. That is to say that as long as the material as a whole appears homogeneous and continuous in all directions and the measured physical properties appear to be homogeneous in all directions then these concepts may apply. This concept has long been accepted in the study of metals and ceramics as is discussed below.

Steel, as an example for purposes of illustration, is composed of a multitude of small metallic crystals called grains. These grains may be either a single phase as in ferrite or multiphase as in pearlite depending upon alloying and heat treatment. Furthermore, the grains themselves are not homogeneous in their mechanical properties. That is to say that the modulus of elasticity, for example, along one crystallographic axis is not necessarily the same as that of another axis. The result is that steel is not a truly continuum solid. But when the collection of grains is treated as a whole, the body takes on the characteristics of a continuum solid if the grains are randomly oriented. That is to say that the modulus of elasticity of the body, for example, is the same in any direction. Furthermore, the mechanical properties of the body as a whole may be changed by changing the individual characteristics of each grain. The same steel may have a high fracture strength and be brittle if it is heat treated and quenched or it may be lower in

strength and tough if it is heat treated and slowly cooled to pearlite and ferrite. The only difference between the two is the microstructure.

The same analytical approach is suggested for a material which is exposed to stresses produced by thermal gradients. Again, measurable changes in properties of the body are produced by changes in the microstructure while the intrinsic properties of the material remain the same. The result is that the mechanical behavior of the body can be described by either the effective properties of the body or by the intrinsic properties of the material in conjunction with knowledge of the microstructure. It is hoped that the present model bridges this gap in the understanding of the thermal stress resistance of truly elastic materials. Hasselman (1969b) has recently developed a theory of thermal shock fracture initiation and propagation which is based upon the intrinsic properties of the material and the microstructure. The model parallels the present one based upon in the final analysis the mechanical properties of the body as a whole. His analysis develops along quite similar lines in that the total energy per unit volume of material at constant strain is established:

$$W_t = \frac{3(\alpha\Delta T)^2}{2(1-2\nu)} E_{int} \left[1 + \frac{16(1-\nu)Mc^3}{9(1-2\nu)} \right]^{-1} + 2\pi Mc^2 \gamma \quad (28)$$

where M is the number of parallel cracks per unit volume. The Griffith criteria for crack instability is imposed:

$$dW_t / dc = 0 \quad (29)$$

and the following temperature differential is obtained:

$$\Delta T = \left[\frac{\pi \gamma (1-2\nu)^2}{2 E_{int} (1-\nu) \alpha^2} \right]^{1/2} \left[1 + \frac{16(1-\nu^2) M c^3}{9(1-2\nu)} \right] \left[c \right]^{1/2} \quad (30)$$

The temperature differential vs. crack half length from this expression is plotted in Figure 12. This plot is nearly identical to that of Figure 10 in which the Griffith strain of the present model is substituted for the temperature differential. The temperature differential in Hasselman's expression is a function of the intrinsic materials parameters of coefficient of thermal expansion, modulus of elasticity, and surface energy as well as the crack size. For the present model the same plot is obtained when the temperature differential is a function of the measured coefficient of thermal expansion, fracture strength, and effective modulus of elasticity or a function of the strain to failure to coefficient of thermal expansion ratio.

Comparison of Equations (26) and (30) indicate the similarity of the two approaches if due compensation is made for the differences in strain conditions:

present model

$$\Delta T = \left[\frac{2\gamma}{E_{int} \pi c \alpha^2} \right]^{1/2} \left[1 + 2\pi N c^2 \right] \quad (26)$$

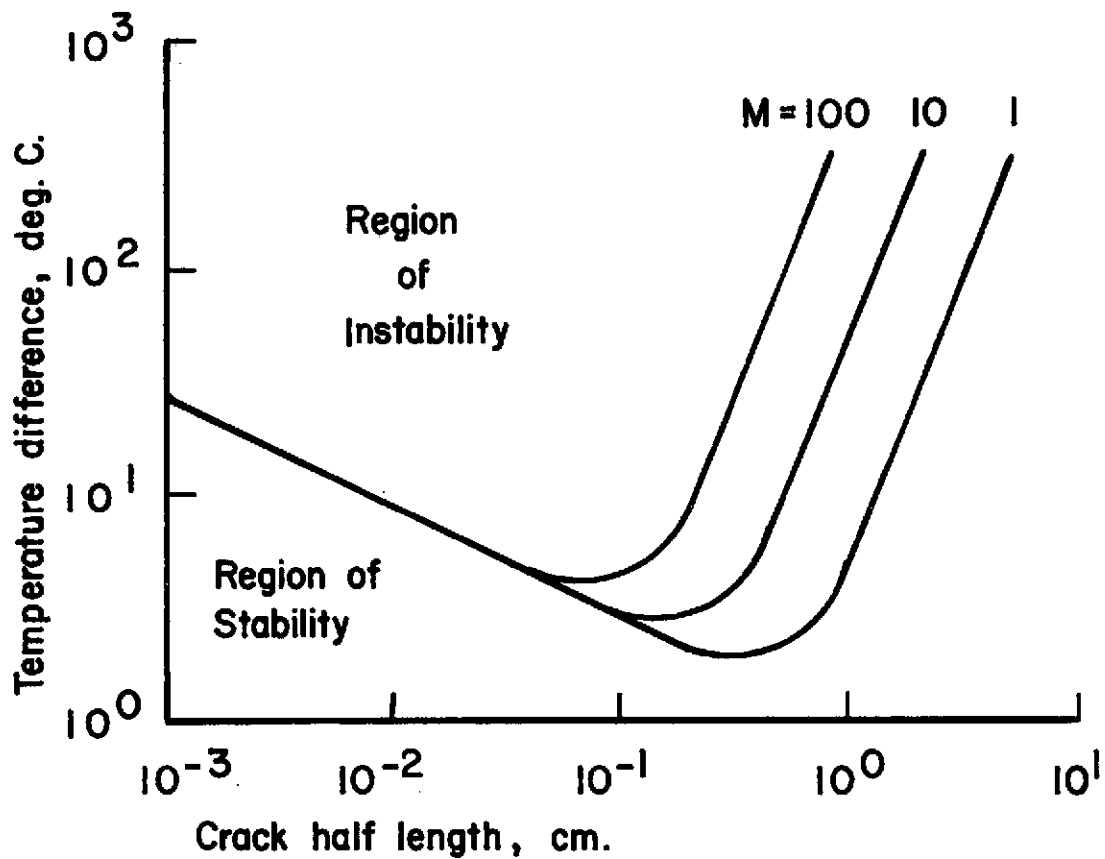


Figure 12. Minimum thermal strain required to initiate crack propagation as a function of crack length and crack density (after Hasselman, 1969b)

Hasselmann's model

$$\Delta T = \left[\frac{\pi \gamma}{2 E_{int} c \alpha^2} \right]^{1/2} \left[1 + \frac{16 M c^3}{9} \right] f(v) \quad (30)$$

The product of the Poisson's ratio terms approach unity and the two expressions become nearly identical.

Earlier Hasselman (1969a) had suggested also that the thermal shock resistance of a material might be increased as a result of an increase in the strain to failure to introducing microcracks. Here again an analysis was made of a material containing parallel microcracks. In this analysis, however, no minimum strain was shown to occur.

On the basis of the comparison of these two approaches it appears that the thermal stress resistance of elastic materials may then be made on the basis of either the bulk or effective properties of the material or on the intrinsic properties of the material and the associated microstructure.

For Hasselman's approach, the number of cracks and their size must be measured as well as the intrinsic properties. These properties then may be used to predict the maximum temperature differential. For the present model, the number of cracks and their size need not be measured as their effect is measured indirectly by the fracture strength and the effective modulus of elasticity. The surface energy term is also incorporated in the fracture strength term. That is to say that the present model treats the body as a homogeneous continuum with the ef-

fects of its microstructure being measured in changes in bulk parameters. Thus the present model allows the use of existing expressions for predicting the thermal shock resistance while information about the type of failure may be gathered by comparison of the effective modulus of elasticity with the intrinsic modulus of elasticity.

APPLICATION OF THE MODEL TO THE DATA

Over the past fifty years a large amount of data has been gathered concerning the thermal shock resistance of various ceramic materials. If the mechanical properties of these materials were measured as an integral part of the researcher's program, then the present model may be applied directly to these data if due allowances are made for specimen geometries and specimen environments. Because of the complications associated with these latter variables, no attempts will be made to predict absolute temperature differentials but if the geometries and environments are the same for a number of materials then the present model may be used to predict relative temperature differentials.

The thermal shock resistance data in the literature appear generally in one of three forms. In the older data specimens are quenched from a given higher temperature to a lower temperature and the percentage weight loss or percentage spalling loss is measured. Newer data are presented for specimens which are quenched as previously described but measures are made of percentage loss of fracture strength. Finally, measures are made of temperature differentials necessary to cause a "defined" failure of the material such as "catastrophic" failure.

Perhaps the most obvious data is that in which the change in strength as the result of a given quench is measured. According to the present model no change in strength occurs if the Griffith stress is not reached or exceeded. If the Griffith stress is reached or exceeded then, as a result of crack growth, the strength decreases with "catastrophic" failure being the manifestation of rapid decreases in strengths. The per-

centage drop in strength according to the present model depends upon the position of the Griffith criteria on the locus of the Griffith criteria: if the position is such that the Griffith stress is above the stress necessary to produce the minimum Griffith strain, the drop in strength is likely to be greater than if the position of the stress is below that to produce the minimum strain.

Hasselmann (1970a) has observed such behavior to occur in high strength alumina (Al_2O_3) rods. The strengths of the rods quenched in still water from various temperatures was measured in four point bending. A representative portion of the data is presented in Figure 13. Here, temperature differentials below approximately 225 deg C. do not produce reductions in strength. That is to say that the Griffith stress has not been reached or exceeded. At higher temperature differentials the strength drops abruptly to levels of only 25 percent or less of the original strength. The resultant strength decreases mildly with increasing temperature differentials after the critical differential for the given specimen geometry and environment has been reached.

Application of the present model suggests that the starting material had a microstructure containing flaws of a very small size as evidenced by the relatively high fracture strength and the modulus of elasticity of $41-45 \times 10^6$ psi. The implication is that the Griffith stress is above that necessary to produce the minimum strain (the knee of the locus of the Griffith criteria) and that once this stress was reached the flaws or cracks grew instantaneously to a much larger size as a result of the excess kinetic energy available. Higher temperature differentials resulted in larger strain energies and correspondingly lower

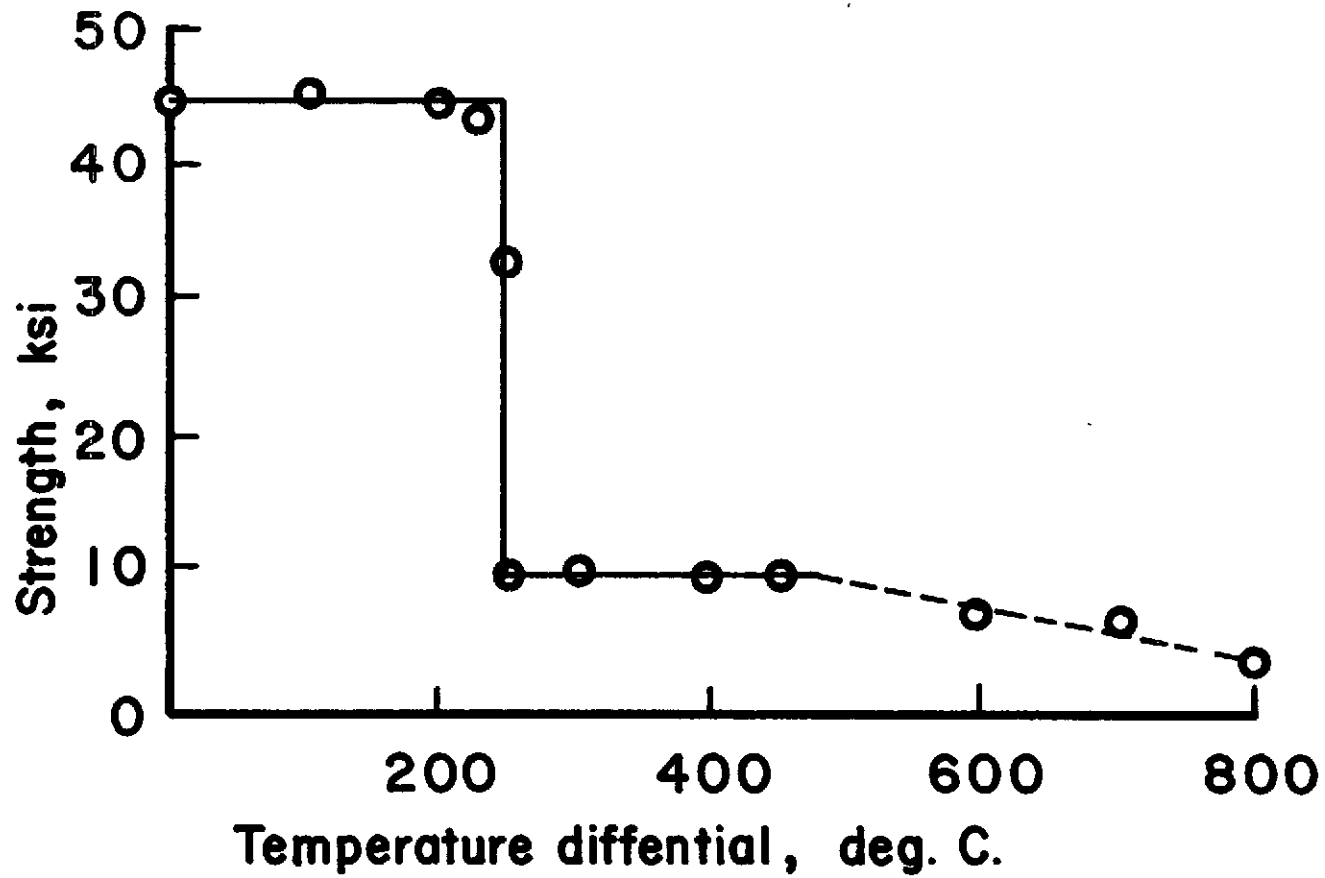


Figure 13. Strength vs. quenching temperature differential
(after Hasselman, 1970a)

strengths. Hasselman (1970a) gives microscopic evidence supporting this implication. Micrographs of the shocked materials revealed relatively large cracks which had grown and interacted as a result of the thermal stresses generated. Although Hasselman was unable to measure the modulus of elasticity of the shocked specimens, he estimated the modulus to be approximately 10 percent of the original. Because the strength after thermal shock exposure was approximately 25 percent of the original, the implication is that the strain to failure has been increased approximately 2.5 times that of the initial strain to failure and Hasselman indicates such behavior.

On the basis of the present model and as indicated by Hasselman the temperature differential necessary to propagate the cracks again would be approximately 2.5 times the initial temperature differential if the coefficient of thermal expansion is unaffected by the presence of the cracks. Hasselman (1970a) found this to be the case with certain larger rods but unfortunately he did not report their strengths after this second thermal shock exposure. On the basis of the present model the damage would not be as extensive as after the first exposure because as a result of the first exposure the Griffith stress lies below the knee of the locus as evidenced by the very low modulus of elasticity. It is to be expected that temperature differentials 2.5 times that of the initial temperature differentials and higher, produce only slightly lower strengths as a result of crack propagation.

The above data represents a "strong" thermal shock resistant material. That is to say that thermal stress fracture may be avoided by not

exceeding the critical temperature differential. Once the critical differential is exceeded the material suffers "catastrophic" loss of strength. This sudden loss of strength during crack propagation may be avoided if a material is picked which requires a Griffith stress lying on the locus below the knee. McKee and Adams (1950) performed extensive investigations of the thermal shock resistances of extruded and slip cast zircon ($ZrO_2 \cdot SiO_2$). They found that their material had a four point bend strength of 15×10^3 psi and a modulus of elasticity of 13.30×10^6 psi. Ryshkewitch (1960) found a maximum modulus of elasticity of 33.10×10^6 psi for zircon in a separate investigation. On this basis it appears that the Griffith criteria for the materials of McKee and Adams is below the knee of the locus of the Griffith criteria as the effective modulus of elasticity is only 50 percent of the intrinsic.

After establishing the initial fracture strengths and the moduli of elasticity, the remaining specimens were exposed to various temperature differentials. The fracture strengths and moduli of elasticity of these specimens were subsequently determined. A representation of these data is presented in Figures 14 and 15. From Figure 14 it is obvious that large changes in the modulus of elasticity did not occur as they did in Hasselman's data. These smaller changes are to be expected as previously discussed if the Griffith criteria for the given material lies below the knee of the locus. Perhaps the data in Figure 15 are more to the point. After the critical temperature differential of 300 deg C. is reached the percentage decrease in strength increases constantly with increasing temperature differential from a value of zero at 300 deg C. to 44 percent

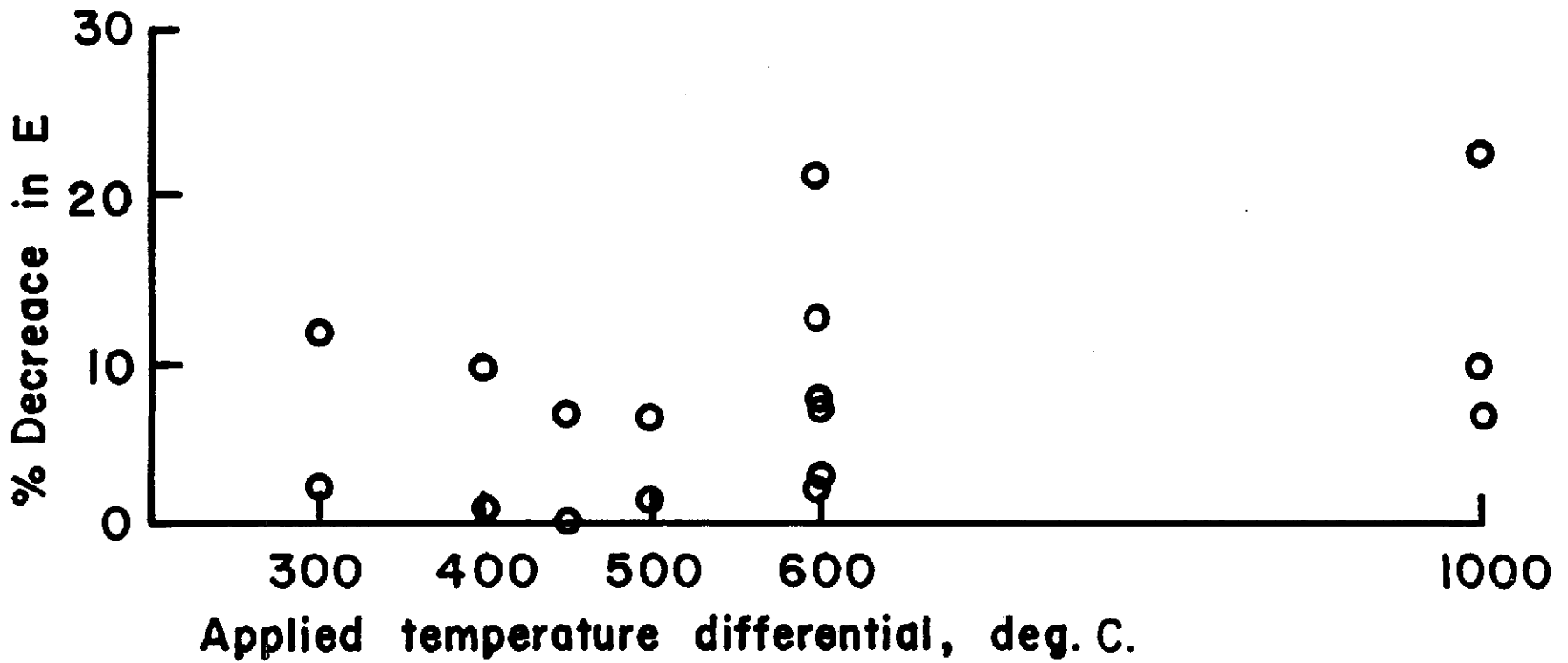


Figure 14. Applied temperature differential vs. percentage decrease in modulus of elasticity for zircon (after McKee and Adams, 1950, from tabular data)

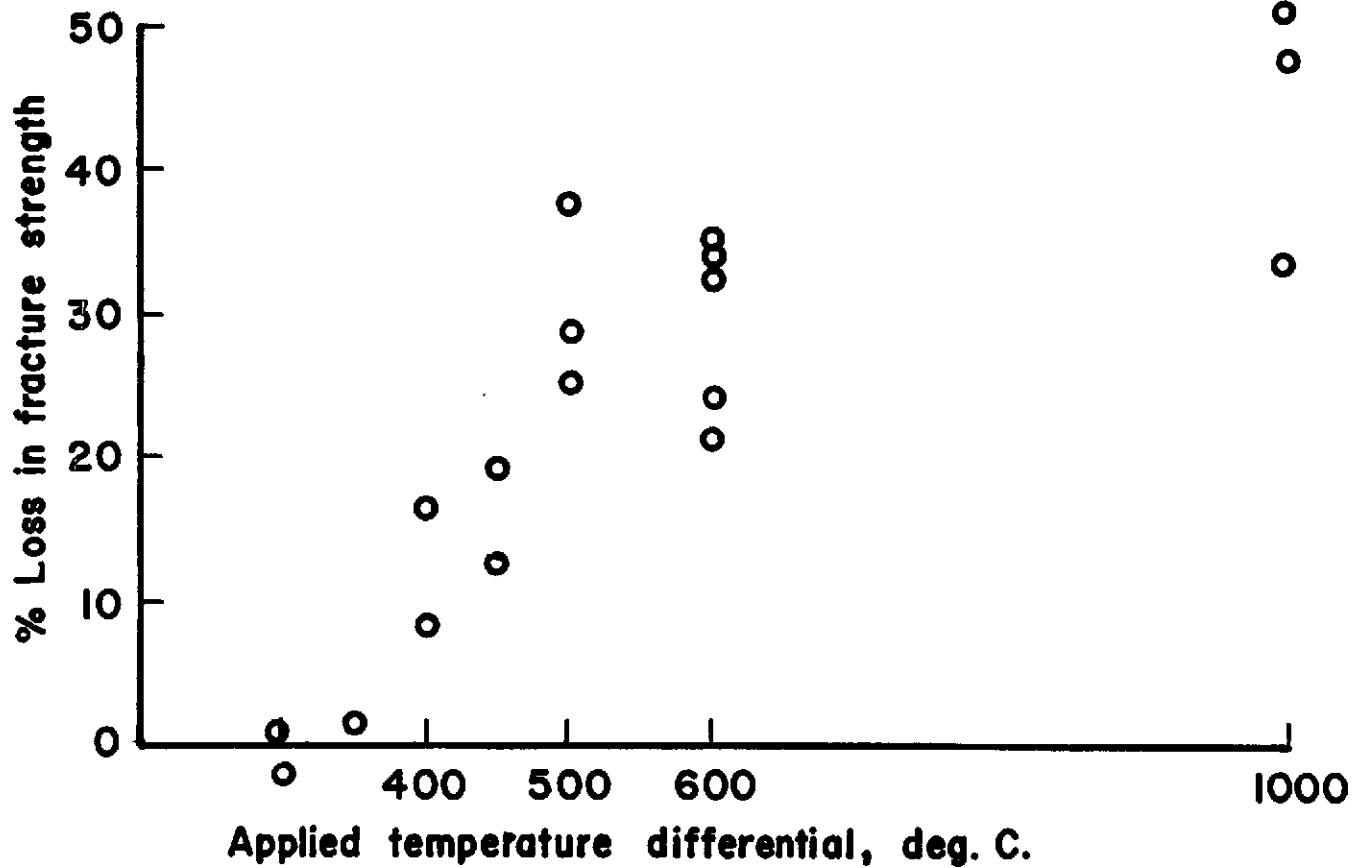


Figure 15. Applied temperature differential vs. percent loss in strength of zircon after thermal shock exposure (after McKee and Adams, 1950, from tabular data)

at 1000 deg C. That is to say that the cracks grow in a "quasi-static" manner as suggested by Hasselman (1969b) and the large initial decrease in strength due to the large "excess" kinetic energy is avoided as the present model suggests.

The amount of thermal shock damage for this material is then a direct result of the amount of overstressing (that is, the amount of stress above the Griffith stress) as the result of the thermal stresses generated by the temperature differential. As a result "catastrophic" decreases in strength do not occur.

Triaxial bodies were fired by Chaudhuri and Chatterjee (1968) which also appear to have mechanical properties associated with a Griffith criteria below the knee of the locus. Again, bend strengths were measured on both shocked and unshocked specimens. Unfortunately the modulus of elasticity was measured on only unshocked specimens. The specimens were shocked by slowly heating to 900 deg C. and subsequently quenching in still air for ten cycles. Figure 16 indicates that this temperature differential results in larger percentage decreases in strength for the weakest and the strongest materials and that the lowest percentage decreases occurred in materials having intermediate strengths.

The percentage decrease in the transverse strength varied linearly with the modulus of elasticity as may be seen in Figure 17. Similarly the decrease in strength varied linearly with the coefficient of thermal expansion (Figure 18). The decrease in transverse strength was subsequently plotted against the strength to modulus of elasticity ratio (or strain to failure) and against the strain to failure:coefficient of thermal expansion ratio.

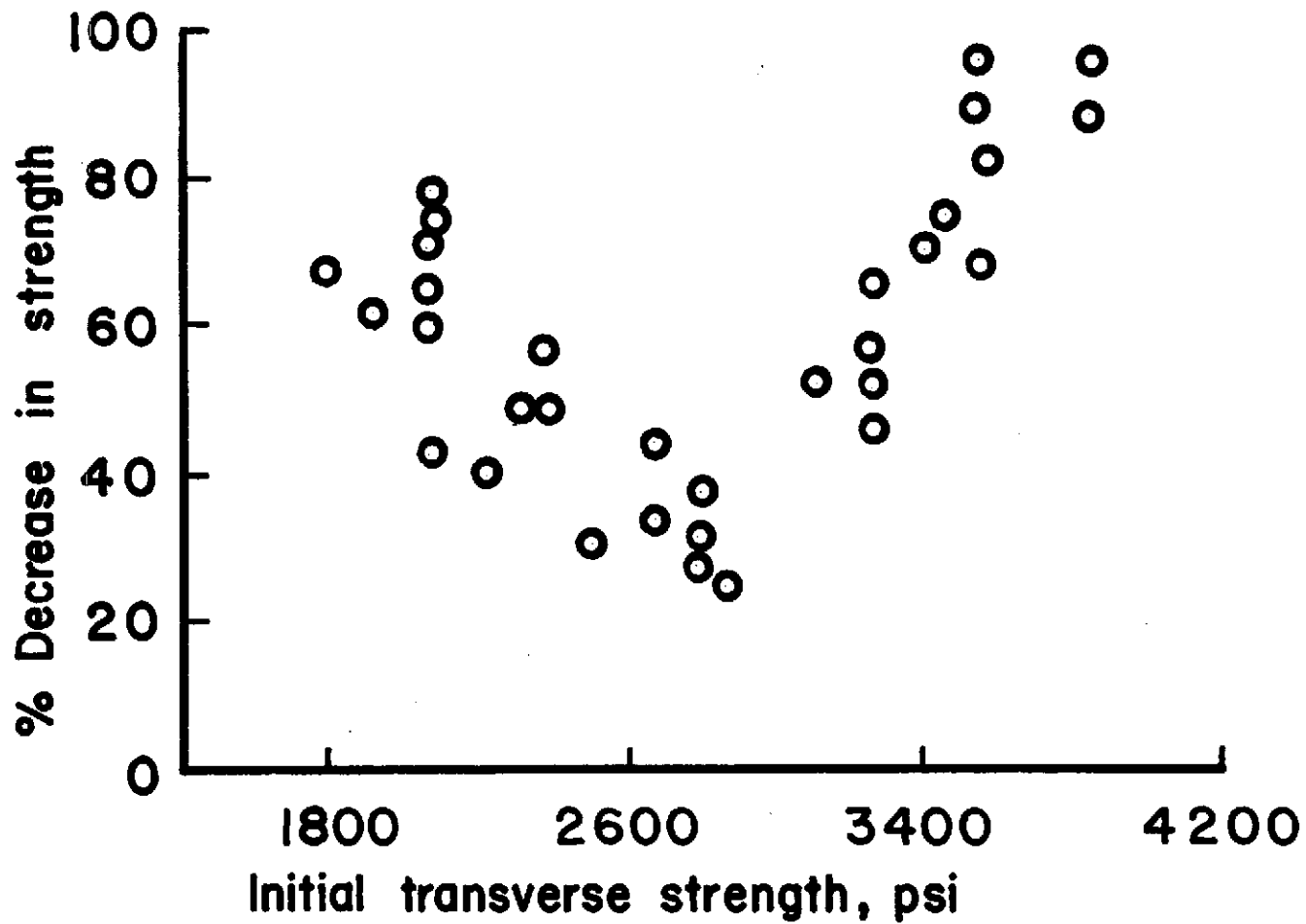


Figure 16. Relationship between mechanical strength and spalling loss (after Chaudhuri and Chatterjee, 1968)

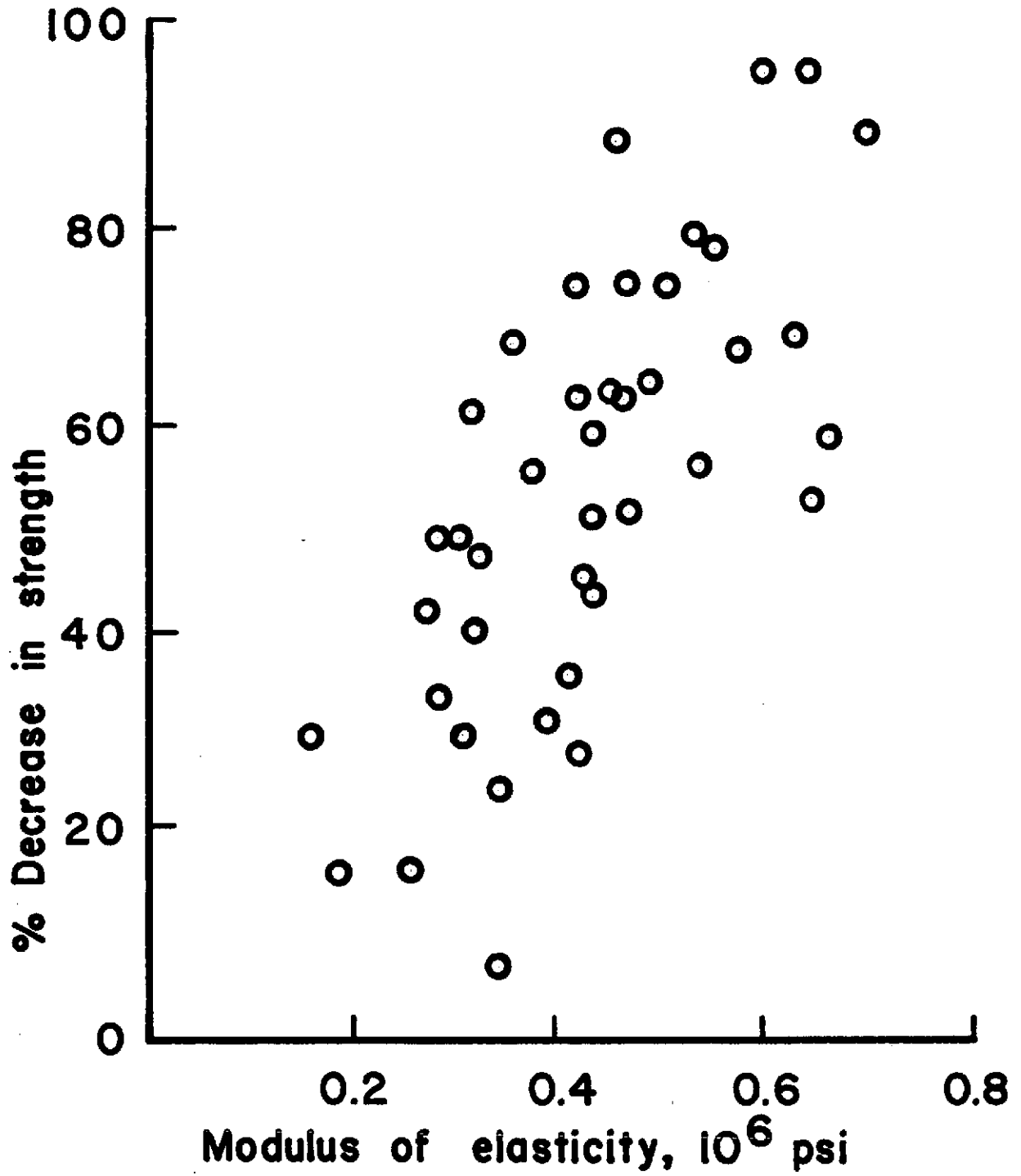


Figure 17. Relationship between modulus of elasticity and spalling loss (after Chaudhuri and Chatterjee, 1968)

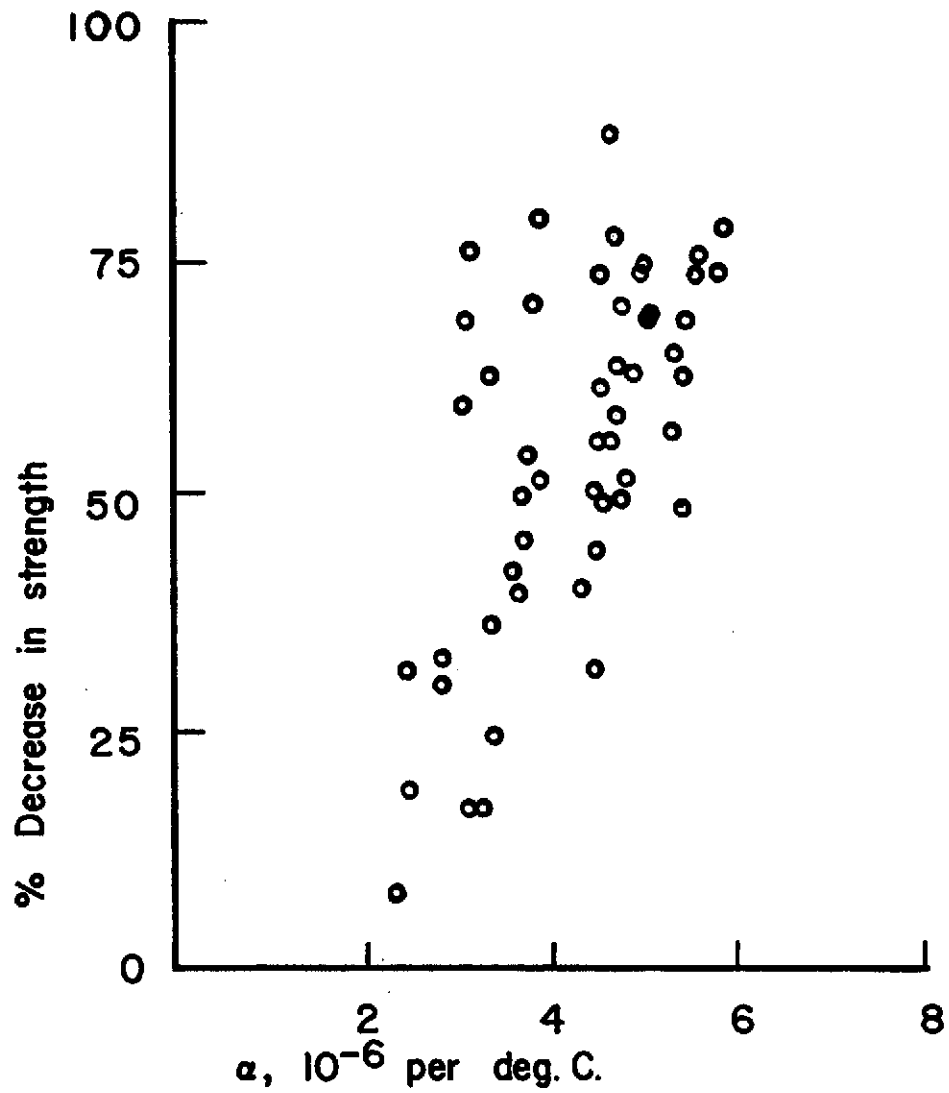


Figure 18. Relationship between coefficient of linear thermal expansion and spalling loss (after Chaudhuri and Chatterjee, 1968)

It is obvious from Figure 16 that the critical temperature differential has been reached as all specimens experienced decreases in transverse strength. What is not as obvious is the amount of stressing above the Griffith stress. Nonetheless, it is significant that for the given experimental conditions neither the weakest nor the strongest materials were the most thermal shock damage resistant but that an intermediate strength material was.

The decrease in strength appears to be strongly related to the initial modulus of elasticity as shown in Figure 17. The percentage decrease in the initial strength is clearly larger for higher moduli of elasticity. It should be recalled from the present model that for a given material the Griffith criteria on the lower portion of the locus indicates that the modulus of elasticity decreases as the criteria moves away from the knee. The Griffith stress also decreases slowly but the strain to failure and consequently the critical temperature differential increases. Furthermore, recalling that in this region of the locus of the Griffith criteria, the amount of crack growth and subsequently the decrease in strength is directly related to the amount of overstressing, it follows from the model that, for a given temperature differential large enough to produce a stress equal or larger than the Griffith stress, the decrease in strength will be greater for the materials having the higher moduli of elasticity. This is a direct result of the applied temperature differential becoming increasingly nearer the critical temperature differential when the modulus of elasticity and subsequently the Griffith stress decreases as a result of the growth of flaws or cracks.

The above results are shown in Figure 19 as percent decrease in strength vs. the strength to modulus of elasticity ratio. Although a large amount of scatter is present in the data, the figure indicates that larger strains to failure give lower percentage decreases in transverse strength as predicted above. Here it must be recalled that a range of compositions was employed in this investigation. Thus some variation in the relative position of the locus of the Griffith criteria may be present and thus the amount of stressing above the Griffith stress for a given strain to failure may vary from composition to composition with the result being larger or smaller decreases in strength. Here the major portion of the data scatter may be attributed to variations in the coefficients of thermal expansion.

The strong relationship between the coefficients of thermal expansion and the losses of transverse strength is shown in Figure 18. Those materials having high coefficients of thermal expansion also have high losses in strength. Thus if these data are applied as suggested by the present model in the strain to failure:coefficient of thermal expansion ratio then the scatter in data in Figure 19 is reduced as shown in Figure 20. Here high losses in strength are associated with low strain to failure:coefficient of thermal expansion ratios (more specifically, lower "temperature differentials"). Again the amount of overstressing above the Griffith stress for the applied thermal gradient and the "damage" or loss of strength is directly related to the overstressing. Here again the scatter may be attributed to the variations in compositions. If it were possible to separate the data and plot the results separately then there should be considerably less scatter in the data.

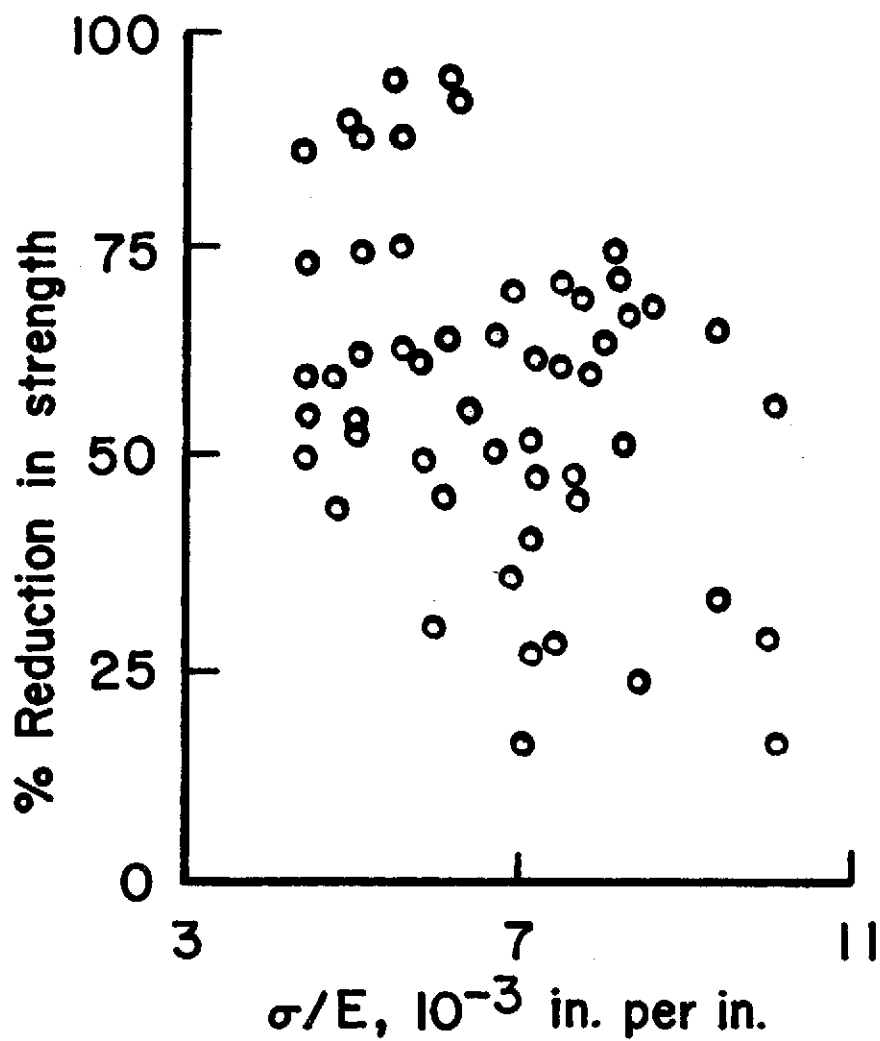


Figure 19. Relationship between σ/E and spalling loss (after Chaudhuri and Chatterjee, 1968)

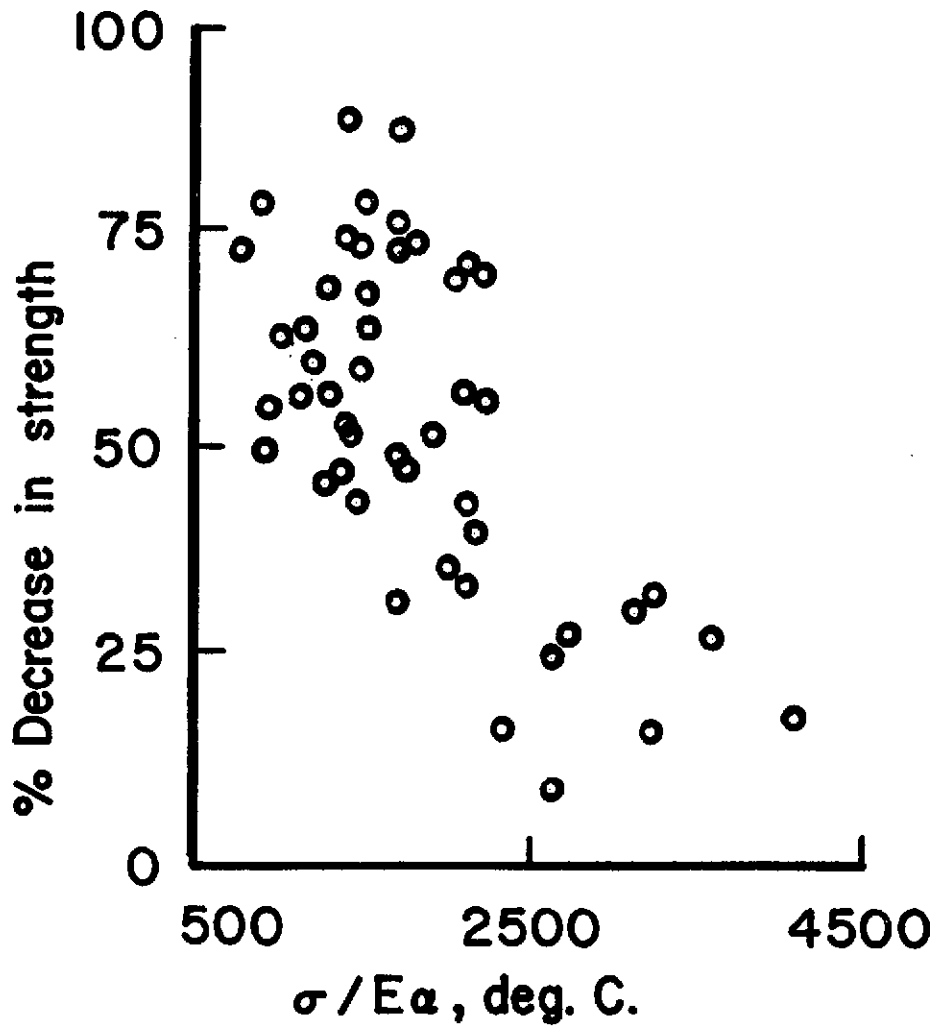


Figure 20. Relationship between $\sigma/E\alpha$ and spalling loss (after Chaudhuri and Chatterjee, 1968)

Chaudhuri and Chatterjee (1968) have attributed the behavior of these materials to the presence of microcracks formed during processing. The specimens giving higher percentages of loss of strength at lower strengths in Figure 16 were those specimens higher in alumina while those giving higher percentages at higher strengths were higher in silica content. They indicated that higher silica or glassy content of these materials gave less flexibility and favored crack growth in these bodies.

Parmelee and Westman (1928) had performed, at an earlier time, similar experiments on several commercial firebricks of more nearly the same composition. These bricks were heated to 1100 deg C. and were thermally shocked by subjecting one face of the brick to an air blast. The transverse strength of both shocked and unshocked bricks were obtained and their results are presented in Figure 21. Unfortunately the moduli of elasticity were not measured.

The data suggests that the Griffith criteria of these materials lies below the knee of the locus. It appears again that the applied temperature differential is sufficiently large to produce a stress exceeding the Griffith stress such that flaws grow "quasi-statically" in size. As indicated by Figure 21 the bricks having higher initial strengths and presumably having Griffith criteria lying near the knee suffer larger percentages of loss of strength. It is significant here that the final strengths of the initially stronger materials are generally higher than those of the initially weaker bricks. That is to say that the thermal shock damage is not "catastrophic."

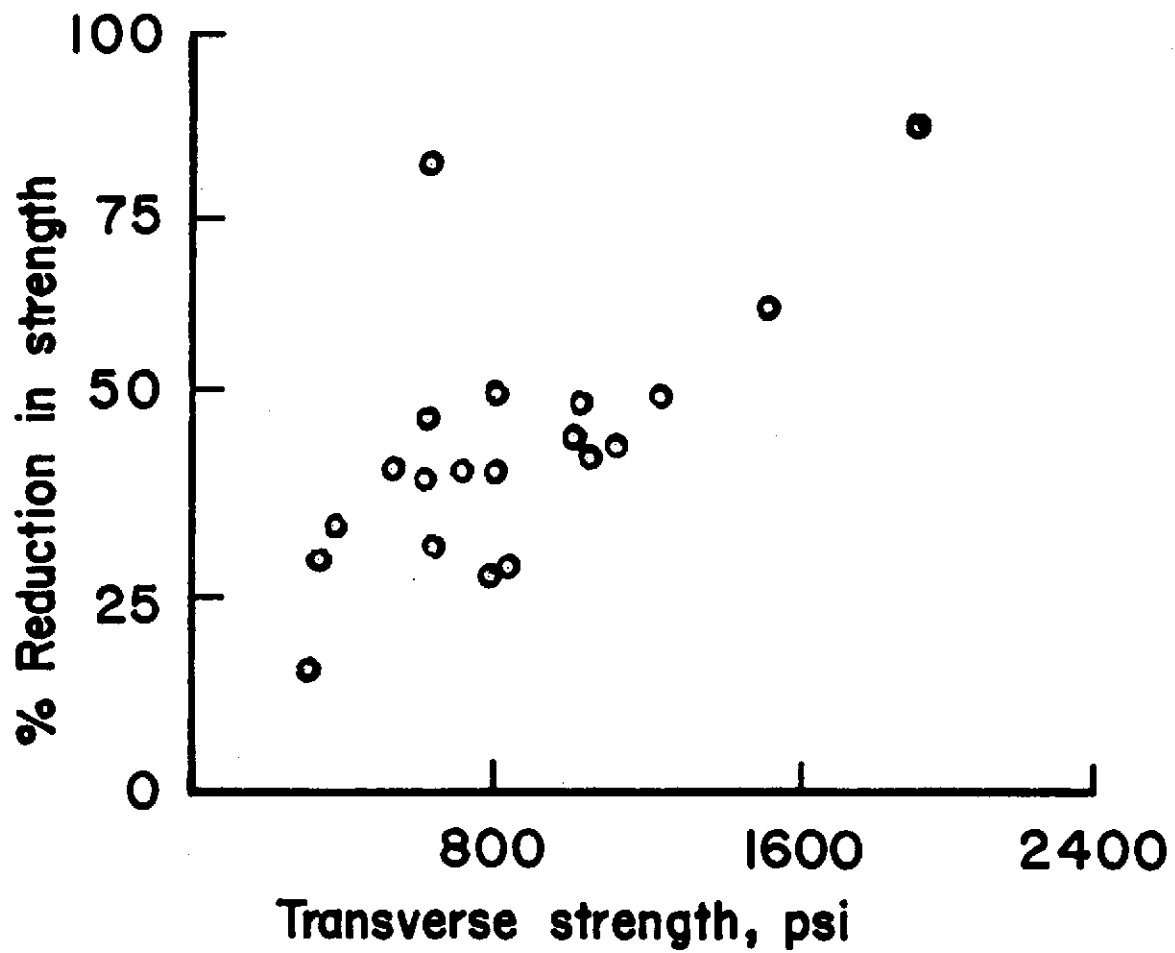


Figure 21. Effect of thermal shock on fracture strength
(after Parmelee and Westman, 1928)

Several years later Morgan (1931) performed similar experiments on similar firebricks and obtained similar results as shown in Figures 22, 23, and 24. Again the percentage reduction in transverse strength as a result of thermal shock exposure is larger for the initially higher transverse strength materials as shown by Figure 23. Here, for the very strongest bricks the final strengths are lower for the initially stronger bricks than for the initially medium strength bricks as shown in Figures 22 and 24. This type of behavior is hinted at in the data of Parmelee and Westman (1928) (Figure 21) and may be seen in the data of Chaudhuri and Chatterjee (1968) (Figure 16) if it is replotted as in Figure 25. As discussed by these latter investigators, this behavior may be due to the effects of the microstructure upon crack propagation in the various compositions.

It should be noted that the behavior of the Chaudhuri and Chatterjee materials and the Morgan materials is not identical. Those of Morgan which have low initial strengths suffer very small reductions in strength such that the initial and final transverse strengths extrapolate to zero while those of Chaudhuri and Chatterjee suffer larger losses in strength and do not extrapolate to zero. The variations in compositions of the Morgan materials are probably smaller such that the locus of the Griffith criteria are more nearly the same for these materials. The present model would then suggest that these initially low strength materials have Griffith criteria further from the knee such that the critical temperature differential is higher and a smaller reduction in strength results as a result of the given applied temperature differential. With

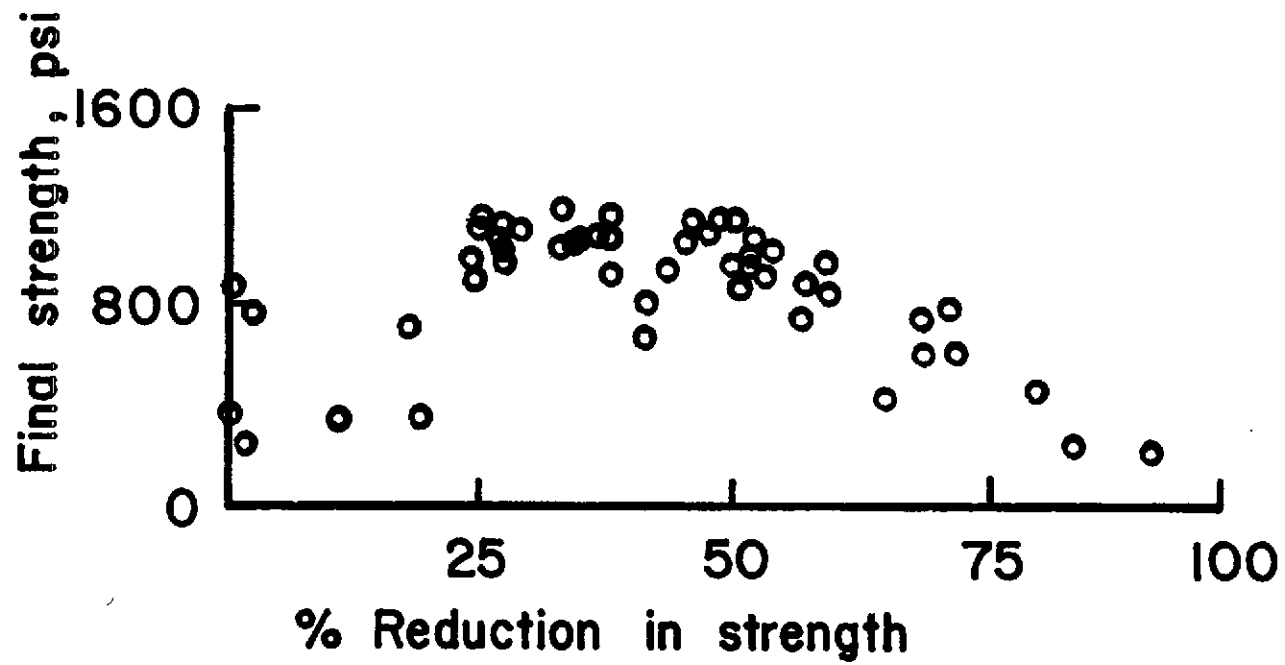


Figure 22. Experimental data showing relation between final strength and percent reduction in strength (after Morgan, 1931)

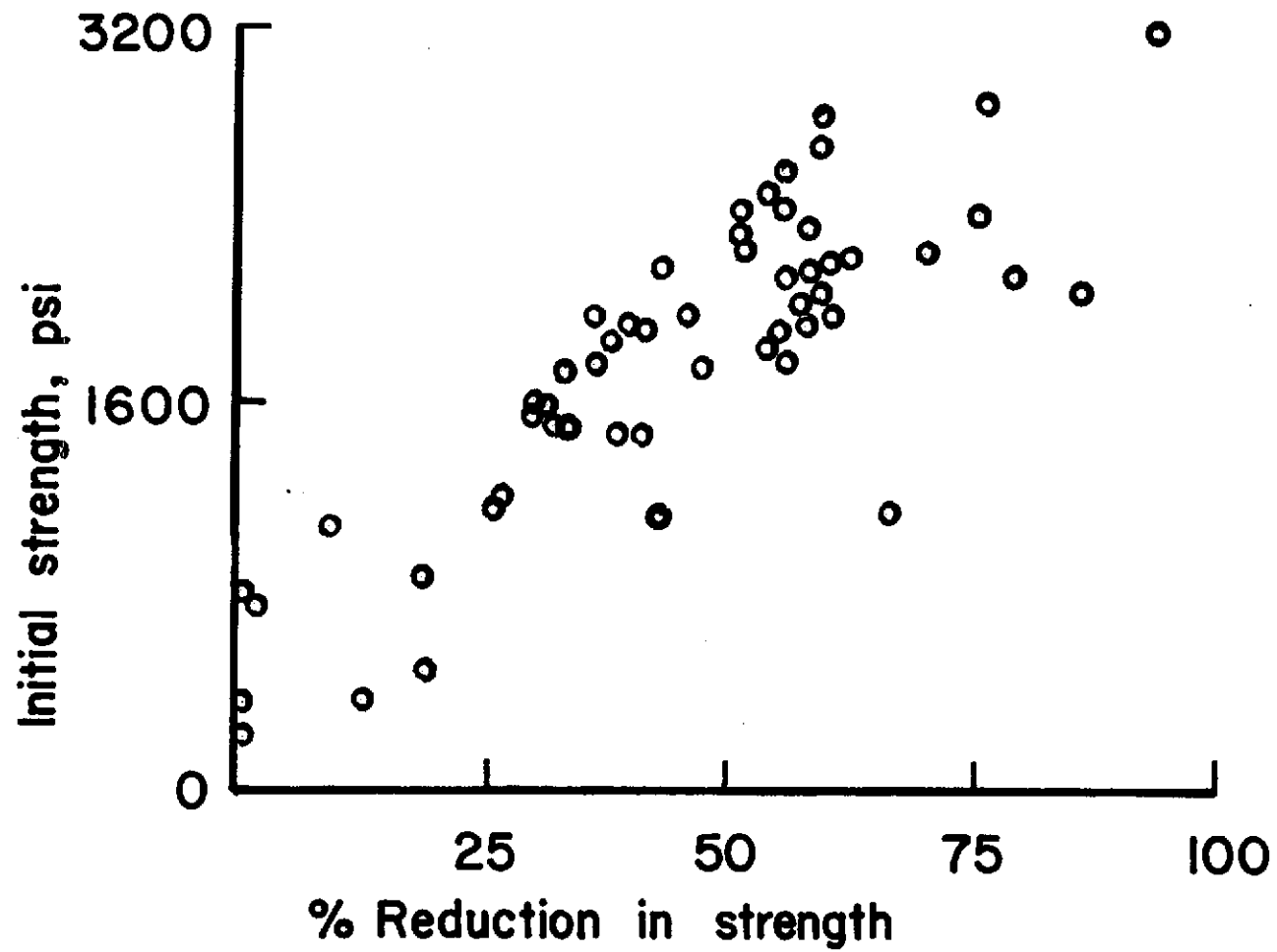


Figure 23. Experimental data showing relation between initial strength and percent reduction in strength (after Morgan, 1931)

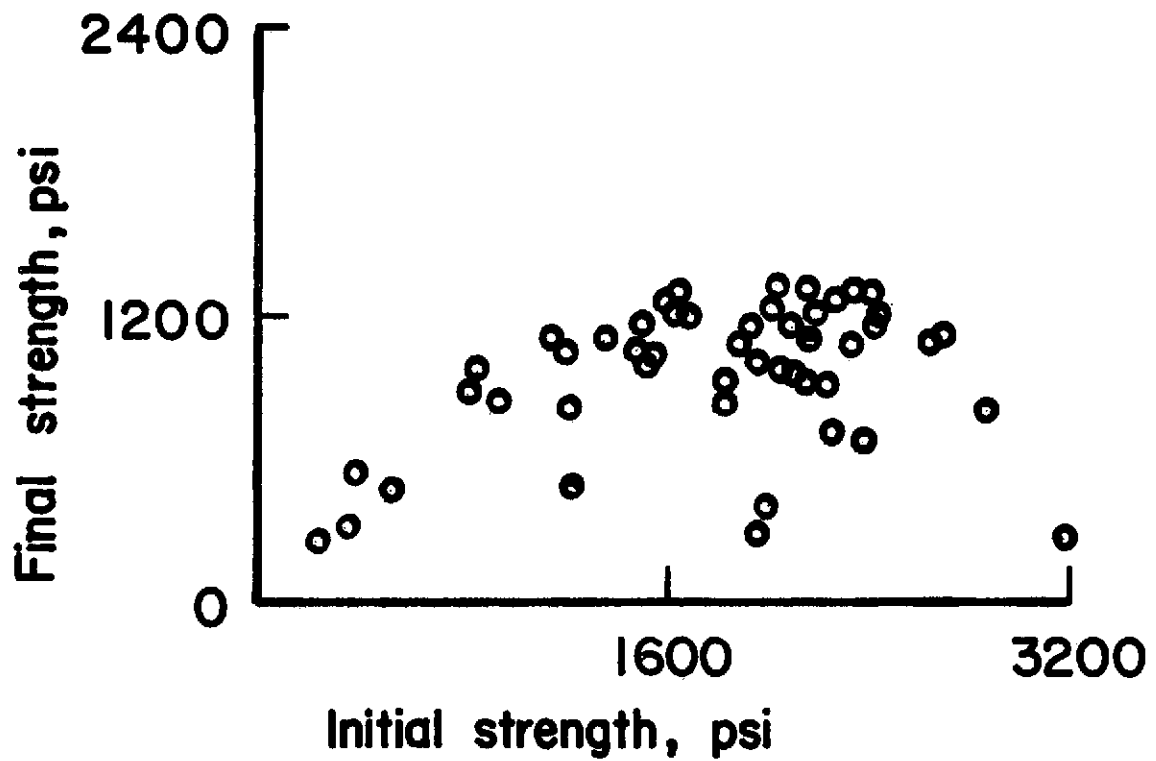


Figure 24. Experimental data showing relation between initial and final strength (after Morgan, 1931)

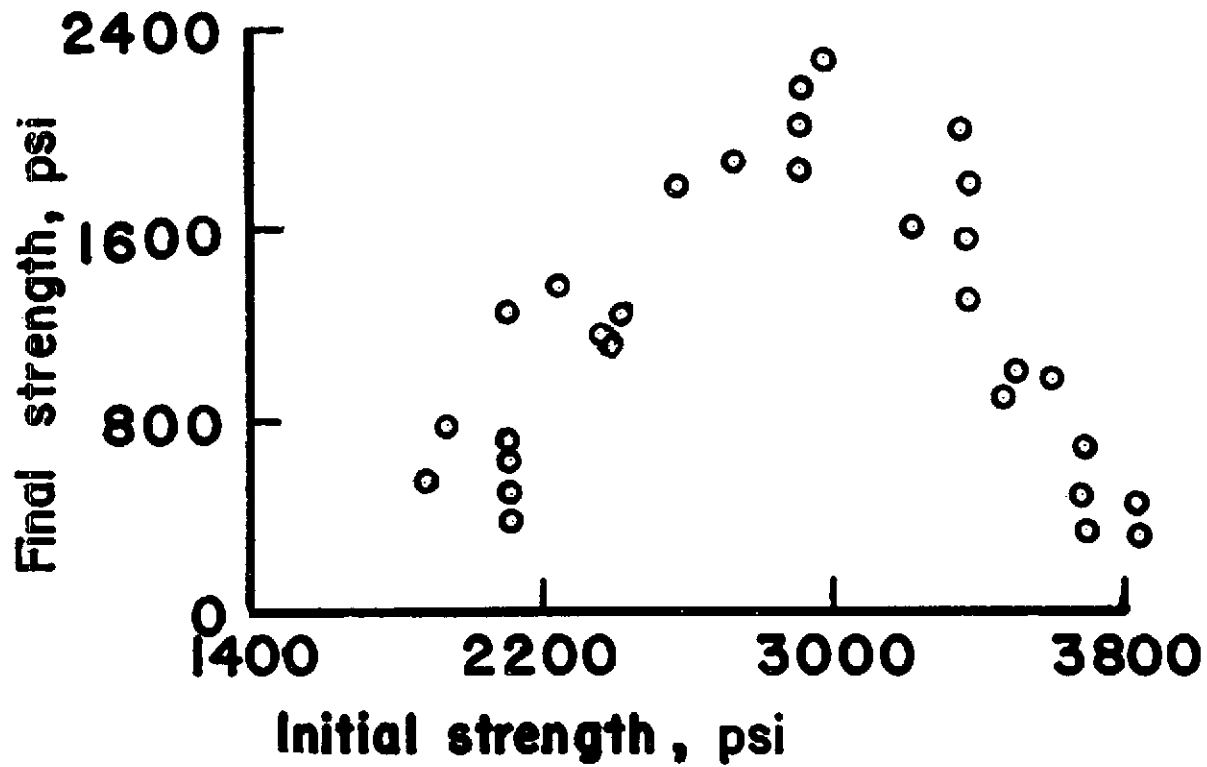


Figure 25. Initial transverse strength vs. final transverse strength after thermal shock exposure for various triaxial bodies (after Chaudhuri and Chatterjee, 1968)

the Chaudhuri and Chatterjee materials, on the other hand, the Griffith criteria of the weaker materials were probably nearer the knee than the weaker Morgan materials such that for the applied temperature differential a greater degree of damage was done on the Chaudhuri and Chatterjee materials.

The present model may be used to analyze thermal spalling resistance data in a manner similar to the above. If, for a given material, the measured mechanical properties are determined before the thermal exposure, the spalling trend may often be predicted. Nakayama and Ishizuka (1966) recently presented some data for high alumina firebricks which may so be analyzed. These investigators heated spall resistant, clay bonded (A and B type) and normal clay bonded (D and E type) firebricks as well as normal chamotte firebricks to 1200 deg C. and subsequently quenched them in running water. The bricks were cycled until five percent body weight was lost due to spalling. They reported that bricks of the A and B types were able to survive more than fifteen cycles, while bricks of the D and E types were able to survive more than five cycles. The chamotte bricks (C type) were able to survive more than seven cycles.

Using the data from Table 1 the strain to failure:coefficient of thermal expansion ratios (calculated temperature differentials) for these materials are as follows:

- A type - 39 deg C
- B type - 49 deg C.
- C type - 43 deg C.
- D type - 56 deg C.
- E type - 107 deg C.

Table 1. Physical property data for firebricks (Nakayama and Ishizuka, 1966, data)

Brick	Strength, σ_f	Coefficient of Thermal Expansion	Modulus of Elasticity, E
	kgms/sq cm	per deg C.	kgms/sq cm
A	40	6.7×10^{-6}	1.5×10^5
B	40	5.4×10^{-6}	1.5×10^5
C	40	6.2×10^{-6}	1.5×10^5
D	180	5.3×10^{-6}	6.0×10^5
E	170	5.3×10^{-6}	3.0×10^5

The immediate implication of this ratio is that the thermal shock resistance of D and E type bricks is superior and it is probably a correct assumption. The implication that the thermal spalling resistance is superior is obviously not correct as the weaker bricks are more spall resistant. The present model may be used to eliminate the discrepancy.

The modulus of elasticity of the D and E type bricks are four and two times greater than those of the A, B, and C type. The fracture strengths of these former two are also four times higher. The higher values of these strengths and moduli of elasticity suggest that the Griffith criteria for these two materials lie above the knee of the locus. Due to the fact that spalling occurs it is obvious that the Griffith stress has been reached for all the materials. The critical temperature differentials are significantly higher for the D and E types than for the A, B, and C types but the present model indicates that they would fail "catastrophically" if their Griffith criteria are

located above the knee. That is to say that the "damage" or crack growth is larger for D and E type bricks. As a result more thermal spalling may be expected to occur per cycle. That is to say that for these materials the most thermal shock damage resistant are the least spall resistant materials.

Nakayama and Ishizuki indicated that they believed the behavior of these materials to be related to the method of growth of cracks in the materials. They measured the effective fracture energy and applied these values to Hasselman's (1970b) thermal shock damage resistance factor with good results.

Earlier Heindl and Pendergast (1957) performed panel spalling tests on twenty-four brands of fireclay plastic refractories. The transverse strength and modulus of elasticity were measured before spall tests in four point bending. No properties were measured after the spall tests. The modulus of elasticity of these materials is plotted against the modulus of rupture in Figure 26. The nearly straight line relationship indicates that the Griffith criteria for these materials is below the knee of the locus and that failure can be expected to be "quasi-static" in nature. It appears that the plot in Figure 26 may be leveling at the higher values of the moduli of elasticity and this may indicate that these values are near the knee of the locus.

Although a large amount of scatter is present in the data, Figure 27 indicates that the spalling loss is greater for the stronger materials. Similar results were observed in the data of Nakayama and Ishizuki. Figure 28 indicates that for the materials investigated by Heindl and Pendergast spalling loss was higher for materials having higher moduli

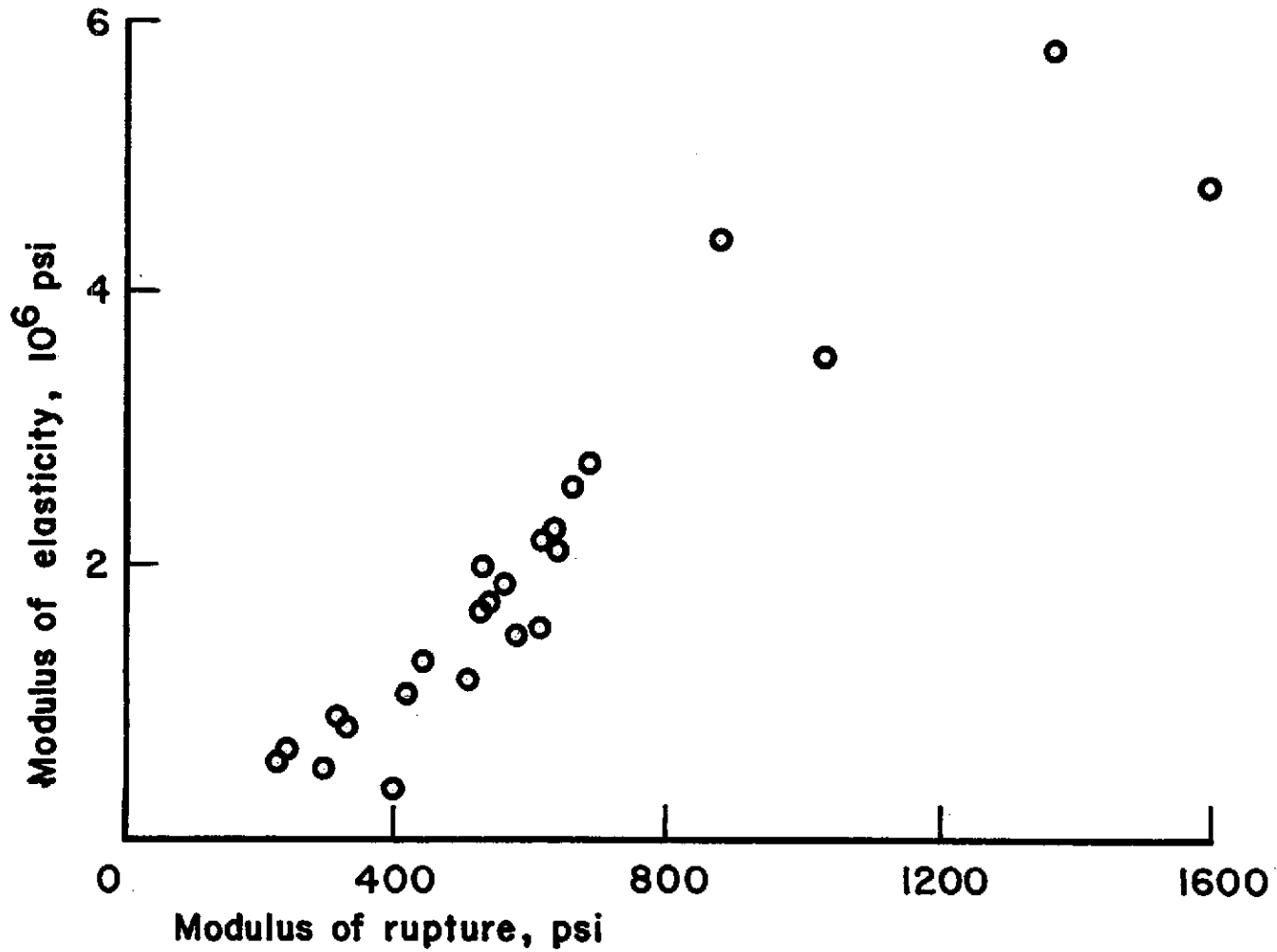


Figure 26. Modulus of rupture vs. modulus of elasticity for selected fireclay plastic refractories (after Heindl and Pendergast, 1957, from tabular data)

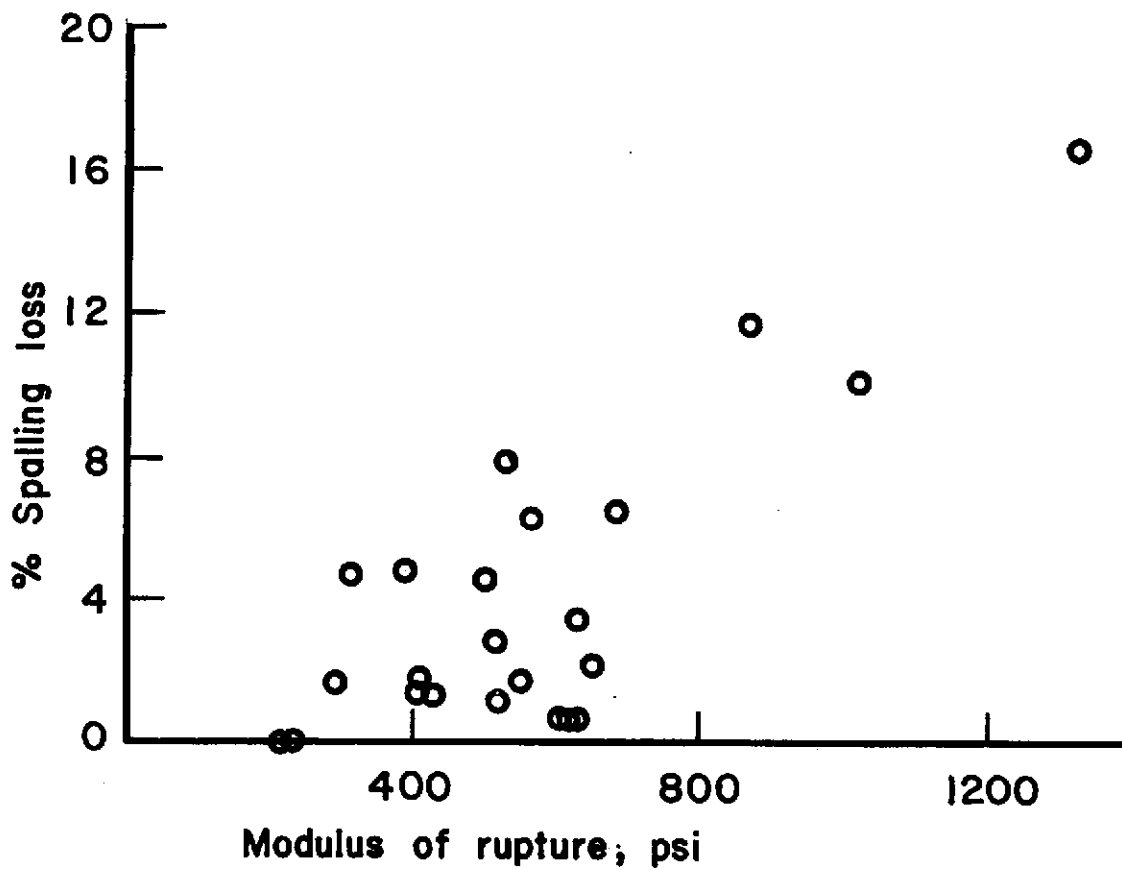


Figure 27. Modulus of rupture vs. percent spalling loss for selected fireclay plastic refractories (after Heindl and Pendergast, 1957, from tabular data)

of elasticity. Again the results are similar to those of Nakayama and Ishizuki. If the modulus of rupture:modulus of elasticity ratio is plotted against spalling loss for the data of Heindl and Pendergast as in Figure 29 it may be observed that, unlike the data of Nakayama and Ishizuki, the spalling loss is greater for lower strains to failure. Again a large amount of scatter exists in the data as it did for the similar materials of Chaudhuri and Chatterjee in the similar plot in Figure 19. Heindl and Pendergast did not measure the coefficients of thermal expansion but if these values were available it is reasonable to assume that the plot of strain to failure:coefficient ratio vs. percentage spalling loss would show less scatter.

These data of Heindl and Pendergast appear contradictory to those of Nakayama and Ishizuki at first glance because the previously discussed ratio or critical temperature differential is larger for lower amounts of spalling in the former's data and smaller for lower amounts of spalling in the latter's data. Again, the present model appears to explain the contradiction. If the Griffith criteria for Heindl and Pendergast's materials lie below the knee of the locus then the critical temperature differential increases as the modulus of elasticity and fracture strength decrease. Then for a given specimen geometry and applied temperature differential the lesser strains to failure result in larger overstresses and as a result, larger amounts of thermal shock damage or in this case larger amounts of spalling occurs. That is to say that the stronger materials are the most susceptible to spalling damage but but for different causes.

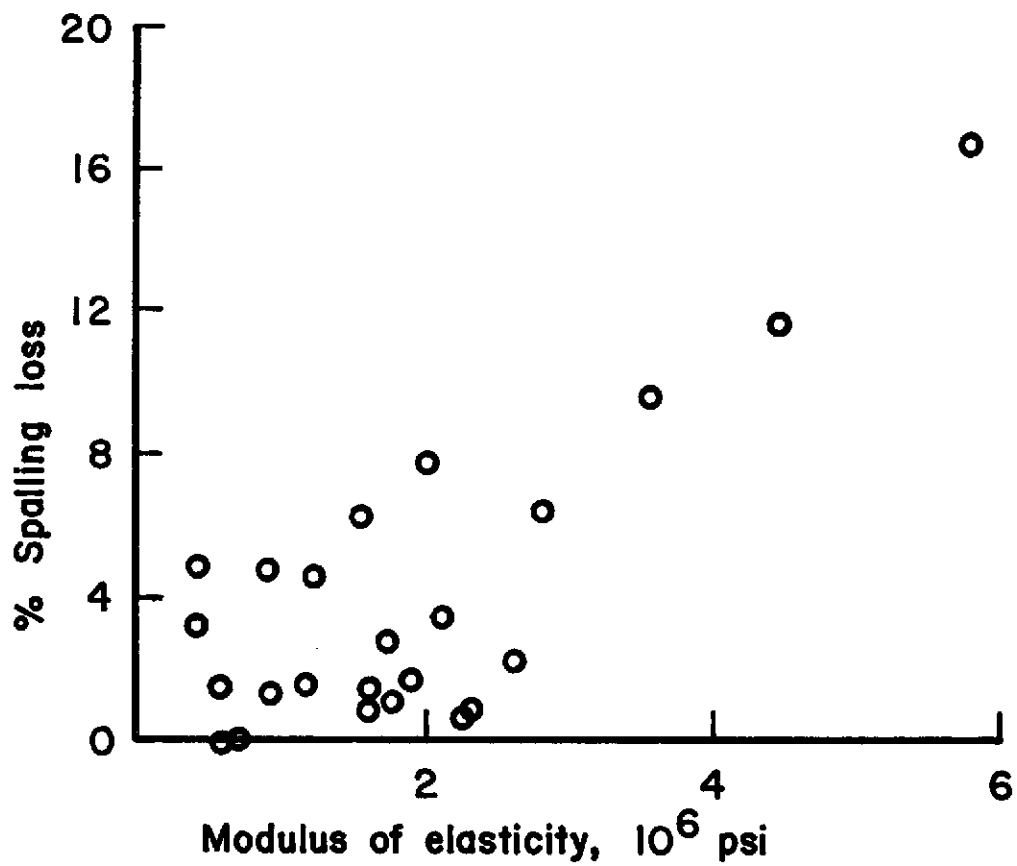


Figure 28. Modulus of elasticity vs. percent spalling loss for selected plastic refractories (after Heindl and Pendergast, 1957, from tabular data)

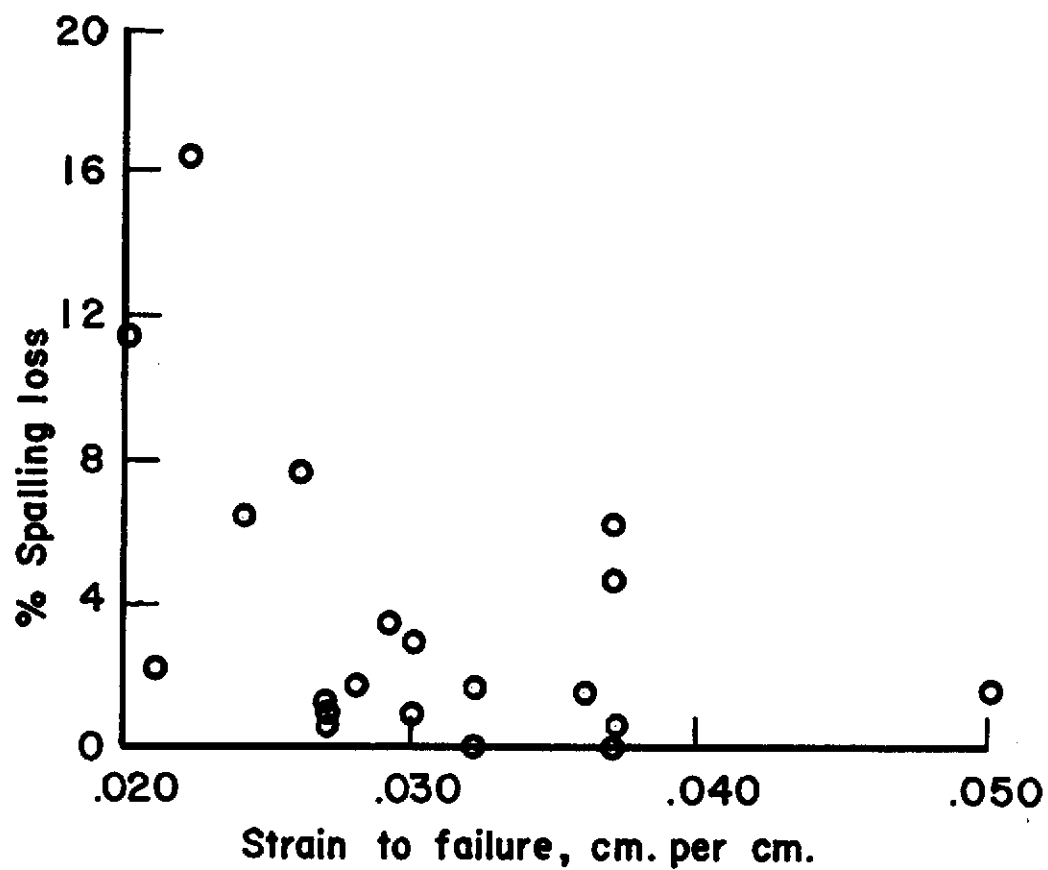


Figure 29. Strain to failure vs. percent spalling loss for selected fireclay plastic refractories (after Heindl and Pendergast, 1957, from tabular data)

Earlier Norton (1925) working with firebricks had observed that "small increases in flexibility greatly increases the resistance to spalling." He slowly heated bricks to 2900 def F. and cooled them in a stream of air. They were cycled until "observable" spalling damage occurred. He measured the shearing strain and shear modulus as well as the coefficients of thermal expansion and these data are presented in combined form in Figure 30. Here the number of cycles to produce "observable" damage increases as the critical temperature increases which indicates behavior similar to that observed both by Heindl and Pendergast and by Chaudhuri and Chatterjee.

The term thermal shock resistance is perhaps most accurately applied when it is used as a measure of the temperature differential necessary to initiate thermal shock damage. A large volume of data has been gathered concerning this phenomenon. Unfortunately most of the analysis of these data has been performed on the basis of materials parameters reported elsewhere and not on materials parameters measured on the materials at hand. The heat transfer conditions also hamper the analysis as the thermal stresses are usually transient. That is to say that few tests, if any, are truly constant strain tests.

Twenty years ago Schwartz (1952) studied the thermal shock resistances of three refractory oxides: alumina, zirconia (ZrO_2), and magnesia (MgO). Hollow tubes of these oxides were heated until fracture occurred and the temperatures necessary to produce these failures were noted. The tensile strengths, moduli of elasticity, and coefficients of thermal expansion were measured on the test materials and the results are tabulated in Table 2.

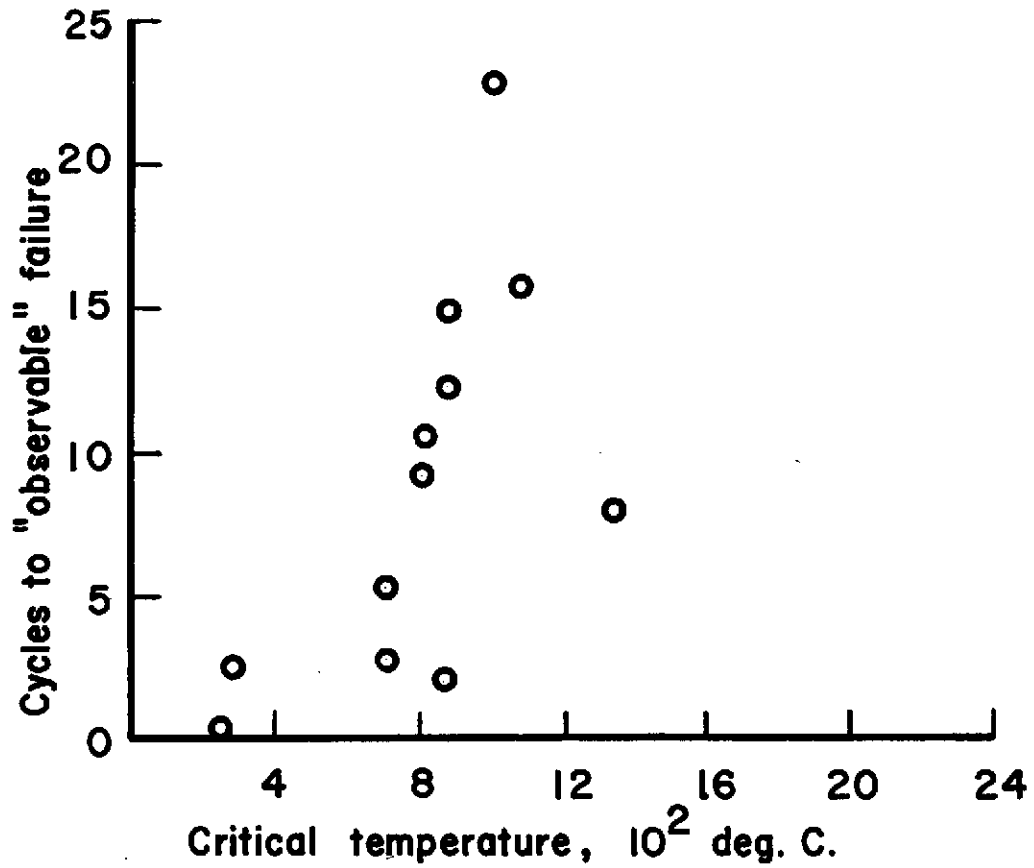


Figure 30. Number of cycles to failure vs. critical temperature differential for selected firebricks (after Norton, 1925, from tabular data)

Table 2: Physical property data for alumina, zirconia, and magnesia (Schwartz mechanical properties data)

Material	Tensile Strength	Modulus of Elasticity	Coefficient of Linear Thermal Expansion	Temperature Differential
	psi	psi	per deg C.	deg C.
Al_2O_3	21×10^3	51×10^6	5.5×10^{-6}	85
ZrO_2	20×10^3	21.5×10^6	6.7×10^{-6}	185
MgO	14×10^3	30×10^6	10.0×10^{-6}	50

The modulus of elasticity of alumina is very high and the Griffith criteria is certainly above the knee of the locus while that of zirconia is probably below the knee of the locus on the basis of a theoretical modulus of elasticity of approximately 36×10^6 psi (Smith and Crandall, 1964). On this basis alone it may be expected that alumina will fail "catastrophically" while zirconia will fail "quasi-statically."

If the simplistic assumption is made of one dimensional constant strain, then the calculated critical temperature differentials to initiate fracture are as follows:

Al_2O_3	-	74 deg C.
ZrO_2	-	185 deg C.
MgO	-	50 deg C.

These values are in excellent agreement with those given in Table 2 as measured values taken near room temperature. While the alumina and zirconia materials have the same fracture strengths, the zirconia has

a critical temperature differential nearly twice that of alumina as a result of the lower modulus of elasticity. Magnesia, on the other hand, has a critical temperature differential of slightly more than one-half that of alumina even though the strain to failure (strength to modulus of elasticity ratio) are very nearly equal. The difference in thermal shock behavior is due to the coefficients of thermal expansion. The coefficient for magnesia is nearly twice that of alumina and the critical temperature was nearly one-half that of alumina as a result.

Schwartz made similar tests at higher temperatures and obtained similar results when the high temperature mechanical properties were employed. On the basis of the low values for the modulus of elasticity of zirconia and the high value for alumina it appears that, on the basis of the present model, a material under the knee of the locus of the Griffith criteria and containing a significant number of flaws has more thermal shock resistance than does a dense, strong material having a Griffith criteria above the knee. Ryshkewitch (1960) has commented upon the superior thermal shock resistance of zirconia having similar properties:

A low modulus of elasticity means a correspondingly great elastic deformability of sintered zirconia, considerably greater than that of sintered alumina. Therefore, balls of sintered zirconia, bounced to the floor, jump back almost like solid rubber balls, without breaking or cracking. The high elastic deformability of sintered zirconia explains its surprisingly good thermal shock resistance, in spite of the low heat conductivity and great thermal expansion (Ryshkewitch, 1960, p.380).

Davidge and Tappin (1967) later quenched into water a number of fully dense materials to determine the critical temperature differentials

and they measured the mechanical properties of unquenched materials. Although primary attention was paid to alumina, seven other materials listed in Tables 3 and 4 were investigated. The results are shown in Figure 31 where the applied critical temperature differential is plotted against their stress resistance factor or calculated critical temperature differential:

$$R = \frac{\sigma_{fs} (1-\nu)}{3 E\alpha} \quad \text{deg C.}$$

There appears to be excellent agreement between the value of the calculated critical temperature differential and the applied value. As was the case with the alumina of Schmidt, the applied critical temperature differential was larger for alumina than for magnesia. The excellent thermal shock resistance of silicon nitride (Si_3N_4) is shown here.

In view of the present model all the materials tested appear to have Griffith criteria above the knee of the locus. The thermal shock resistance of these materials is then dependent upon high fracture strengths, low intrinsic moduli of elasticity, and low coefficients of thermal expansion or more specifically the ratio of the first to the product of the latter two. The failures were "catastrophic" in these materials as large cracks were observed to occur at failure.

The importance of the ratio described above is borne out by the above investigation. The most thermal shock resistant material investigated was not the strongest (silicon nitride) but a rather mediocre strength material (silica glass). The high critical temperature differential was due to the extremely low coefficient of thermal expansion.

Table 3. Properties of various ceramic materials (after Davidge and Tappin, 1967)

Material	Fracture Strength (σ_b)	Young's Modulus (E)	Coefficient of Linear Thermal Expansion (α)	Critical Temperature (T_c)	Thermal Stress Resistance Parameter $\sigma_b(T-v)/3E\alpha$
	10^9 dyn.cm^{-2}	$10^{12} \text{ dyn.cm}^{-6}$	$10^{-6} \text{ }^\circ\text{C}^{-1}$	$^\circ\text{C}$	$^\circ\text{C}$
Sodium Chloride	0.5	0.4	40	95	8
Magnesia	1.9	3.0	13.5	125	12
Various Aluminas	See Table 4 for data		8.0	180 to 220	17 to 59
Bone China	0.9	0.96	8.0	215	29
Borosilicate Glass	1.4	0.61	3.3	275	185
Si_3N_4 ($d=2.2 \text{ g.cm}^{-3}$)	2.3	0.7	2.5	425	330
Si_3N_4 ($d=2.6 \text{ g.cm}^{-3}$)	2.5	0.9	2.5	500	280
Silica Glass	1.0	0.70	0.55	1,400	690

Table 4. Properties of alumina ceramics (after Davidge and Tappin, 1967)

Code No.	Fracture Strength		Young's Modulus	Thermal Stress Resistance Parameter	Critical Temperature
	Initial	Quenched from 270°C			
	σ_b	σ_q	E	$\sigma_b(1-\nu)/3E\alpha$	T_c
	10^9 dyn.cm^{-2}	10^9 dyn.cm^{-2}	$10^{12} \text{ dyn.cm}^{-2}$	°C	°C
1	3.77	1.39	3.98	32	190
2	4.72	1.09	4.00	39	195
3	2.44	1.40	3.78	21	180
4	1.93	1.18	3.76	17	185
5	3.49	1.07	3.76	31	200
6	4.44	1.07	3.81	39	190
8	1.93	1.40	3.10	21	190
9	3.33	1.57	3.49	32	200
10	4.39	1.38	3.67	40	200
11	3.71	1.16	2.92	42	210
12	3.75	0.81	2.99	42	195
13	3.34	1.40	3.00	37	205
14	4.30	1.16	3.18	45	215
15	4.16	1.89	3.02	46	210
17	3.41	1.05	2.96	38	200
18	3.72	1.44	3.05	41	205
19	4.57	1.70	2.81	54	210
20	4.78	1.72	2.70	59	220

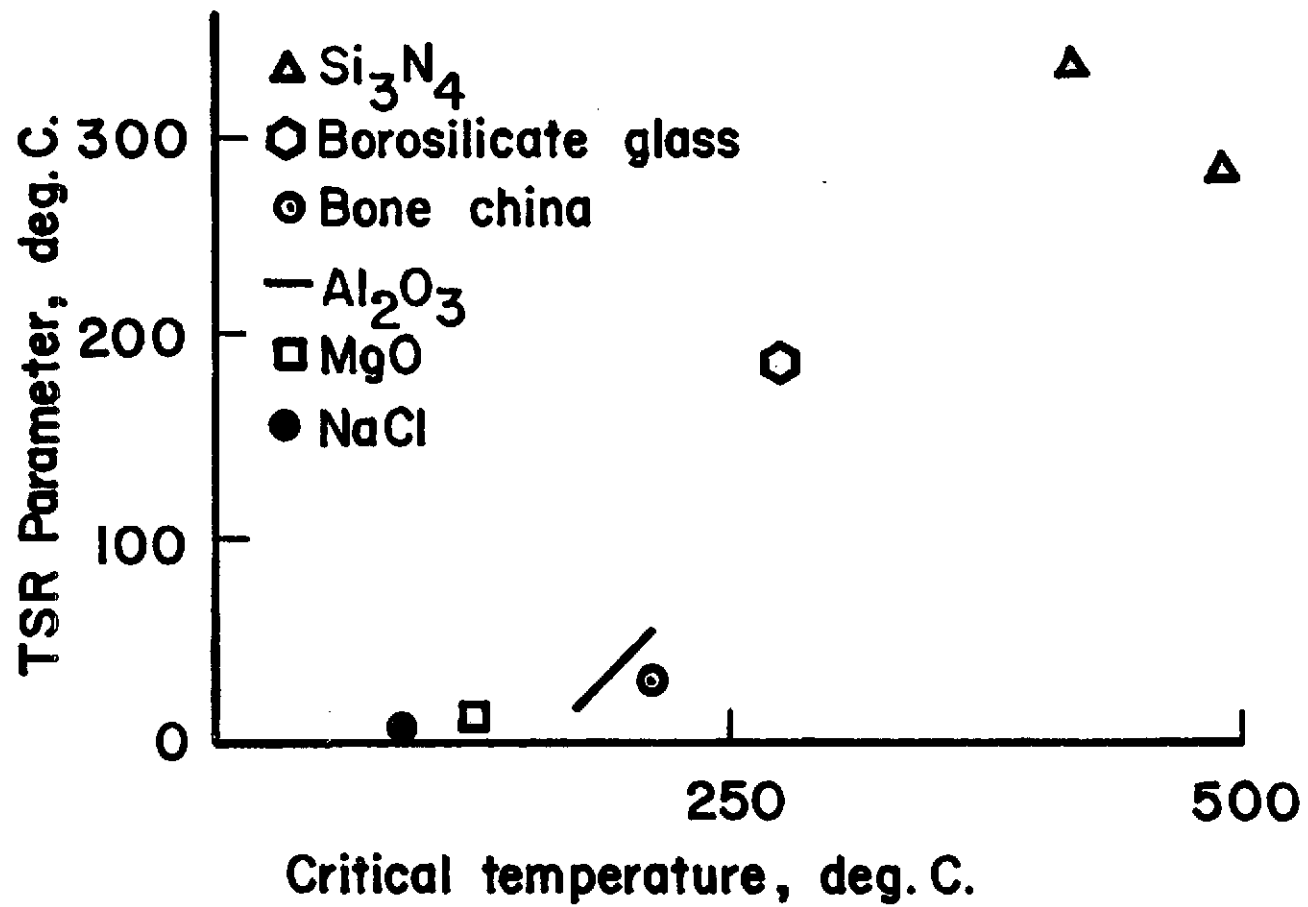


Figure 31. Correlation between thermal-stress-resistance parameter and critical temperature for various substances (after Davidge and Tappin, 1967)

The least thermal shock resistant material (table salt) was also the weakest. Nonetheless, the strain to failure of sodium chloride is approximately equal that of silica glass! The coefficient of linear thermal expansion of sodium chloride is approximately eighty times that of the silica glass and as a result the critical temperature differential is approximately one-eightieth that of silica glass. On the other hand the coefficients of thermal expansion of borosilicate glass and silicon nitride are nearly the same but the strain to failure and consequently the critical temperature differential of silicon nitride are nearly twice that of the borosilicate glass.

Davidge and Tappin made a closer study of the alumina. The straight line in Figure 31 representing these data is enlarged in Figure 32. Here for a given composition the critical temperature differential for a given specimen geometry and environment is shown to be related to the ratio of the fracture strength and the product of the modulus of elasticity and coefficient of thermal expansion in the same manner that completely different materials having the same specimen geometry and environment. The differences in the thermal shock resistances of materials of the same composition can be attributed to differences in the microstructures which are reflected in the measured or effective material parameters. That is to say, as predicted by the present model, the thermal shock resistance of a material is directly related to the intrinsic properties of a material and the effect of defects upon them as manifested in the effective material properties.

Davidge and Tappin (1967) measured the fracture strengths of the alumina after exposure to various temperature differentials and they

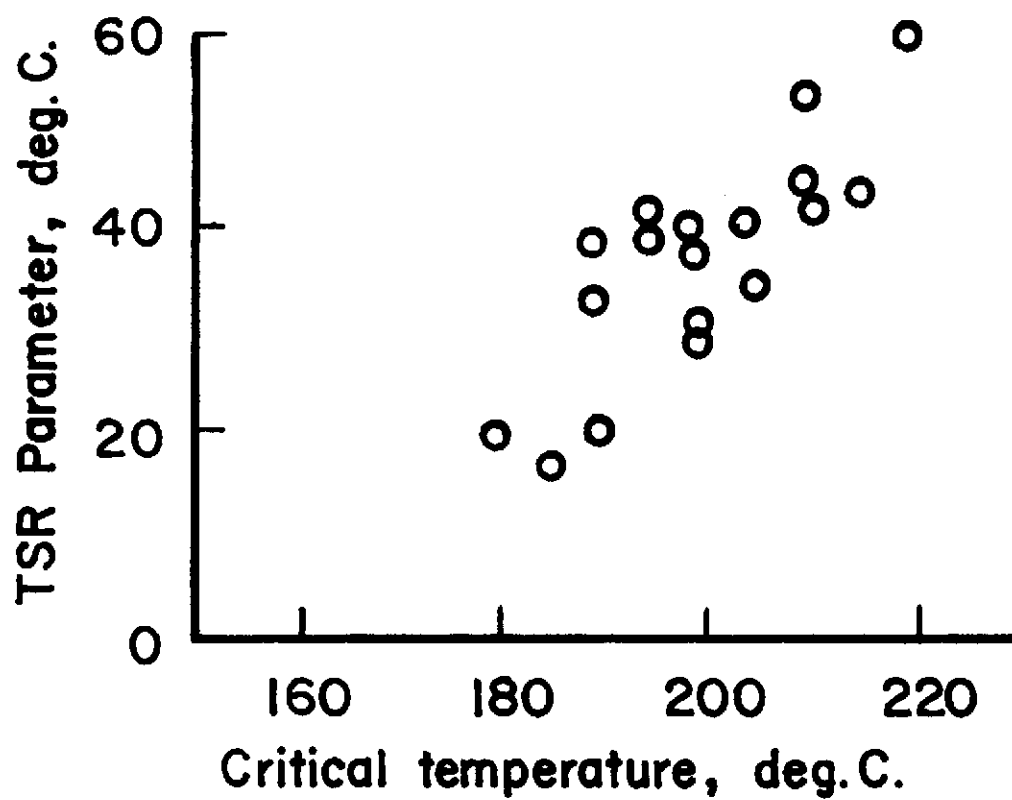


Figure 32. Correlation between thermal-stress-resistance parameter and critical temperature for aluminas (after Davidge and Tappin, 1967)

observed the behavior represented in Figure 13. No loss in strength occurred until the critical temperature differential was reached. When this value was reached "catastrophic" thermal shock occurred with the growth of many cracks. They observed that these cracks grew only slightly larger when the critical temperature differential was exceeded and that the resultant strengths were only slightly lower as a result. It was upon these data that Hasselman (1969b) developed his previously discussed theory.

Heindl and Pendergast (1927) in other work determined the critical temperature for several sagger clays which are similar to those clay materials discussed previously. These clays were relatively weak and probably have Griffith criteria below the knee of the curve as opposed to the above discussed materials of Schmidt, and Davidge and Tappin. Properties were measured on unshocked materials by means of bending tests as before. As may be seen in Figures 33 and 34 no apparent relationship exists between the modulus of rupture and the critical temperature differential or between the modulus of elasticity and the critical temperature differential.

Figure 35 indicates that the modulus of rupture increases as the modulus of elasticity increases. Again the suggestion is that the Griffith criteria are below the knee of the locus. The strain to failure: coefficient of thermal expansion ratio is plotted against the measured critical temperature differential in Figure 36. This ratio again gives an indication of the temperature differential necessary to initiate thermal shock fracture. In this case the fracture is expected not to

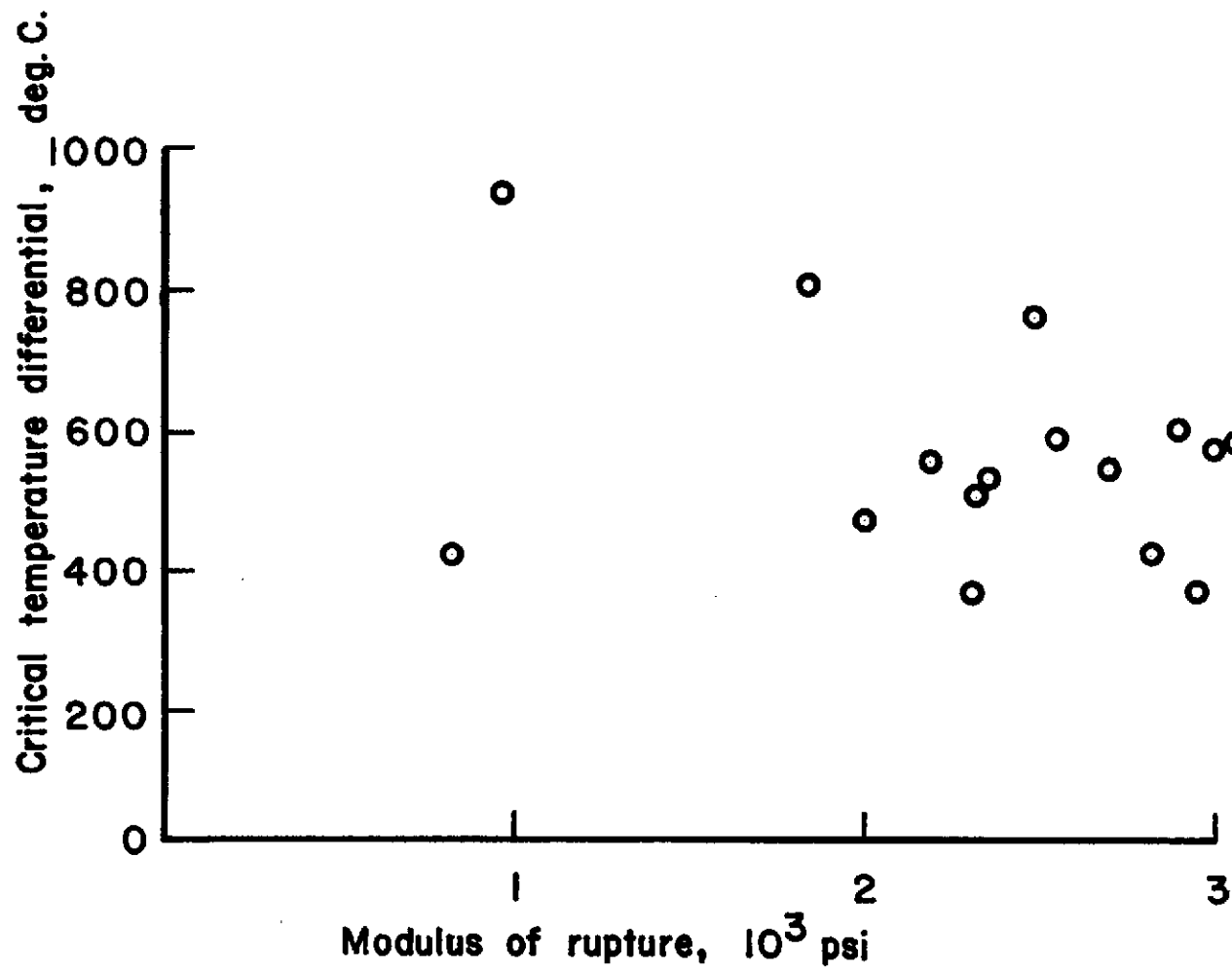


Figure 33. Modulus of rupture vs. critical temperature differential for sagger clays (after Heindl and Pendergast, 1927, from tabular data)

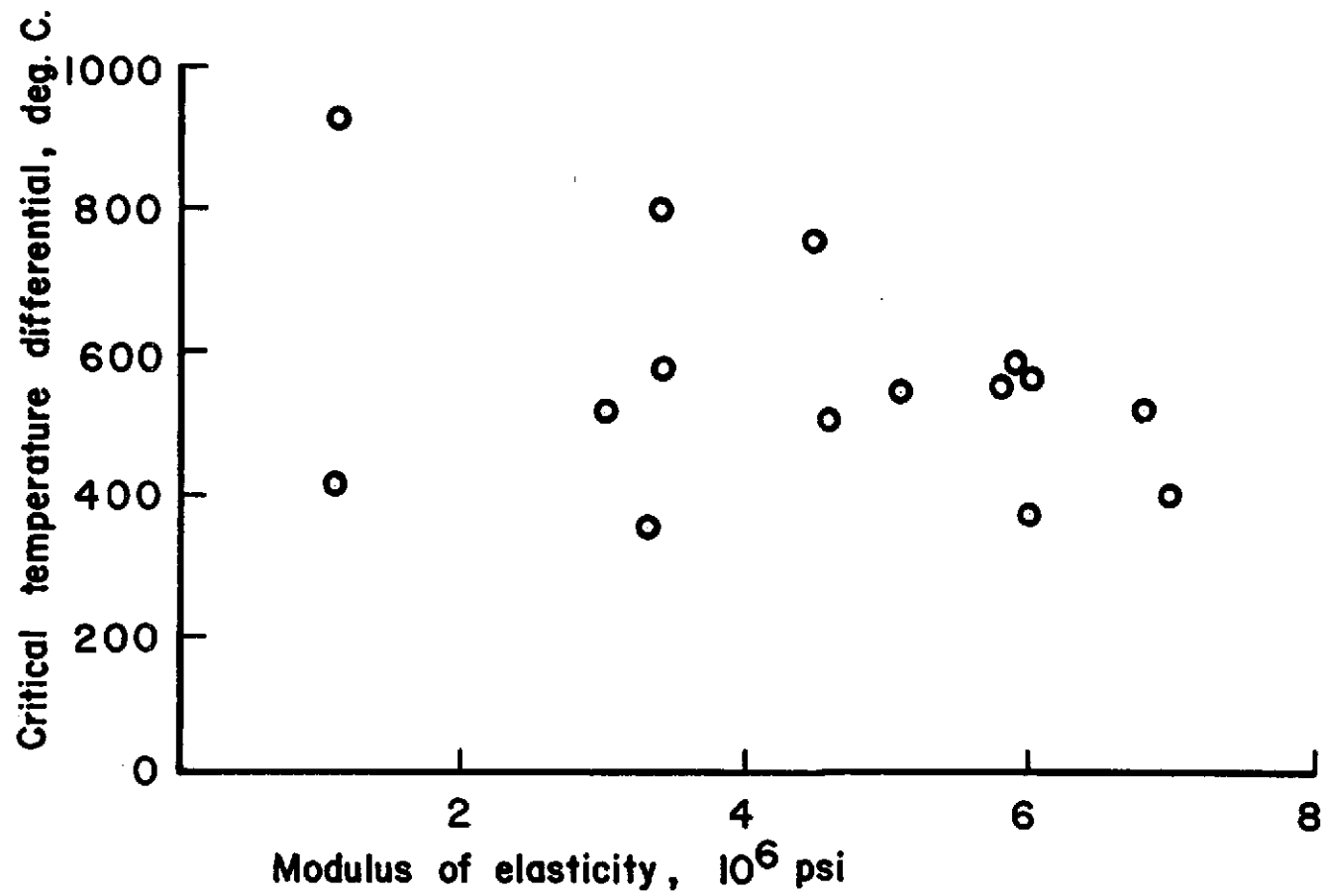


Figure 34. Modulus of elasticity vs. critical temperature differential for sagger clays (after Heindl and Pendergast, 1927, from tabular data)

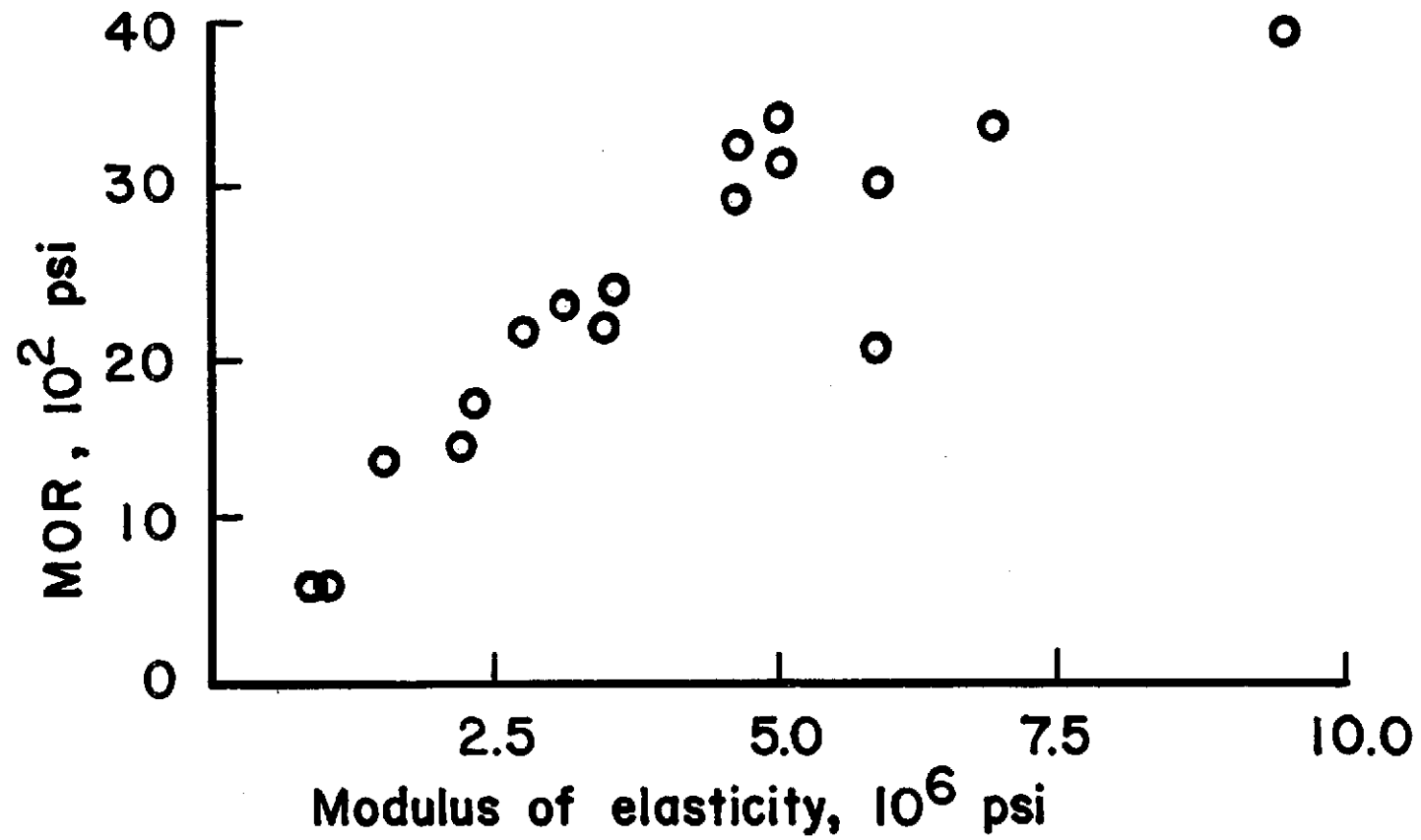


Figure 35. The relationship between modulus of elasticity and transverse strength determined at room temperature (after Heindl and Pendergast, 1927)

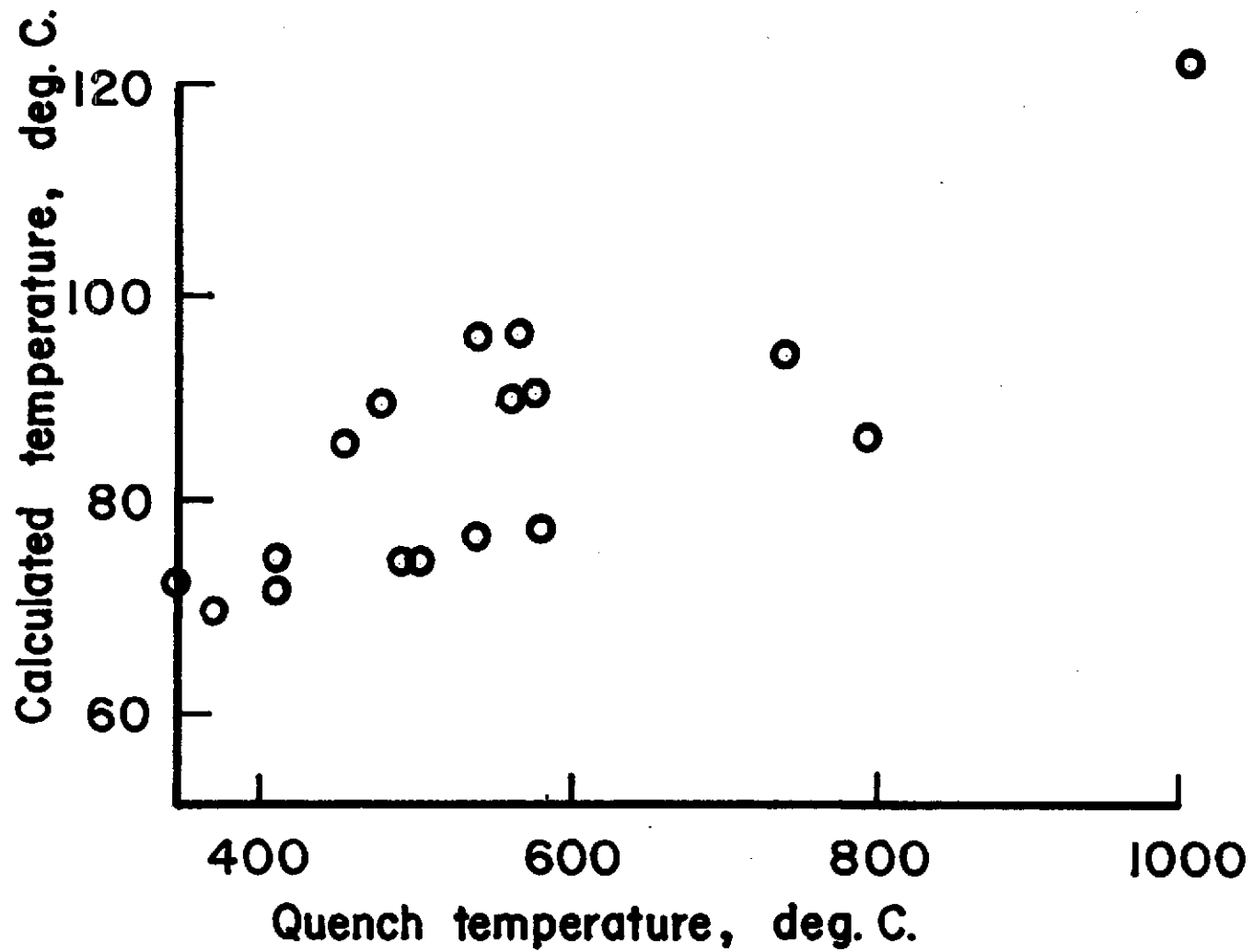


Figure 36. Resistance of saggars to spalling (after Heindl and Pendergast, 1927)

be "catastrophic" but rather "quasi-static." Indeed the applied temperature differentials which caused fracture were nearly an order of magnitude larger than those predicted. This observation suggests that a large amount of overstressing was necessary to fracture the material into separate pieces.

If the thermal shock resistance of materials is influenced by the microstructure as the present model suggests, then composite materials should be of some significance because the microstructure can be carefully controlled by controlling the dispersed phase. Arias (1966a and 1966b) has developed a titanium-zirconia composite having a thermal shock resistance superior to unaltered zirconia. This investigator mixed small diameter titanium metal powder with calcia stabilized zirconia, hydrostatically pressed the mixture, and vacuum sintered the body. The room temperature properties of zirconia with and without the titanium additions were measured. He found the modulus of elasticity of the composite to be higher (29.6×10^6 psi) than that of the zirconia without titanium (20.45×10^6 psi). He also found the bend strength of the composite to be higher: 27.5×10^3 psi for the composite and 14.0×10^3 psi for the zirconia. The strain to failure then is 9.1×10^{-4} for the composite and 7.0×10^{-4} for the zirconia. The coefficient of thermal expansion of the composite is reported as approximately 6.6×10^{-6} per deg C. at temperatures below the inversion point of zirconia.

Arias concludes that the thermal shock resistance of the composite is superior to that of zirconia at temperatures below the inversion point but that it is inferior at temperatures above the inversion point. Limiting the temperatures below the inversion point, Arias concludes

that the metal additions inhibit grain growth (decrease the flaw size) and subsequently a higher strength is obtained. He further concludes that the addition of metals induce plastic deformation at failure because the metal is found in the grain boundaries in the microstructure. These assumptions may be accurate. On the basis of the present model, the thermal shock resistance should be only slightly higher for the composite as the strain to failure is only slightly higher than for zirconia. The most significant result of these materials appears in Figure 37. At room temperatures the thermal conductivity is approximately four times that of zirconia. At higher temperatures the values converge.

With respect to the present model, the improved thermal shock resistance of the composite appears to be primarily related to heat transfer rather than to the strength of the materials. The effective modulus of elasticity to intrinsic modulus of elasticity ratio is greater than 0.80 for the composite but not for the zirconia. Thus the Griffith criteria for the composite are above the knee while the criteria for zirconia are not. The metal additions effectively reduce the defect size such that the strength is increased. The calculated critical temperature differentials are approximately the same however. Here the thermal conductivity is significantly higher for the composite such that for a given temperature differential the transient thermal stresses developed in the composite are significantly lower or for the same transient stress in both materials the temperature differential can be significantly higher for the composite. Thus the composite material at lower temperatures is more thermal shock resistant than the zirconia.

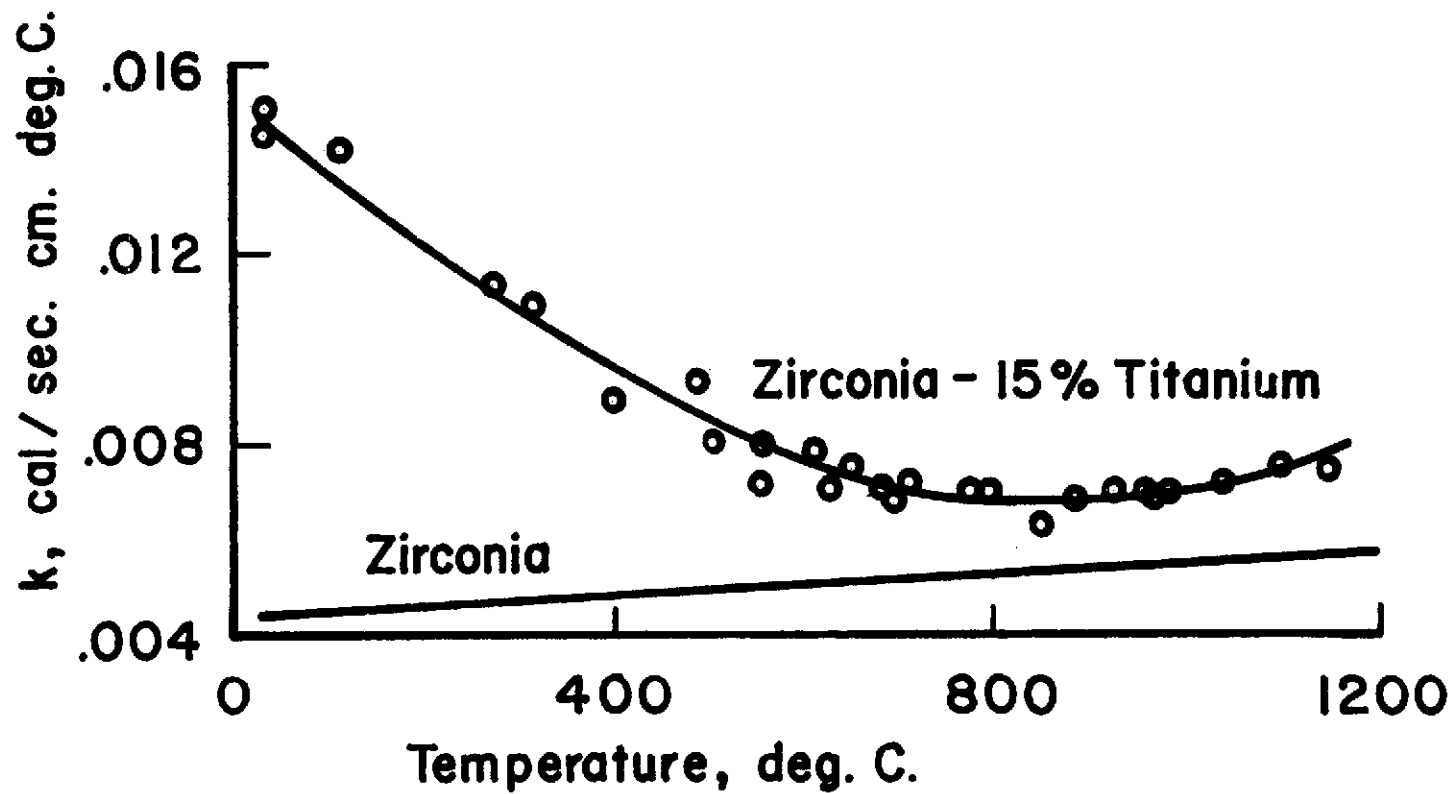


Figure 37. Thermal conductivity of zirconium oxide with 15 percent titanium as a function of temperature compared with that of stabilized zirconia (after Arias, 1966a)

Recently, Lineback and Manning (1971) have investigated the thermal shock resistance of a number of yttria stabilized hafnia based composite materials some of which contained tungsten metal fiber additions (Lineback and Manning, 1972). The thermal shock resistance of composites containing ten weight percent fibers was found to be clearly superior to zirconia containing no fibers. The thermal shock resistance has been attributed directly to the strength:modulus of elasticity ratio.

Lineback and Manning found that large additions of metal fibers increased the thermal conductivity of the composites. Small additions, however, decreased the conductivity particularly in the ten weight percent region which exhibited the best thermal shock resistance. Thus, unlike the previous work of Arias, the increases in thermal shock resistance of the composite materials cannot be attributed to increases in thermal conductivity.

Additions of metal fibers of up to thirty weight percent were found to decrease slightly the low temperature coefficients of thermal expansion. These small changes were not believed to be responsible for the observed behavior. The compressive fracture strengths and the modulus of elasticity of unshocked materials were measured. Again small additions of metal fibers initially decreased the strengths. Larger additions of fibers yielded materials stronger than the zirconia without fibers. The weakest materials contained about ten weight percent fibers. Similarly small additions of metal fibers decreased the effective modulus of elasticity. Additions of about ten weight percent yielded the lowest values while larger additions again increased the

modulus of elasticity. That is to say, the materials having the lowest values of strength and moduli of elasticity were the most thermal shock resistant. Figure 38 indicates that the strength to modulus of elasticity ratio is highest for the materials having the lowest strengths and moduli of elasticity or for the materials having the highest thermal shock resistance. From Figure 39 it can be seen that the lowest modulus of elasticity is less than one-fifth that of the intrinsic modulus of elasticity. From Figure 40 it can be seen that the lowest fracture strength corresponds to the lowest effective modulus. Thus the Griffith criteria of these materials lies below the knee of the locus and failure would be expected to be "quasi-static." Indeed, subsequent quench tests of this material by Manning and Lineback (1971) indicated that unlike "strong" zirconia without fibers, the materials were observed to "spall" rather than fracture into two or more large pieces. For a given specimen geometry and environment, temperature differentials were established which would fracture dense, strong zirconia. The composite materials were cyclically quenched from these temperatures into still water without any gross failure. The specimens did eventually lose weight due to spalling and they did lose strength. Cyclic tests were ended when the specimens could be broken with the fingers.

Microscopic observation of both the shocked and unshocked composite specimens revealed many microcracks. These cracks were observed in many specimens to be associated with the fibers. Cracks were observed in the hafnia matrix away from the tungsten fibers. These cracks upon thermal shock exposure grew and often interacted with the fibers. The cracks

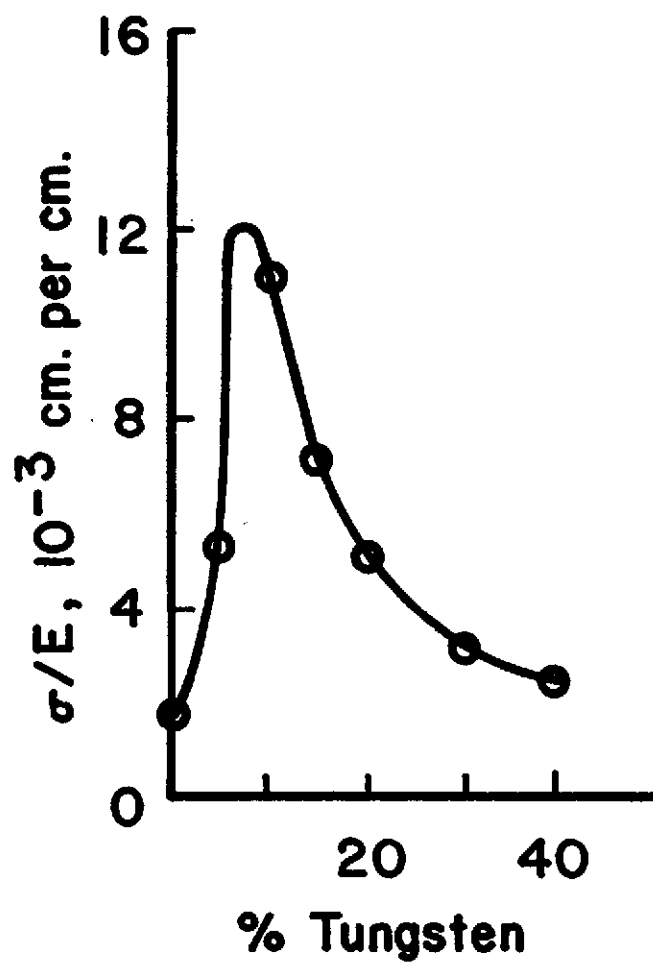


Figure 38. Ratio of compressive fracture stress to modulus of elasticity vs. weight percent tungsten in seventy percent yttria stabilized hafnia (after Lineback and Manning, 1971)

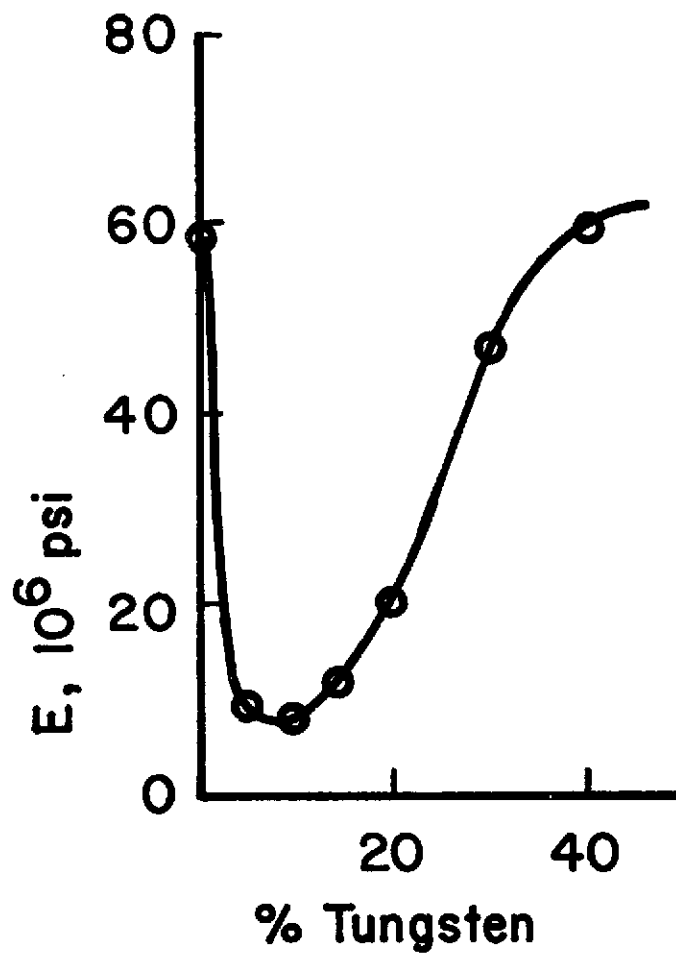


Figure 39. Modulus of elasticity vs. weight percent tungsten in seventy percent yttria stabilized hafnia (after Lineback and Manning, 1971)

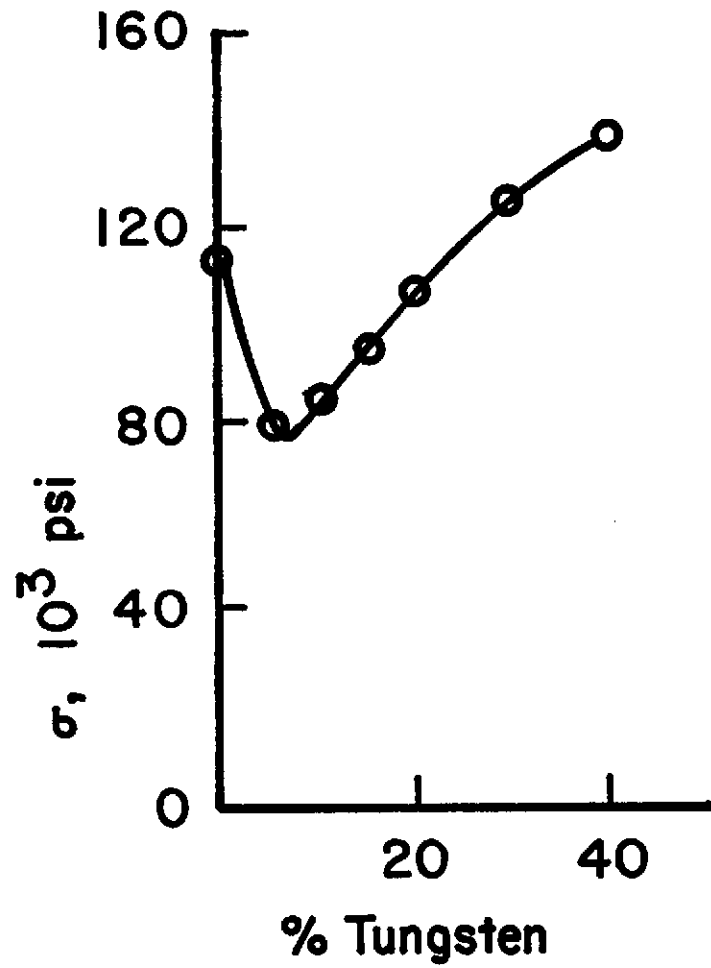


Figure 40. Compressive fracture stress vs. weight percent tungsten in seventy percent yttria stabilized hafnia (after Lineback and Manning, 1971)

were never observed to travel across the fibers. They were observed to travel around the fiber such that the fiber acted to impede their growth. Therefore, it appears that the fibers were both responsible for crack initiation during fabrication and for crack retardation during thermal shock exposure. The cracks were observed to be larger in size after thermal shock exposure but not larger in number.

It is therefore assumed that in this instance the thermal expansion mismatch between tungsten and hafnia resulted in crack formation upon cooling after fabrication by hot pressing. These cracks lowered both the fracture strength and the modulus of elasticity but increased the strain to failure. This combination of events as predicted by the present model resulted in improved thermal shock resistance. Thus, at a given quench temperature the overstressing grew the many cracks in size by a relatively small amount such that the body integrity remained even though the strength was drastically reduced after many quench cycles. That is to say, as predicted by the present model, the thermal shock failure was not "catastrophic."

SUMMARY AND CONCLUSIONS

A model for the thermal stress resistance of truly elastic materials has been developed based upon the intrinsic material properties of surface energy as defined by Griffith (1920) and the modulus of elasticity of a perfect body and upon the physical presence of imperfections as cracks in the body. By incorporation of the criteria for crack growth proposed by Griffith (1920) with the expression for effective modulus of elasticity proposed by Berry (1960a and 1960b), the concept of a Griffith energy which must be applied to a material as strain energy to initiate crack growth was established. The magnitude of this energy was shown to depend upon the surface energy, intrinsic modulus of elasticity, and number of cracks and was reflected in the locus of the Griffith criteria. The position of the Griffith criteria on the locus was determined by the crack size. It was further established that if the Griffith energy was exceeded for a material containing cracks smaller than those necessary to produce the minimum Griffith strain, then the cracks would grow rapidly, resulting in large losses in strength or "catastrophic" failure. Materials, on the other hand, containing cracks larger than those necessary to produce the minimum Griffith strain would fail with smaller losses in strength or "quasi-statically." Finally it was proposed in the model that the temperature differential necessary to produce this Griffith energy in a material at constant uniaxial strain depended only upon the following measured or effective properties of the body; fracture strength, modulus of elasticity, and coefficient of ther-

mal expansion. More specifically, the temperature differential to cause failure depends upon the ratio of the fracture strength to effective modulus of elasticity or the strain to failure for the truly elastic body. Even more specifically, the temperature differential to cause failure depends upon the ratio of the strain to failure to coefficient of thermal expansion. Because it was assumed that the presence of cracks had no effect on the coefficient of thermal expansion, their effect was reflected in the strain to failure. It was suggested in the model that, as cracks grow in size from zero, the strain to failure initially decreases (the material becomes less thermal shock resistant) until the minimum strain to failure is reached and that to this point in size the material would fail "catastrophically." With subsequent increases in crack size the strain to failure increases (the material becomes more thermal shock resistant) and the material is expected to fail "quasi-statically."

The model was applied to the data in the literature. The trends in degree of damage in terms of spalling losses and losses in strength were successfully predicted. The trends in temperature differentials necessary to initiate fracture were also successfully predicted. On this basis the following conclusions were reached:

1. The temperature differential necessary to cause thermal shock damage in elastic materials containing microcracks may be increased by increasing the fracture strength to effective modulus of elasticity ratio which is the strain to failure,

2. Materials having high effective modulus of elasticity to intrinsic modulus of elasticity ratios as a result of microcracks fail with large initial decreases in strength.
3. Materials having low effective modulus of elasticity to intrinsic modulus of elasticity ratios as a result of microcracks may fail with smaller initial decreases in strength.
4. The spalling resistance of elastic materials is greater (the spalling loss is smaller) for weaker materials and is not dependent upon the ratio of the effective modulus of elasticity to intrinsic modulus of elasticity except to the extent that weaker materials have lower ratios.
5. The thermal shock resistance of a material may be increased by adding a second dispersed phase which produces microcracks in the body.
6. Lower coefficients of thermal expansion are beneficial to thermal shock resistance.
7. The fracture strength, the effective modulus of elasticity, and the coefficient of thermal expansion must be considered in concert to ascertain the thermal stress resistance of the body.

Assuming that the present model is a correct approximation to reality on the basis of the above conclusions then the following conclusions concerning the intrinsic properties of the material can be reached:

1. Large surface energies are beneficial to thermal shock resistance.
2. Small intrinsic moduli of elasticity are beneficial to thermal shock resistance.
3. Large numbers of cracks are beneficial to thermal shock resistance if the crack size is large.
4. Small crack sizes are beneficial to thermal shock resistance.

LIST OF REFERENCES

- Arias, A. 1966a. Thermal shock resistance of zirconia with 15 mole percent titanium. *J. Am. Cer. Soc.*, 49, (6), 334-338.
- Arias, A. 1966b. Mechanisms by which metal additions improve the thermal shock resistance of zirconium. *J. Am. Cer. Soc.*, 49, 339-341.
- Berry, J. P. 1960a. Some kinetic considerations of the Griffith criteria for fracture - I equations of motion at constant force. *J. Mech. Phys. Solids*, 8, (3), 194-206.
- Berry, J. P. 1960b. Some kinetic considerations of the Griffith criteria for fracture - II equations of motion at constant deformation. *J. Mech. Phys. Solids*, 8, (3), 207-216.
- Chaudhuri, S. P. and Chatterjee, M. K. 1968. Studies on the thermal shock resistance of aluminosilicate refractories in relation to strength, thermal expansion, and modulus of elasticity. *Trans. Indian Cer. Soc.*, 27, (2), 63-68.
- Davidge, R. W. and Tappin, G. 1967. Thermal shock and fracture in ceramics. *Trans Brit. Cer. Soc.*, 66, (8), 405-422.
- Griffith, A. A. 1920. Phenomena of rupture and flow in solids. *Phil. Trans. Royal Soc. London*, 221A, (4), 163-198.
- Griffith, A. A. 1924. Further considerations on the phenomenon of rupture and flow in solids, pp. 55-63. In J. Waltman, Jr. (ed.), *Proceedings of the First International Congress of Applied Mechanics*. Delft Univ. Press, Delft, Holland.

- Hasselmann, D. P. H. 1969a. Analysis of the strain at fracture of brittle solids with high densities of microcracks. *J. Am. Cer. Soc.*, 52, (8), 458-459.
- Hasselmann, D. P. H. 1969b. Unified theory of thermal shock fracture initiation and crack propagation in brittle ceramics. *J. Am. Cer. Soc.*, 52, (11), 600-604.
- Hasselmann, D. P. H. 1970a. Strength behavior of polycrystalline alumina subject to thermal shock. *J. Am. Cer. Soc.*, 53, (9), 490-495.
- Hasselmann, D. P. H. 1970b. Thermal stress resistance parameters for brittle refractory ceramics: a compendium. *Am. Cer. Soc. Bull.*, 49, (12), 1033-1037.
- Heindl, R. A. and Pendergast, W. L. 1927. Progress report on investigation of sagger clays: their elasticity and transverse strength at several temperatures. *J. Am. Cer. Soc.*, 10, (8), 524-534.
- Heindl, R. A. and Pendergast, W. L. 1957. Results of laboratory tests of high duty and superduty fireclay plastic refractories. *Am. Cer. Soc. Bull.*, 36, (1), 6-13.
- Kingery, W. D. 1955. Factors affecting the thermal shock resistance of ceramic materials. *J. Am. Cer. Soc.*, 38, (1), 1-15.
- Lineback, L. D. and Manning, C. R. 1971. Factors affecting the thermal shock behavior of yttria stabilized hafnia based graphite and tungsten composites, pp. 137-147. In W. W. Kreigel and H. Palmour, III (eds.), *Materials Science Research, Vol. 5: Ceramics in Severe Environments*. Plenum Press, New York.
- Lineback, L. D. and Manning, C. R. 1972. Thermal shock resistant hafnia ceramic material. U. S. Patent 3,706,583. December 19, 1972. U. S. Patent Office, Washington, D. C.

- Manning, C. R. and Lineback, L. D. 1971. Eighth quarterly progress report: Development of high temperature materials for solid propellant rocket nozzle applications. National Aeronautics and Space Administration (Grant NGR 34-002-108), Washington, D. C.
- McKee, J. H. and Adams, A. M. 1950. Physical properties of extruded and slip cast zircon with particular reference to thermal shock resistance. *Trans. Brit. Cer. Soc.*, 49, (8), 386-407.
- Morgan, W. R. 1931. Thermal shock effect on transverse strength of clay bodies. *J. Am. Cer. Soc.*, 14, (12), 913-923.
- Nakayama, J. and Ishizuki, M. 1966. Experimental evidence for thermal shock damage resistance. *Am. Cer. Soc. Bull.*, 45, (7), 666-669.
- Norton, F. H. 1925. A general theory of spalling. *J. Am. Cer. Soc.*, 8, (1), 29-39.
- Parmelee, C. W. and Westman, A. E. R. 1928. Effect of thermal shock on the transverse strength of fireclay bricks. *J. Am. Cer. Soc.*, 11, (12), 884-895.
- Ryshkewitch, E. 1960. *Oxide Ceramics*. Academic Press, Inc., New York.
- Schwartz, B. 1952. Thermal stress failure of pure refractory oxides. *J. Am. Cer. Soc.*, 35, (12), 325-333.
- Smith, C. F. and Crandall, W. D. 1964. Calculated high temperature elastic constants for zero porosity monoclinic zirconia. *J. Am. Cer. Soc.*, 47, (12), 624-627.
- Walsh, J. B. 1965. The effect of cracks on the uniaxial elastic compression of rocks. *J. of Geophys. Res.*, 70, (2), 399-411.